CHAPTER III

RESULTS AND DISCUSSION

Hyptis suaveolens Poit. (Lamiaceae), one of noxious weeds in Thailand, was selected for preliminary screening tests for various activities including cytotoxicity test, antifungal activity, plant growth inhibition and antioxidant activity. The main activity used to investigate for bioactive compounds in this study is plant growth inhibition.

3.1 Weed Growth Inhibition Bioassay Results of Preliminary Screening Tests of *Hyptis suaveolens* Poit.

Air-dried aerial and root parts of *H. suaveolens* Poit. were separately minced to coarse powder and extracted according to the procedure described in Chapter II. Crude extracts were preliminary screened for various activities followed the procedures mentioned in Chapter II. All bioassay results are summarized in Tables 3.1-3.2 and Fig. 3.1.

Table 3.1 Inhibitory effect of the ethanolic crude extracts of *H. suaveolens* Poit. on the growth of *M. pigra* Linn.

Part	% Inhibition at various concentrations			
	Growth of *M.pigra*	0.1 (g)	0.5 (g)	1.0 (g)
Aerial part	Root	5.01	16.93	22.32
	Shoot	14.64	19.86	23.48
Root	Root	11.60	10.12	38.02
	Shoot	-1.99	-4.00	17.24

Table 3.2 Inhibitory effect of the ethanolic crude extracts of *H. suaveolens* Poit. on the growth of *E. crus-galli* Beauv.

Part	% Inhibition at various concentrations			
	Growth of *E. crus-galli*	0.1 (g)	0.5 (g)	1.0 (g)
Aerial part	Root	42.71	80.37	100.00
	Shoot	18.96	38.59	39.86
Root	Root	-14.95	-12.09	70.73
	Shoot	-2.00	5.89	35.45

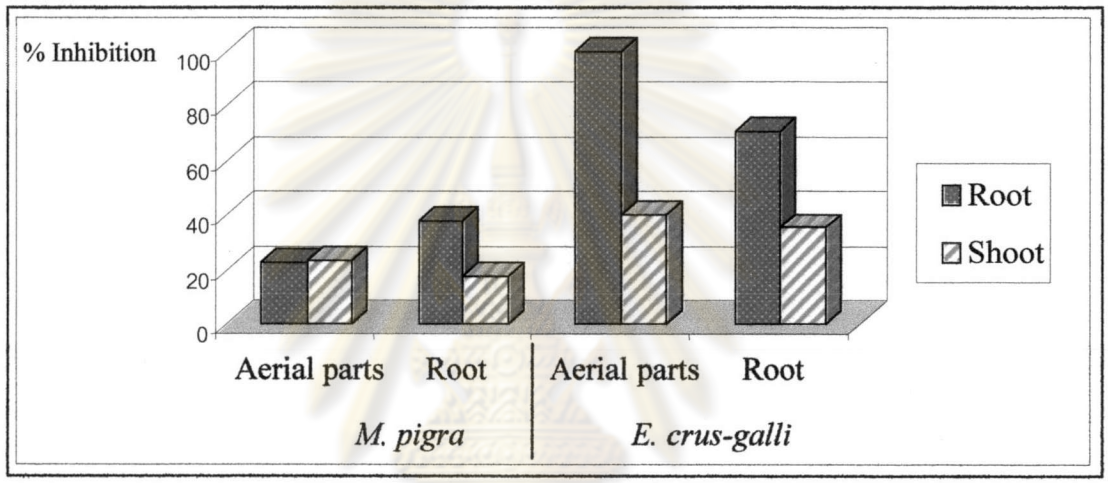

Fig. 3.1 Inhibitory effect of 1.0 g ethanolic crude extracts of *H. suaveolens* Poit. on the seedling growth of *M. pigra* Linn. and *E. crus-galli* Beauv.

Based upon the results of *M. pigra* Linn. growth inhibitory effect, the ethanolic crude extracts of both parts of *H. suaveolens* Poit. revealed not impressive results. To illustrate this, the root growth inhibitory at 1.0 g exhibited 38.02 % whereas at 0.5 g and 0.1 g were 10.12 % and 11.60 %, respectively (Table 3.1).

In contrast to the above results, the ethanolic extract of the aerial part of this plant revealed very good inhibition results against *E. crus-galli* Beauv. The root growth inhibition was noticed to be more effective than that of the shoot growth of aerial parts. The root growth inhibitory was completely 100 % at 1.0 g and for 0.5 g and 0.1 g the percent inhibition were 80.37 % and 42.71 %, respectively (Table 3.2).

Nonetheless, the extracts of the root of *H. suaveolens* Poit. revealed moderate activity. The root growth inhibition effect is higher than that of shoot growth.

The root growth inhibitory effect at 1.0 g was 70.73 % and those of 0.5 g and 0.1 g are -12.09 % and -14.95 %, respectively (Table 3.2).

The ethanolic crude extract of aerial part of *H. suaveolens* Poit. exhibited better growth inhibitory effect on *E. curs-galli* Beauv. than that on shoot and root of *M.* pigra Linn. From the result obtained, it was indicated that ethanolic crude extract significantly inhibited *E. curs-galli* Beauv., which is a monocotyledon. Therefore this crude extract should have allelopathic effect on other monocotyledon. Hence, the present investigation will be focused on the constituents of *H. suaveolens* Poit. and its plant growth inhibition against *E. curs-galli* Beauv.

3.2 Weed Growth Inhibition Activity Results of the Extracts of *H. suaveolens* Poit.

Each crude extract of the aerial parts of *H. suaveolens* Poit. which was derived from the extraction procedure described in Chapter II (2.5.1) was preliminary bioassay for plant growth inhibition activities. The results are presented in Table 3.3 and Fig. 3.2.

Table 3.3 Inhibitory effect of crude extracts of *H. suaveolens* Poit. on the growth of *E. crus-galli* Beauv.

Crude extracts	% Inhibition at various concentrations			
	Growth of *E. crus-galli* part	0.1 (g)	0.5 (g)	1.0 (g)
Hexane	Root	56.95	98.78	100.00
	Shoot	15.04	40.48	41.59
EtOH	Root	15.92	48.37	89.49
	Shoot	-1.01	16.95	32.18
CH_2Cl_2	Root	-3.57	87.91	100.00
	Shoot	-13.79	41.38	59.34
EtOAc	Root	-4.52	-15.40	-5.75
	Shoot	-2.59	-12.64	-17.24
Butanol	Root	17.90	-7.95	15.70
	Shoot	-39.37	-33.05	5.89
Water	Root	26.12	10.12	4.15
	Shoot	22.52	-4.45	3.00

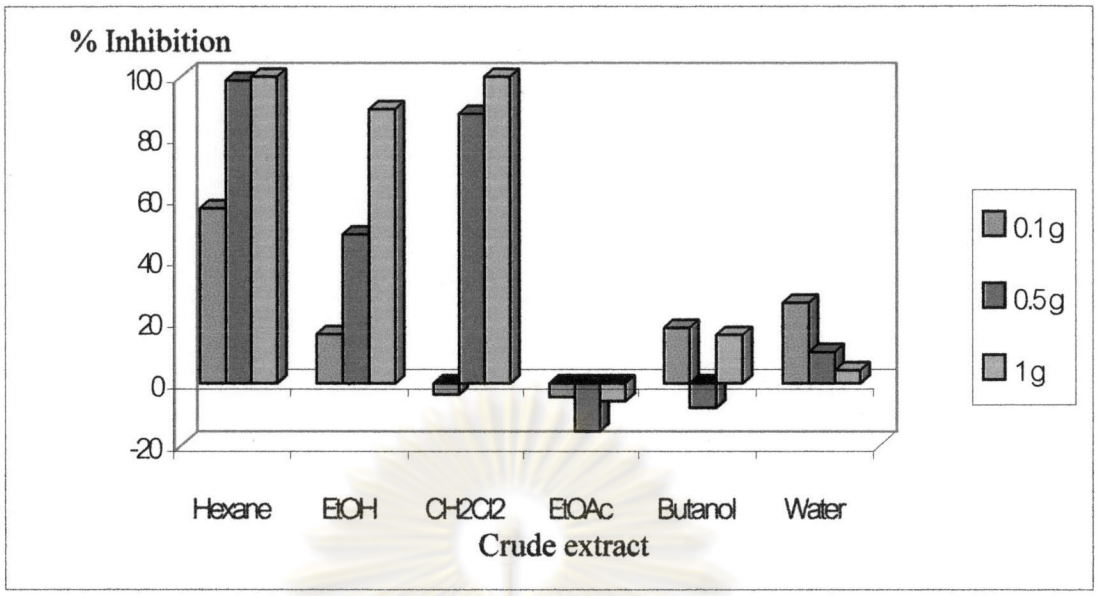

Fig. 3.2 Inhibitory effect of the crude extracts of *H. suaveolens* Poit. on the seedling growth of *E. crus-galli* Beauv.

All fractions revealed a profound effect on the root growth more than the shoot growth. For the inhibitory effect on the root growth of *E. crus-galli* Beauv., hexane and dichloromethane crude extracts showed the strongest inhibitory effect (100%), followed by ethanol, butanol, water and ethyl acetate crude extracts, respectively.

3.3 Weed Growth Inhibition Activity of Fractionation of Hexane and Dichloromethane Extracts of *H. suaveolens* Poit.

According to preliminary plant growth inhibition activities (see Table 3.3), hexane and dichloromethane crude extracts emerged as the most promising fractions to contain allelopathic chemicals against *E. crus-galli* Beauv. The separation of both crude extracts into small portions was carried out and the biological activity tests of each derived fraction was carefully monitored.

3.3.1 Weed Growth Inhibition Activity of Hexane-derived Fractions of *H. suaveolens* Poit.

Each fraction derived from the separation of hexane extract was (Table 2.1) further subjected to plant growth inhibition experiments. The *E. crus-galli* Beauv. growth inhibition results are presented in Table 3.4 and Fig. 3.3.

Table 3.4 Inhibitory effect of hexane-derived fractions crude of *H. suaveolens* Poit. on the growth of *E. crus-galli* Beauv.

Fraction	% Inhibition at various concentrations			
	Growth of *E. crus-galli* part	0.1 (g)	0.5 (g)	1.0 (g)
F	Root	5.9	26.7	42.4
	Shoot	-15.6	17.9	4.14
G	Root	7.2	23.1	33.7
	Shoot	-20.6	11.5	3.0
H	Root	75.3	88.7	98.5
	Shoot	25.1	21.6	46.7
I	Root	32.6	56.1	100.0
	Shoot	15.3	11.7	12.1
J	Root	39.0	65.6	89.6
	Shoot	18.9	10.3	14.4
K	Root	71.3	86.9	93.1
	Shoot	14.8	19.3	29.2

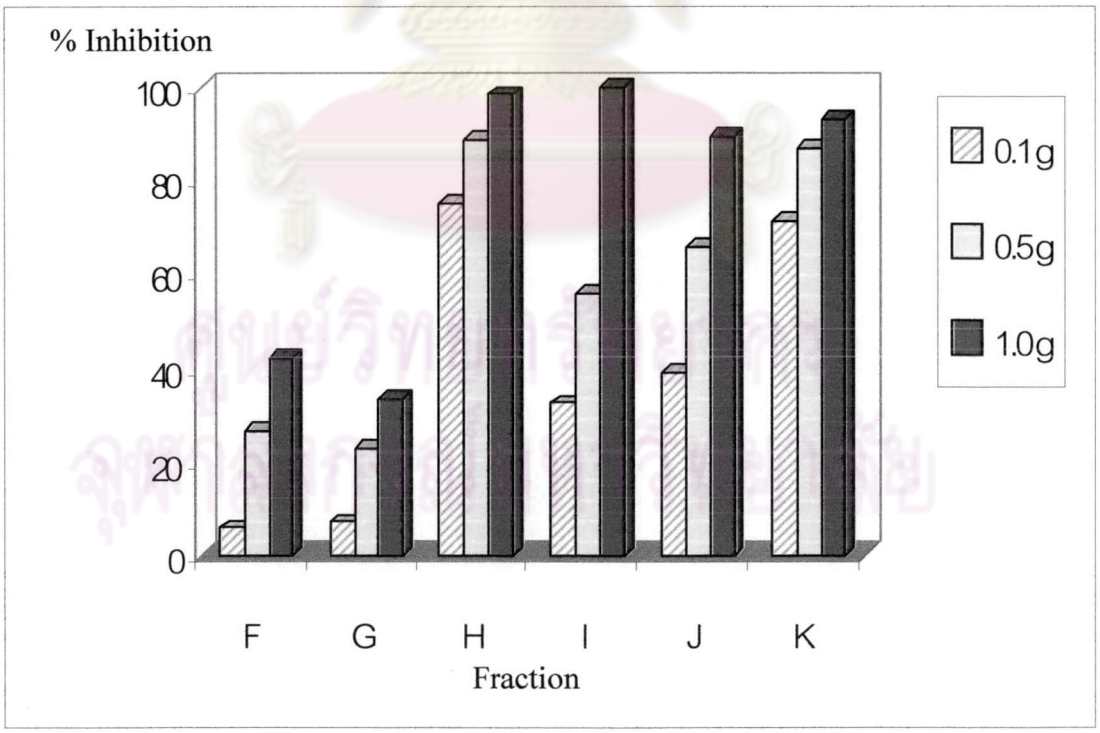

Fig. 3.3 Inhibitory effect of hexane-derived fractions of *H. suaveolens* Poit. on the seedling growth of *E. crus-galli* Beauv.

3.3.2 Weed Growth Inhibition Activity Results of Dichloromethane – derived Fractions of *H. suaveolens* Poit.

Each small fraction derived from the separation of dichloromethane was further subjected to plant growth inhibition experiments. The growth inhibition results against *E. crus-galli* Beauv. of each fraction are shown in Table 3.5 and Fig. 3.4.

Table 3.5 Inhibitory effect of dichloromethane-derived fractions crude extract of *H. suaveolens* Poit. on the growth of *E. crus-galli* Beauv.

Fraction	% Inhibition at various concentrations			
	Growth of *E. crus-galli* parts	0.1 (g)	0.5 (g)	1.0 (g)
A	Root	57.3	55.8	80.5
	Shoot	27.4	7.2	13.5
B	Root	72.1	76.8	91.3
	Shoot	11.2	23.8	30.9
C	Root	6.1	27.6	52.21
	Shoot	-2.2	23.3	24.0
D	Root	21.5	27.7	32.2
	Shoot	30.2	39.0	29.8
E	Root	-6.3	-41.5	-16.2
	Shoot	-6.3	14.8	1.4

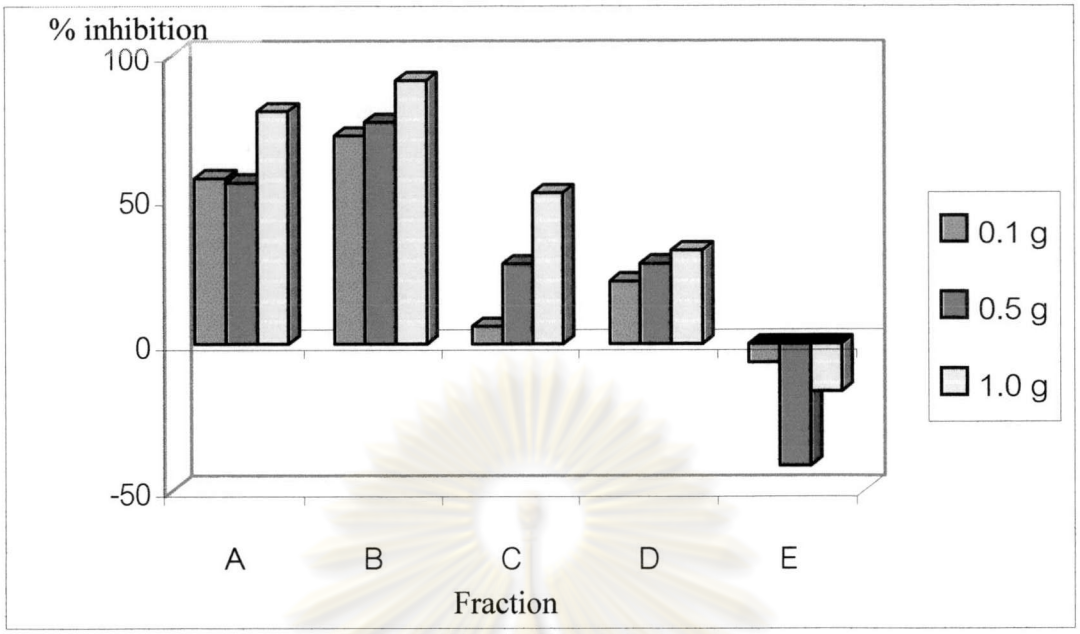

Fig. 3.4 Inhibitory effect of dichloromethane-derived fractions of *H. suaveolens* Poit. on the seedling growth of *E. crus-galli* Beauv.

Based upon the results of the growth inhibitory effect against *E. crus-galli* Beauv., Fractions H, I, J and K attained from hexane extract revealed good activity. The growth inhibition increased when the concentration increased. At low concentration, the root growth inhibition was higher than the shoot growth. Fraction I was found to be the most active fraction with the highest inhibition 100 % at 1.0 g, followed by Fractions H, K, J, F and G 98.5 %, 93.1 %, 89.6 %, 42.4 % and 33.7 % at 1.0 g, respectively. For dichloromethane crude extract, Fraction B displayed the highest percent inhibition with 91.3 % at 1.0 g, followed by Fractions A, C, D and E 80.5 %, 52.21 %, 32.2 % and -16.2 % at 1.0 g, respectively.

From Tables 3.4 –3.5 it was indicated that Fractions A, B, C, H, I, J and K should contain bioactive substances. Thus, it was interesting to isolate, purify and follow the activity in order to find bioactive compounds that affect the growth of *E. crus-galli* Beauv.

3.4 Structural Elucidation of Isolated Compounds.

3.4.1 Structural Elucidation of Mixture HS-1

Mixture **HS-1** was collected from Fraction C3 and recrystallized from a mixture of dichloromethane and methanol to give white needle crystal, m.p. 120-136 °C, 102.1 mg (0.23% w/w of fraction C). This substance gave a deep green color with Liebermann-Berchard's reagent suggesting the presence of steroid skeleton. Two molecular ions at m/z 412 and 414 were observed in EIMS (Fig. 3.5). The IR spectrum (Fig. 3.6) exhibited absorption bands for a hydroxyl group at 3428 cm^{-1}, 2870 cm^{-1} (C-H stretching vibration of $-CH_3$, $-CH_2-$), 1625 cm^{-1} (C=C stretching), 1465, 1381 cm^{-1} (C-H bending vibration of $-CH_3$, $-CH_2-$) and 1061 cm^{-1}(C-O stretching).

Mixture **HS-1** was identified as a mixture of β-sitosterol and stigmasterol by comparison of its ^{1}H and ^{13}C-NMR spectral data with those reported values (Francisco *et al.*, 1994). In addition, the composition of Mixture **HS-1** was verified by using gas-liquid chromatography. From the GC chromatogram of **HS-1**, two major peaks were exhibited at the same retention times as those of authentic β-sitosterol and stigmasterol.

Hence, it was obvious to conclude that **HS-1** was a mixture of β-sitosterol and stigmasterol. The structures of these two steroids are shown below:

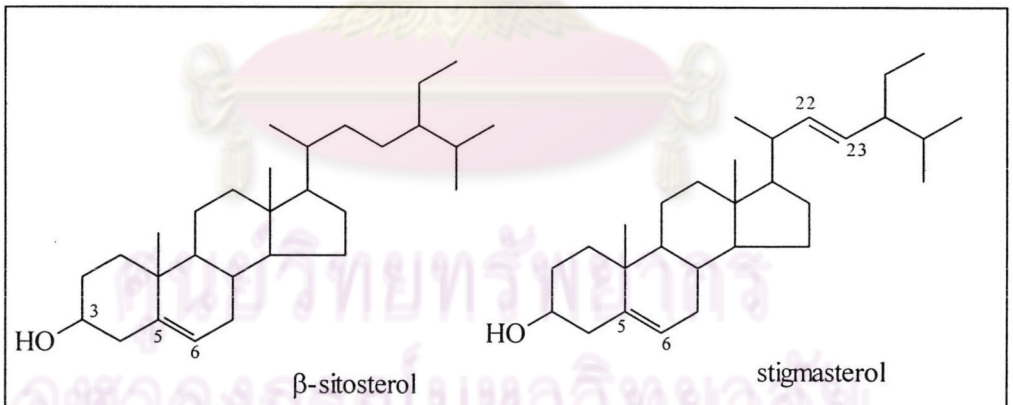

Mixture **HS-1**

The composition of steroids in **HS-1** was presented in Table 3.6.

Table 3.6 The composition of steroids in **HS-1**.

Name	Rt (min.)	% Composition
stigmasterol	28.19	38
β-sitosterol	32.18	62

Additional information was obtained from NMR spectra. ^{1}H-NMR spectrum (Fig. 3.7) revealed the signals at δ 5.07 (1H, dd, *J*=15.5, 8.3 Hz) and 5.13 (1H, dd, *J*=15.53, 8.24 Hz) which could be assigned for H-23 and H-24 of stigmasterol. The signals at 3.47 (2H, m) and 5.34 (2H, d, *J*=5.0 Hz) were assigned to H-3 and H-6 of both β-sitosterol and stigmasterol, respectively.

The ^{13}C-NMR spectrum (Fig. 3.8) of Mixture **HS-1** displayed forty-five signals. These complicated signals, however, were well coincided with those of reported ^{13}C-NMR values of β-sitosterol and stigmasterol (Francisco *et al.*, 1994) as shown in Table 3.7.

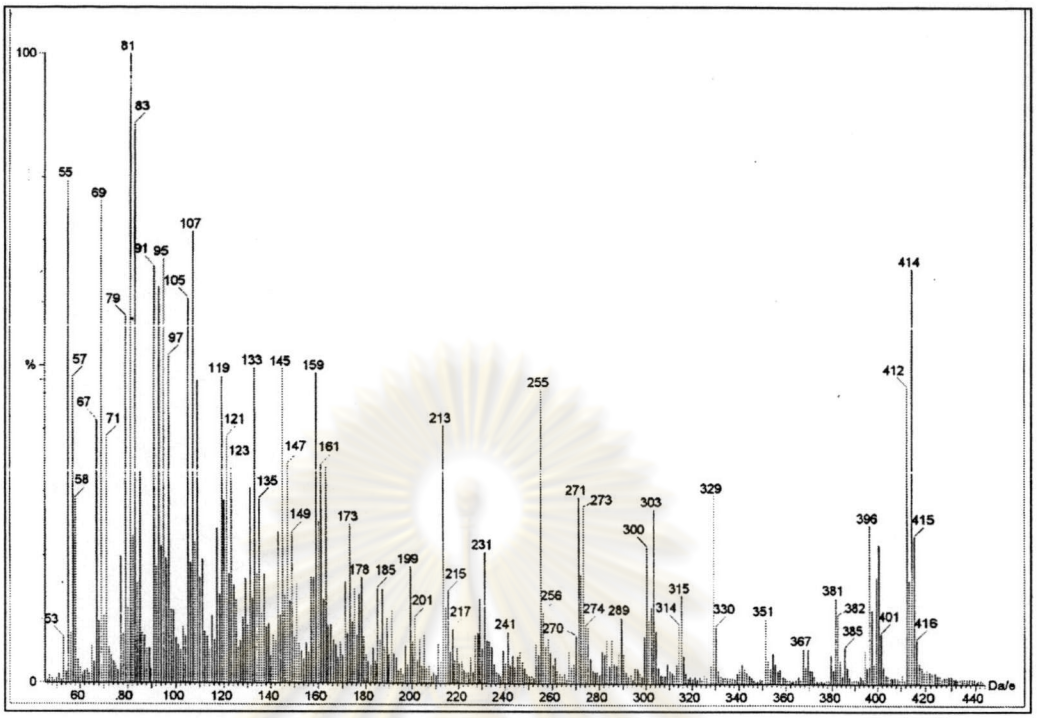

Fig. 3.5 The mass spectrum of Mixture **HS-1**

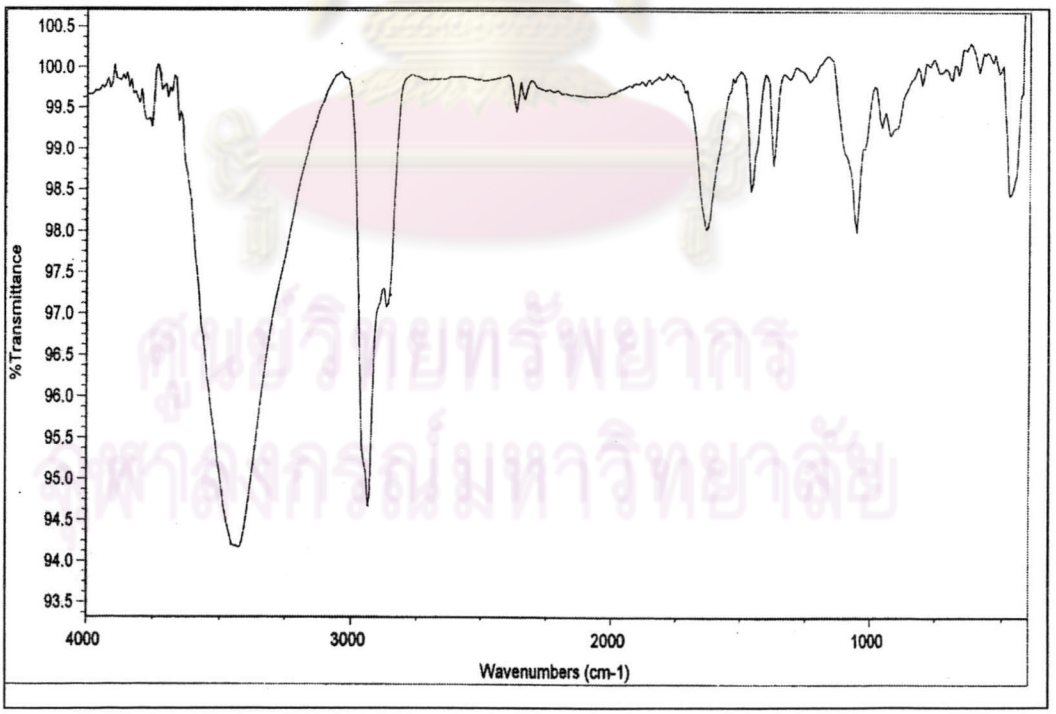

Fig. 3.6 The IR spectrum of Mixture **HS-1**

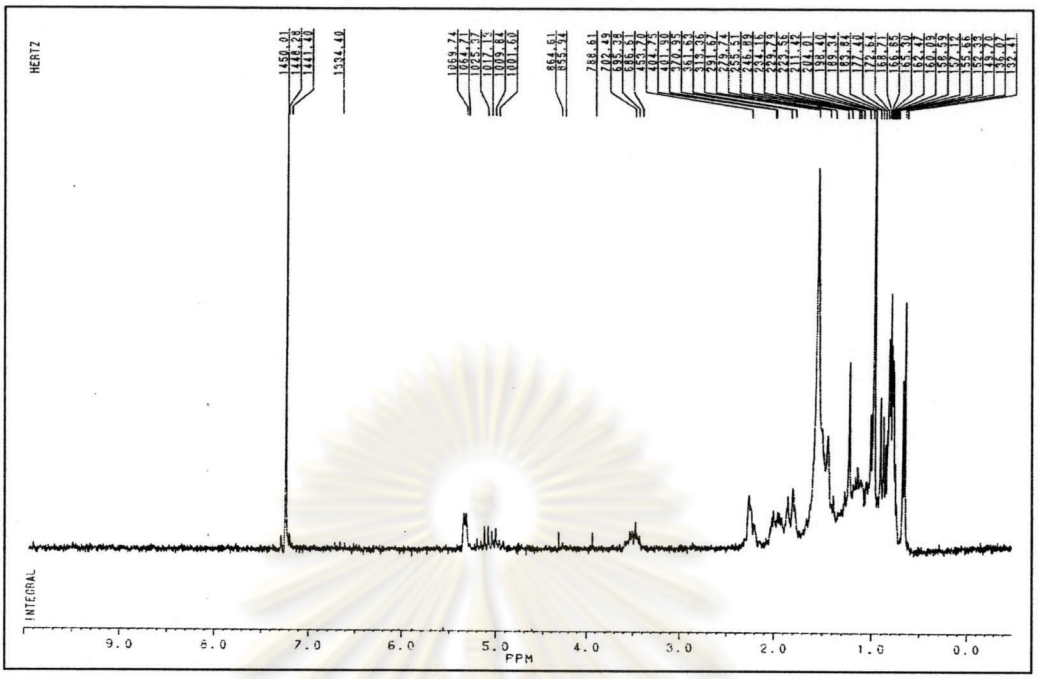

Fig. 3.7 The ^{1}H-NMR spectrum of Mixture **HS-1**

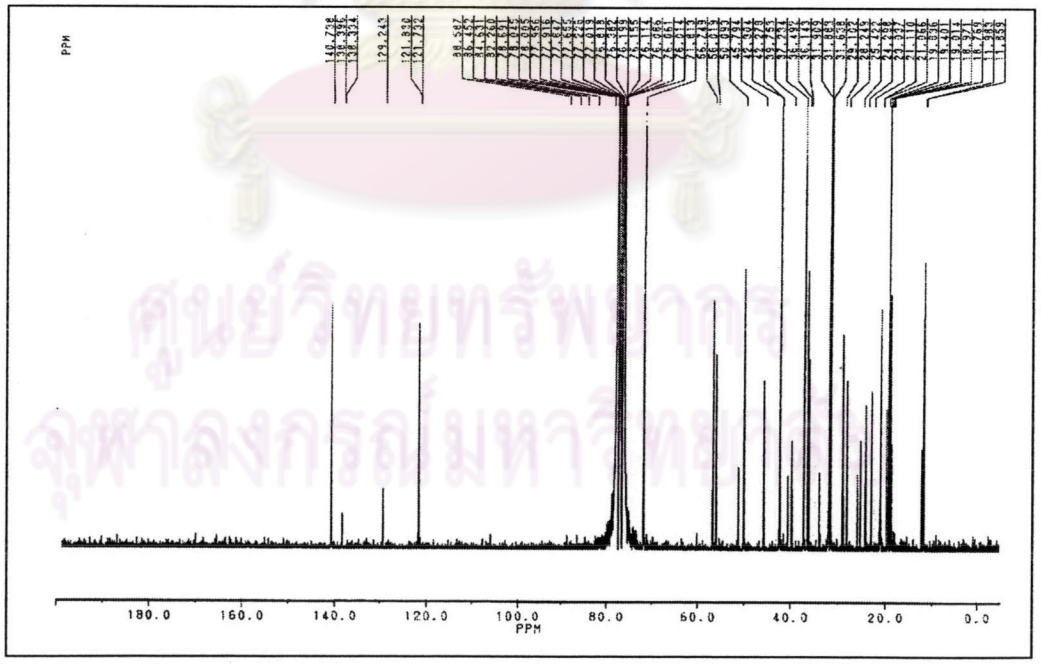

Fig. 3.8 The ^{13}C-NMR spectrum of Mixture **HS-1**

Table 3.7 The ^{13}C-NMR chemical shift assignment of β-sitosterol, stigmasterol and Mixture **HS-1** (in $CDCl_3$)

Carbon	Chemical shift (ppm)		
	β-sitosterol	stigmasterol	**HS-1**
1	37.31	37.31	37.3
2	31.57	31.67	31.6
3	71.69	71.81	71.8
4	42.45	42.35	42.4, 42.3
5	140.76	140.80	140.7
6	121.59	121.69	121.7
7	31.92	31.94	31.9
8	31.92	31.94	31.9
9	51.17	50.20	50.0
10	36.51	36.56	36.5
11	21.11	21.11	21.1
12	39.81	39.74	39.8, 39.7
13	42.33	42.35	42.3
14	56.79	56.91	56.7, 56.8
15	24.32	24.39	24.3, 24.4
16	28.26	28.96	28.2, 28.9
17	56.11	56.06	56.2, 56.0
18	11.87	12.07	11.9, 12.0
19	19.40	19.42	19.4
20	36.17	40.54	36.1, 40.5
21	18.82	21.11	18.8, 21.0
22	33.95	138.37	33.9, 138.3
23	26.13	129.32	26.0, 129.3
24	45.85	51.29	45.8, 51.2
25	29.18	31.94	29.1, 31.9
26	19.84	21.26	19.8, 21.2
27	19.04	19.02	19.0, 18.9
28	23.09	25.44	23.0, 25.4
29	12.32	12.27	12.2

3.4.2 Structural Elucidation of Compound HS-2

Compound **HS-2** (3.12 g) was obtained as colorless needles, m.p. 261-263 °C from Fraction C 75 through recrystallization from ethanol. The yield was 14.61% w/w of Fraction C. A Libermann-Burchard test gave a positive red color, indicative of a triterpeniodal skeleton present in this compound.

The EIMS spectrum of Compound **HS-2** (Fig. 3.9) revealed a molecular ion at m/z 456, suggesting a molecular formula of $C_{30}H_{48}O_3$. The IR spectrum (Fig. 3.10) exhibited absorption bands for a hydroxyl group at 3437 cm^{-1}, 2865 cm^{-1} (C-H stretching vibration of $-CH_3$, $-CH_2-$), 1625 cm^{-1} (C=C stretching), 1465, 1381 cm^{-1} (C-H bending vibration of $-CH_3$, $-CH_2-$) and 1061 cm^{-1}(C-O stretching).

By comparing the ^1H and ^{13}C-NMR spectra of Compound **HS-2** with previously reported spectral data (Takeoka *et al.*, 2000), Compound **HS-2** was identified as oleanolic acid.

The ^1H-NMR spectrum of Compound **HS-2** (Fig. 3.11) showed a methyl signal at δ 0.69, 0.75, 0.88, 0.96 and 1.10 ppm. The signal at δ 5.25 was properly assigned to a hydroxy proton.

The ^{13}C-NMR spectrum (Fig. 3.12) disclosed the presence of 30 carbon resonances. To confirm the structure, the ^{13}C-NMR signals of this compound were compared with those of oleanolic acid (Takeoka *et al.*, 2000). Their carbon assignments are presented in Table 3.8.

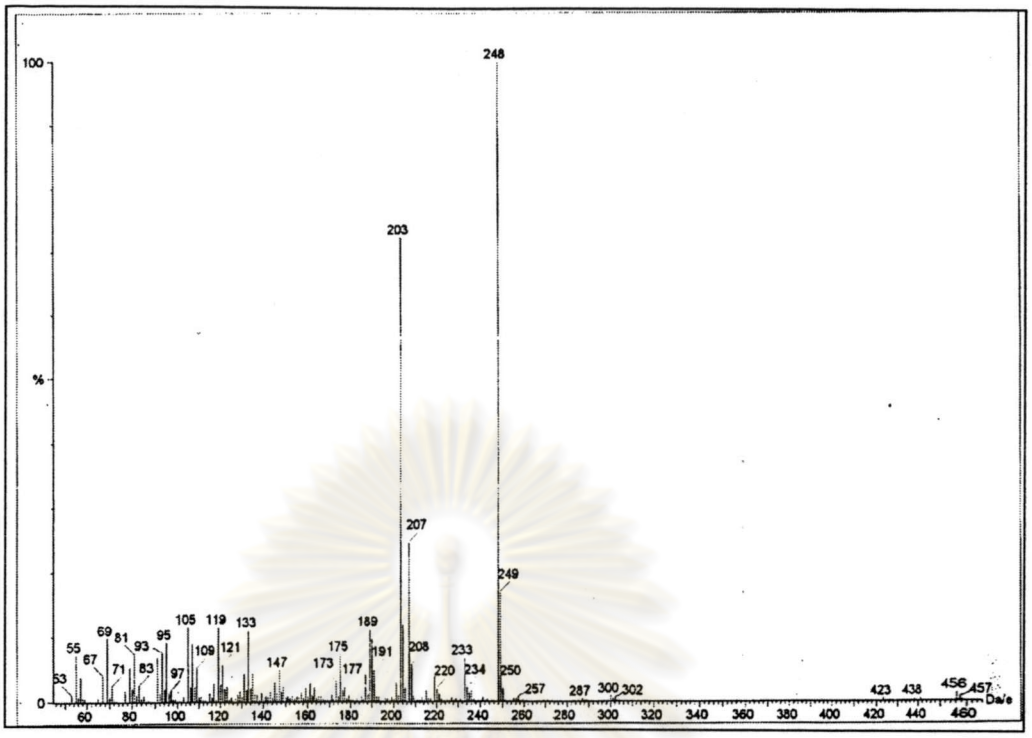

Fig. 3.9 The mass spectrum of Compound **HS-2**

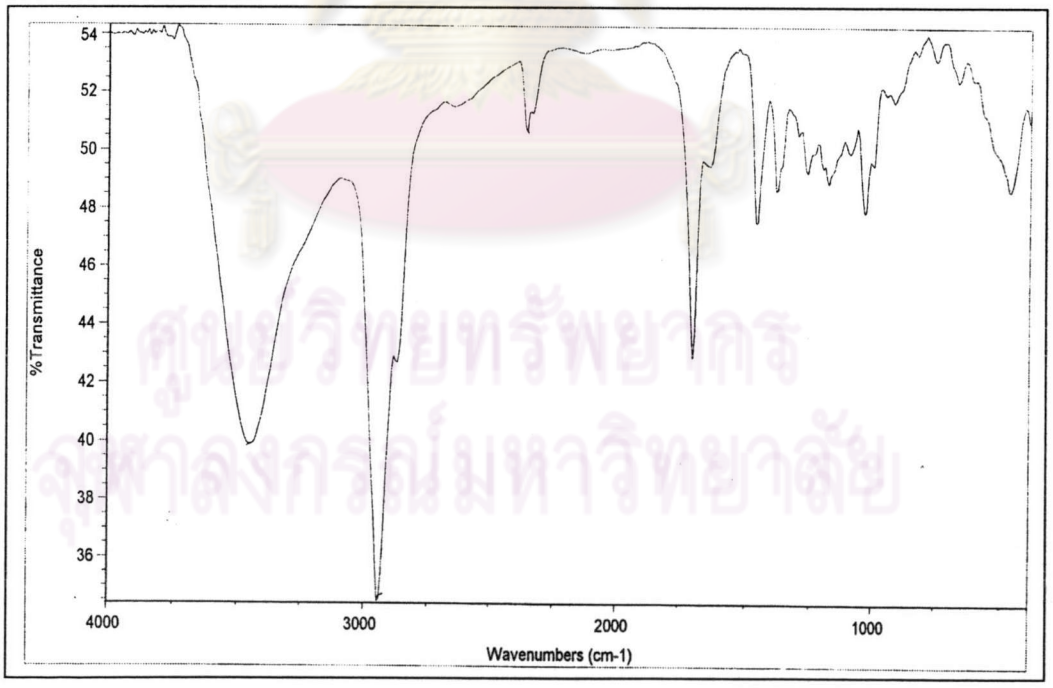

Fig. 3.10 The IR spectrum of Compound **HS-2**

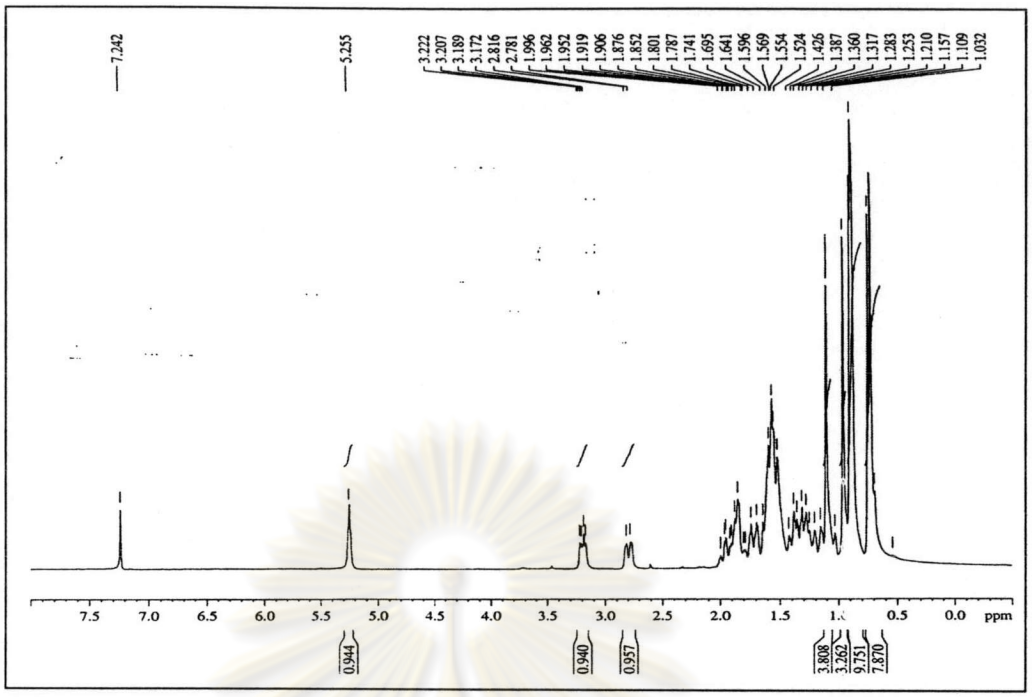

Fig. 3.11 The ^{1}H-NMR spectrum of Compound **HS-2**

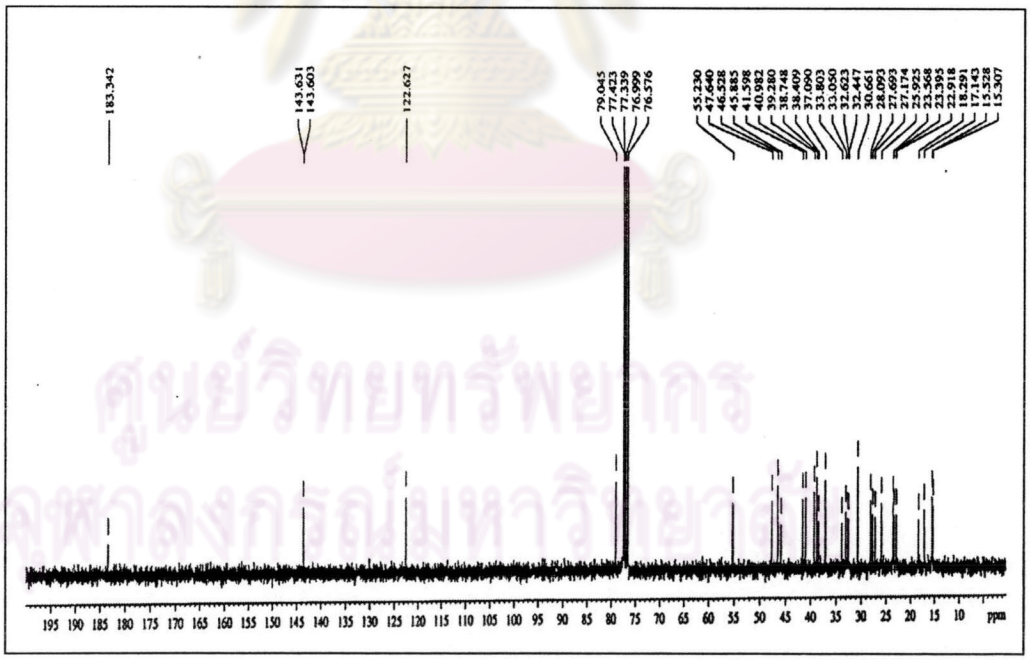

Fig. 3.12 The ^{13}C-NMR spectrum of Compound **HS-2**

Table 3.8 The ^{13}C-NMR spectral assignment of oleanolic acid and Compound **HS-2** (in $CDCl_3$)

Carbon	Chemical shift (ppm)		Carbon	Chemical shift (ppm)	
	oleanolic acid	**HS-2**		oleanolic acid	**HS-2**
1	38.48	37.3	16	23.12	22.9
2	27.24	31.6	17	46.76	46.5
3	79.05	79.0	18	41.35	40.9
4	38.78	38.7	19	45.93	45.8
5	55.28	55.2	20	30.71	30.6
6	18.37	18.3	21	33.90	33.8
7	32.72	32.6	22	32.42	32.4
8	39.32	39.2	23	28.13	28.0
9	47.68	47.6	24	15.58	15.3
10	37.08	37.0	25	15.32	15.2
11	23.44	23.4	26	16.87	17.1
12	122.40	122.6	27	25.97	25.9
13	143.82	143.6	28	178.29	183.3
14	41.69	41.6	29	33.12	33.0
15	27.74	27.6	30	23.66	23.5

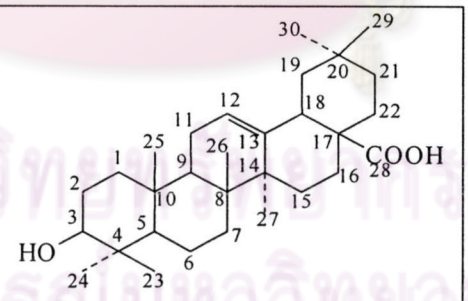

Compound HS-2: Oleanolic acid

3.4.3 Structural Elucidation of Compound HS-3

Compound **HS-3** (25.2 mg) was obtained as yellow crystals from fraction C7523 through recrystallization from methanol. The yield was 0.05% based on dried weight of aerial parts. Compound **HS-3** had a melting point 280-282 °C and Rf value 0.67 (20% EtOAc in CH_2Cl_2).

The EIMS mass spectrum of Compound **HS-3** (Fig. 3.13) revealed a molecular ion at m/z 284, suggesting a molecular formula of $C_{16}H_{12}O_5$.

The IR spectrum (Fig. 3.14) showed characteristic absorption peaks at 3500-3000 cm^{-1} of O-H stretching, 1710 cm^{-1} of C=O stretching, 1630, 1595, 1510 and 1460 cm^{-1} of C=O stretching of aromatic, 900 and 850 cm^{-1} of C-H bending of aromatic.

Followed the data derived from literal review, it was found that comparing the ^{1}H and ^{13}C-NMR spectra of Compound **HS-3** with those previously reported for genkwanin or 4′,5-dihydroxy-7-methoxy flavone (Zahir *et al.*, 1996 and Chang *et. al.*, 1977), Compound **HS-3** was no doubt to be this flavone.

The ^{1}H-NMR spectrum of Compound **HS-3** (Fig. 3.15) indicated the presence of one methoxy (3.85). The remaining signals in the ^{1}H-NMR spectrum indicated the seven aromatic proton at 6.36 (1H, s), 6.76 (1H, s), 6.83 (1H, s), 6.91 (2H, d, J=8.53 Hz) and 7.94 (2H, d, J=8.56 Hz).

The ^{13}C-NMR spectrum (Fig. 3.16) exhibited 16 signals. The signals at 181.4 ppm indicated the presence of a carbonyl group, possibly carbonyl of α,β-unsaturated lectone. In addition, seven methine carbons (129.6, 129.6, 117.2, 117.2, 104.2, 99.2, and 93.7), eight quaternary carbons (181.4, 167.1, 166.0, 162.8, 159.0, 157.4, 122.9 and 106.5) as well as a methoxy carbon (56.7) were detected.

From all spectroscopic data, it could be concluded that this compound was genkwanin. To our best knowledge, this is the first time to report this compound as the constituent in this particular species. The comparison of ^{13}C-NMR signals of genkwanin and Compound **HS-3** was tabulated in Table 3.9.

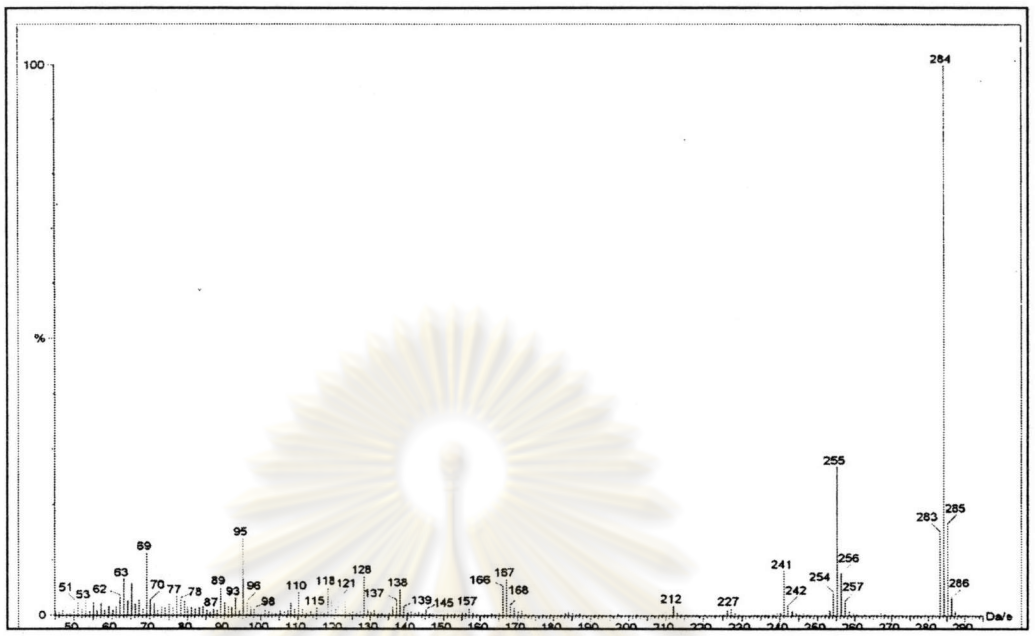

Fig. 3.13 The mass spectrum of Compound **HS-3**

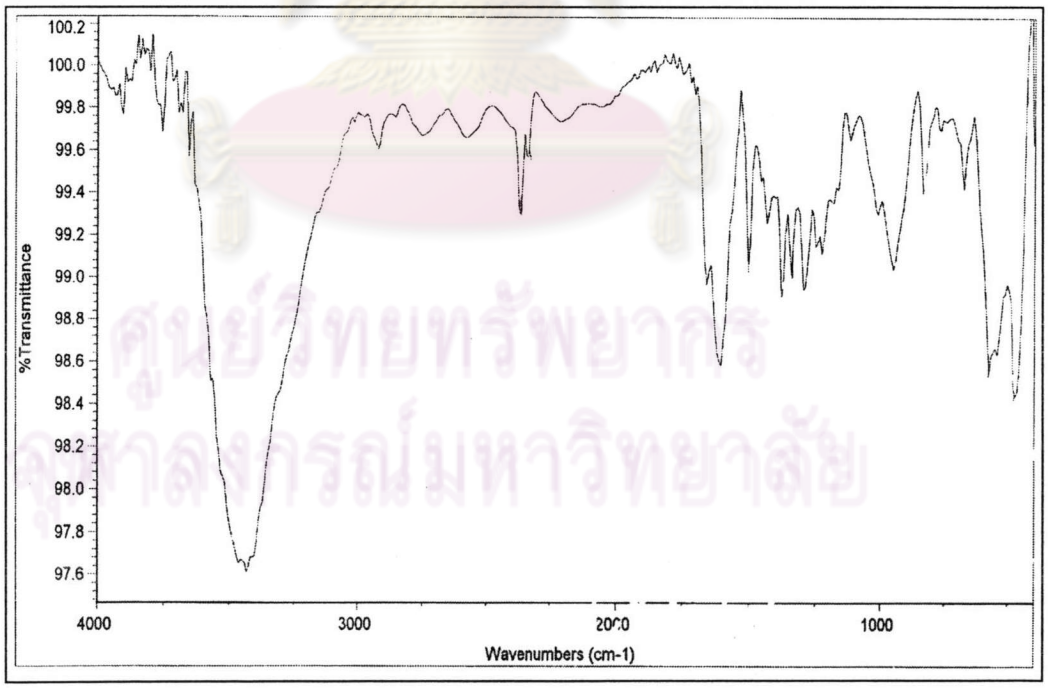

Fig. 3.14 The IR spectrum of Compound **HS-3**

Table 3.9 The ^{13}C-NMR spectral data assignment of genkwanin and Compound **HS-3** (in DMSO-d_6).

Position	Chemical shift (ppm)			
	genkwanin		**HS-3**	
	Carbon	Proton	Carbon	Proton
2	166.0		164.3	
3	104.2	6.82 (1H, s)	103.1	6.83 (1H, s)
4	181.4		182.1	
4a	106.5		105.	
5	159.0		161.3	
6	99.2	6.74 (1H, d, *J*=2.2)	98.1	6.76 (1H, s)
7	167.1		165.3	
8	93.7	6.36 (1H, d, *J*=2.2)	92.8	6.36 (1H, s)
8a	157.4		157.4	
1′	122.9		121.2	
2′	129.6	7.95 (2H, d, *J*=8.9)	128.7	7.93 (2H, d, *J*=8.5)
3′	117.2	6.93 (2H, d, *J*=8.9)	116.1	6.90 (2H, d, *J*=8.5)
4′	162.8		161.5	
5′	117.2	6.93 (2H, d, *J*=8.9)	116.1	6.93 (2H, d, *J*=8.5)
6′	129.6	7.95 (2H, d, *J*=8.9)	128.7	7.95 (2H, d, *J*=8.5)
7′-OMe	56.7	3.87 (3 H, s)	56.2	3.85 (3 H, s)

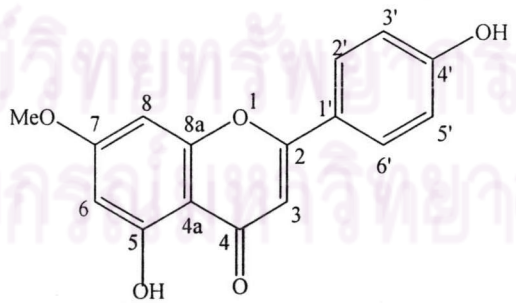

Compound **HS-3** : genkwanin

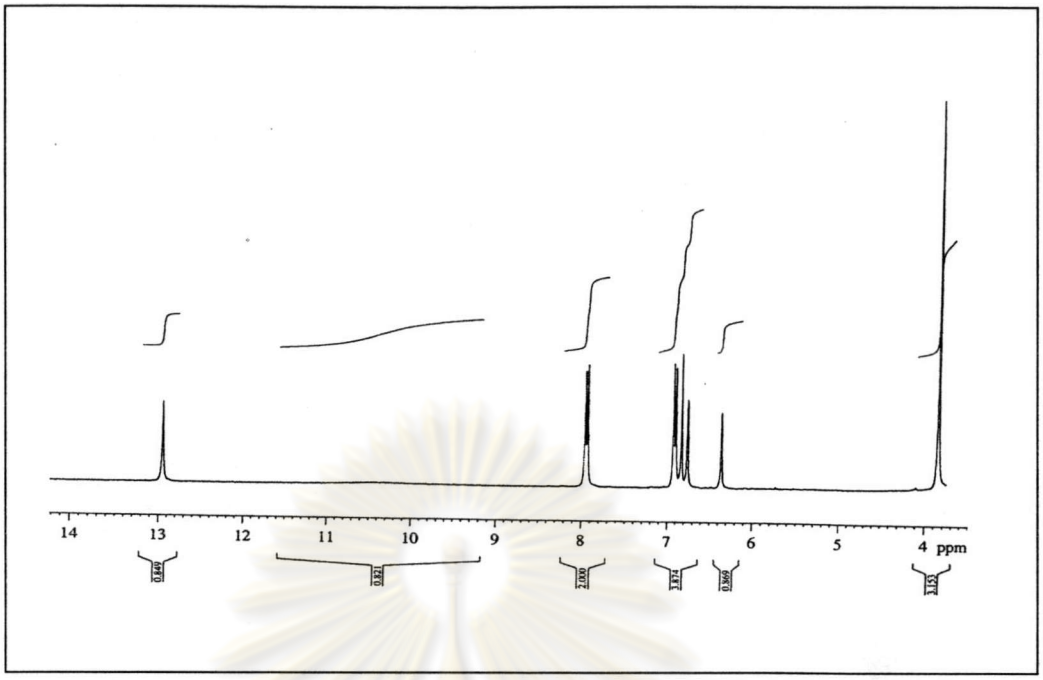

Fig. 3.15 The ^{1}H-NMR spectrum of Compound **HS-3**

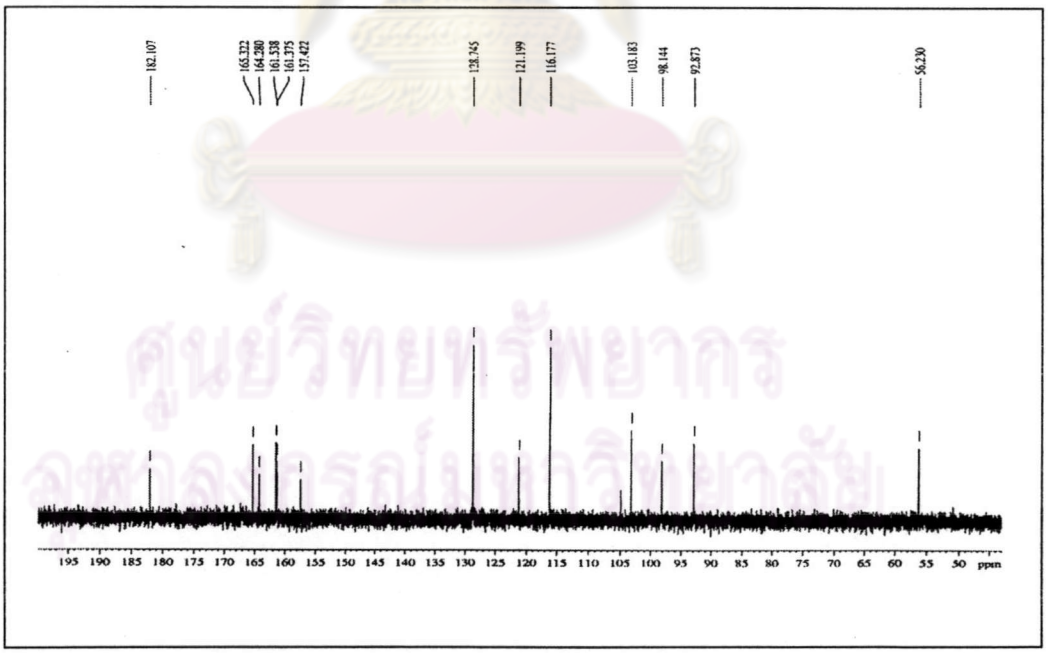

Fig. 3.16 The ^{13}C-NMR spectrum of Compound **HS-3**

3.4.4 Structural Elucidation of Compound HS-4

Compound **HS-4** 14.5 mg was orange viscous oil, obtained from dichloromethane extract.

The presence of a carbonyl group was suggested from the IR spectrum (1685 cm^{-1}) (Fig. 3.17). In addition, there were absorption bands of hydroxyl (3375 cm^{-1}) and furan ring (1028 cm^{-1}). The molecular ion at m/z 126 was observed in EIMS (Fig. 3.18) gave ($C_6H_6O_3$) formula.

The ^{1}H-NMR spectrum (Fig. 3.19) also exhibited signals corresponded to those assigned functional group such as aldehyde and methylene protons resonated at δ 9.50 (1H, s) and 4.70 (2H, s), respectively. The signals of furano protons were detected at δ 6.25 (1H, d, *J*=3.67 Hz) and δ 7.20 (1H, d, *J*=3.35 Hz). Magnitude of coupling constants, 3.35-3.67 Hz, resulted from the coupling of H-3 and H-4. This information implied that this furan should be disubstituted furan, possibly 2,5–disubstituted one (Miltan, 1976. and Nshibe *et. al.*, 1973).

The ^{13}C-NMR spectrum (Fig. 3.20) exhibited the most downfield tertiary carbon at δ 177.6 and a methylene carbon which directly attached to oxygen atom at δ 57.6. There were two substituent groups attached to a furan ring. One was certainly an aldehyde and the other should be a hydroxy methyl group ($HOCH_2$-). The four carbon signals at 109.9, 122.6, 152.3 and 160.3 ppm should belong to a furan skeleton.

Form the comparison of physical properties and all spectroscopic data with an authentic sample (Phuwapraisirisan, 1998.) allowed to assign the structure of Compound **HS-4** as 5-hydroxymethyl furfuraldehyde or 5-HMF.

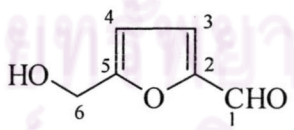

Compound **HS-4** : 5-hydroxy methyl furfuraldehyde

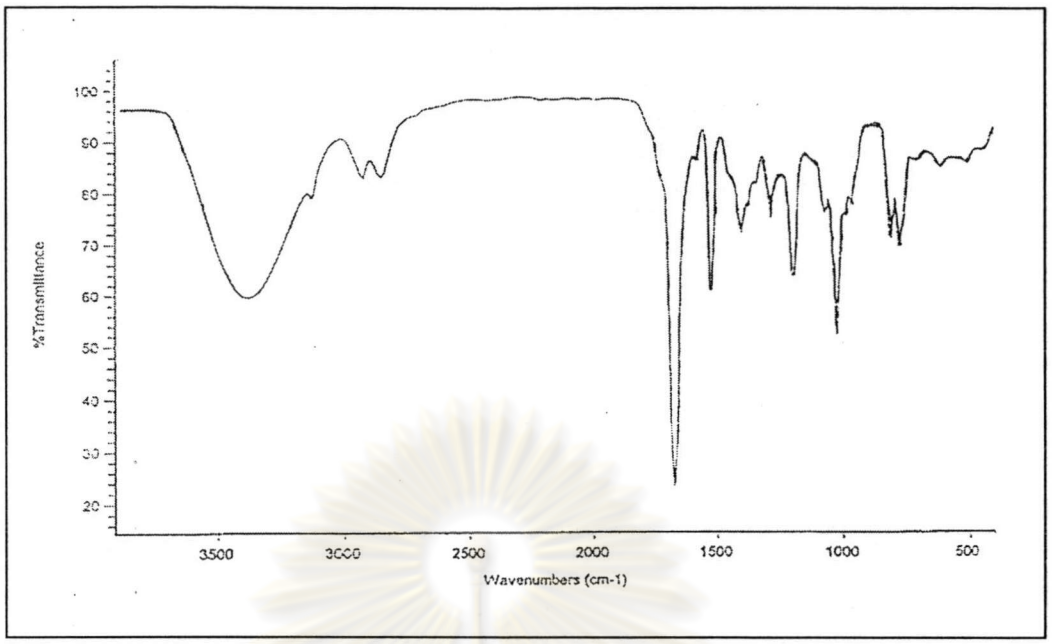

Fig. 3.17 The IR spectrum of Compound **HS-4**

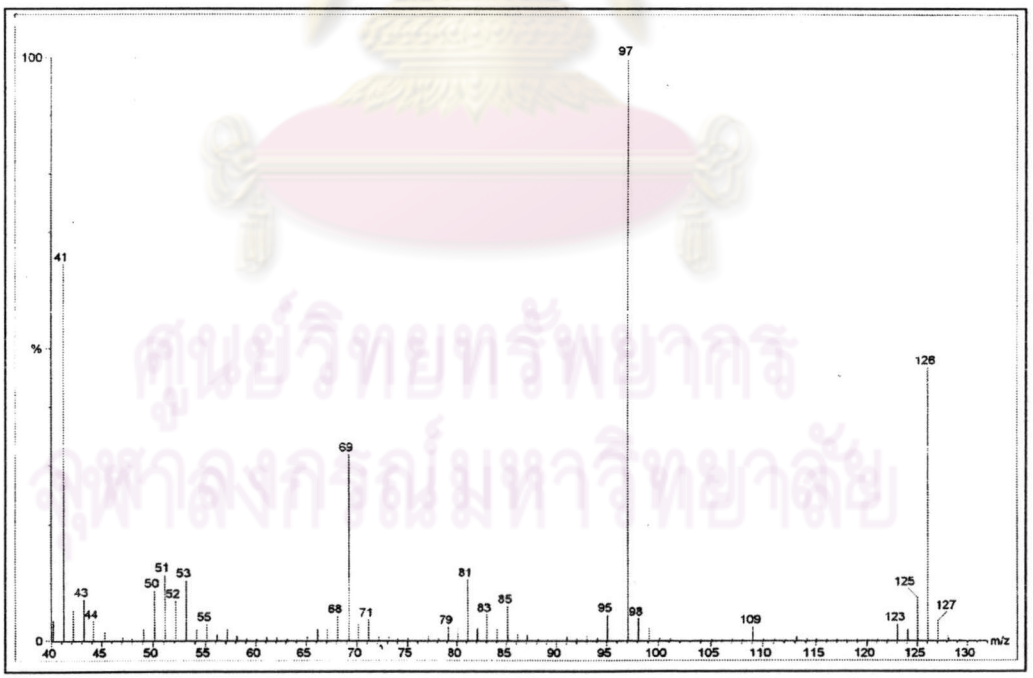

Fig. 3.18 The mass spectrum of Compound **HS-4**

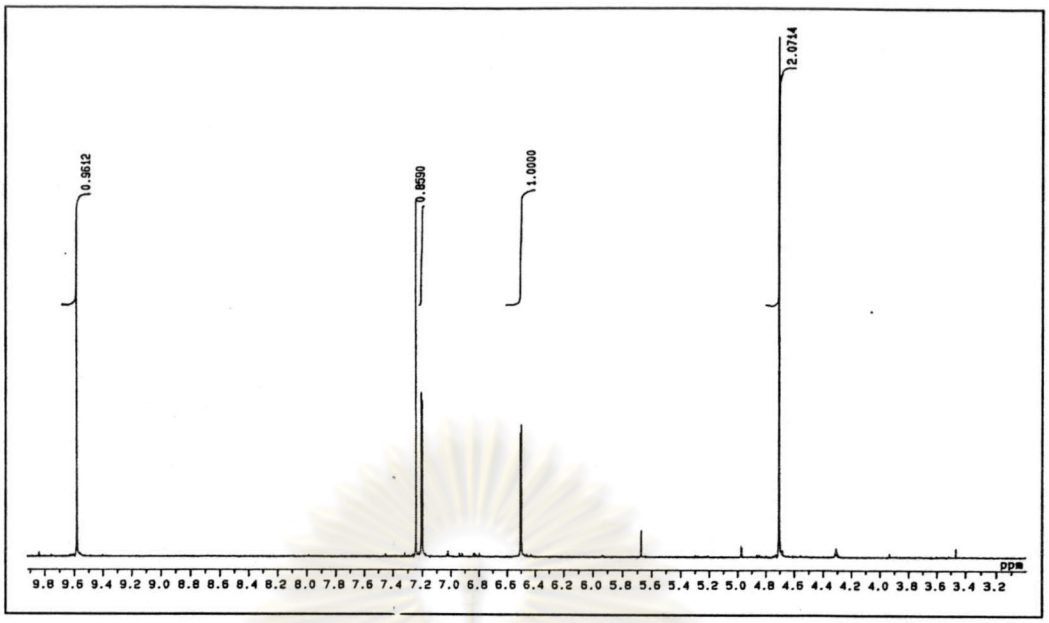

Fig. 3.19 The ^{1}H-NMR spectrum of Compound **HS-4**

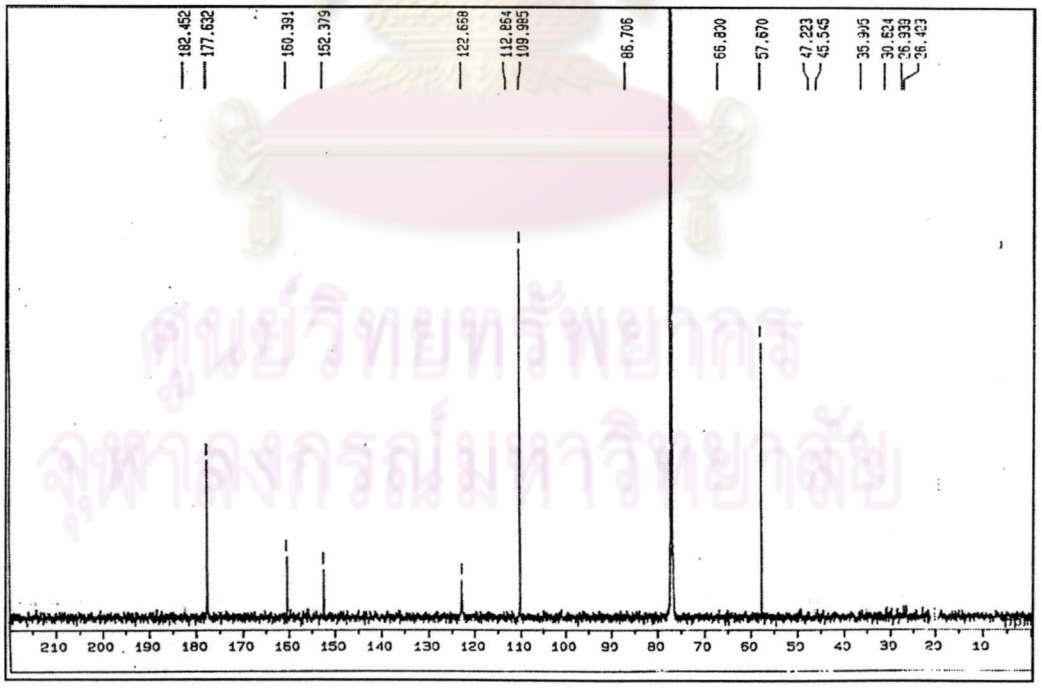

Fig. 3.20 The ^{13}C-NMR spectrum of Compound **HS-4**

3.4.5 Structural Elucidation of Mixture HS-5

Mixture **HS-5** was white amorphous solid, 17.1 mg (0.10% wt/wt of dichloromethane crade extract), mp. 283-285°C, R_f value 0.23 (solvent system: 10% methanol in dichloromethane). This mixture gave positive results (green color) with Liebermann-Burchard's reagent which indicated that it was composed of steroidal skeleton.

The IR-spectrum of Mixture **HS-5** (Fig. 3.21) showed important absorption bawds at 3600-3200 cm^{-1}(O-H stretching vibration of alcohol), 1653 cm^{-1}(C=C stretching vibration of olefin), 1072-1026 cm^{-1}(C-O stretching vibration of OH group of sugar) and 887 cm^{-1}(C-H bending vibration of anomeric axial proton of β-sugar).

The ^{1}H-NMR spectrum of Mixture **HS-5** (Fig. 3.22) showed the signals at 0.63-2.49 ppm, which were the signals of methyl, methylene and methine groups of steroids (-CH_3, -CH_2, -CH respectively). The multiplet signals at 2.85-3.03 ppm were assigned to the protons of a sugar. The proton on carbon attached to sugar (-CH-O-sugar) appeared as the multiplet signal at 3.38 ppm and the signal at 4.18 ppm belonged to the anomeric proton. The multiplet signal at 4.88 ppm was assigned as disubstituted vinyl protons (-CH=CH-). The last signal at 5.32 ppm was the signal of trisubstituted vinyl proton (-CH=C-).

The ^{13}C-NMR spectrum (Fig. 3.23) after the hydrolysis of Mixture **HS-5**, showed carbon signals in the range of 11.6-56.1 ppm which were the signals of CH_3, CH_2, CH of steroid. The olefinic carbon signals were observed at 121.2, 128.5, 138.1 and 140.4 ppm. The ^{13}C-NMR spectrum of aglycone was corresponded to that of a mixture of stigmasterol and β-sitosterol.

The mass spectrum (Fig. 3.24) exhibited the molecular ion peak of stigmasterol, and β-sitosterol at m/z 412 ($C_{29}H_{48}O$), and 414 ($C_{29}H_{50}O$), respectively. The mass fragmentation ion pattern of this mixture indicated that it was a mixture of steroids.

For the glycone part, co-TLC profile with authentic sugar was denoted that the glycone of the Mixture **HS-5** consisted of glucose.

All above data of ^{1}H-NMR, ^{13}C-NMR, EIMS spectra, co-TLC profile and a literature search indicated that Mixture **HS-5** was a mixture of steroidal glycoside; stigmasteryl-3-*O*-β-D-glucopyranoside and β-sitosteryl-3-*O*-β-D-glucopyranoside. Their structures were shown in Table 3.10.

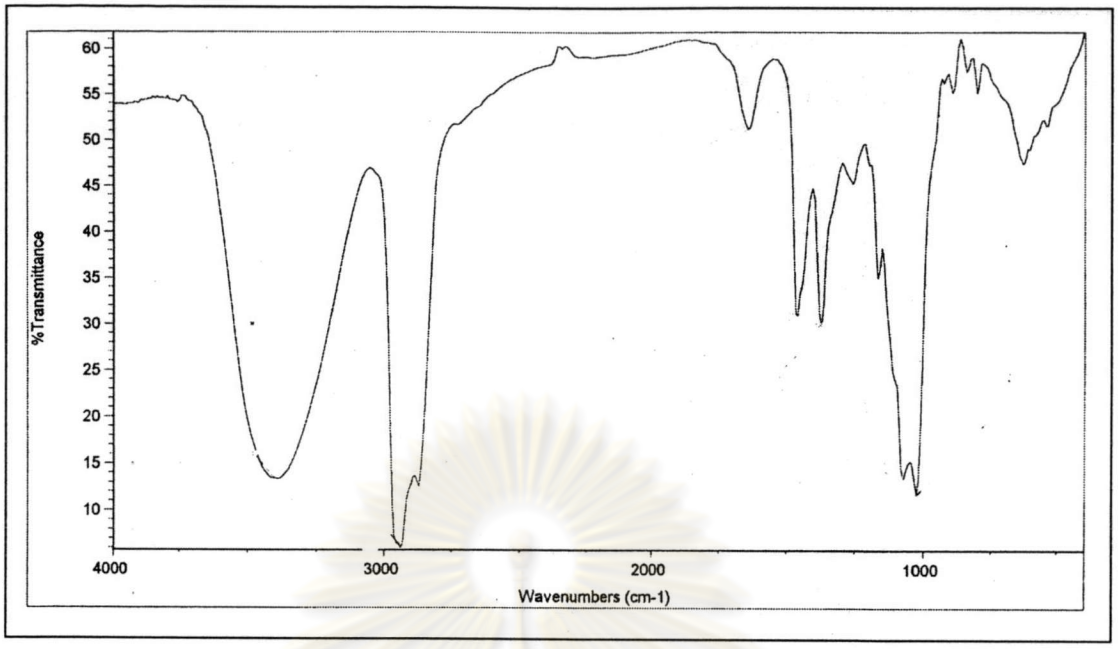

Fig. 3.21 The IR spectrum of Mixture **HS-5**

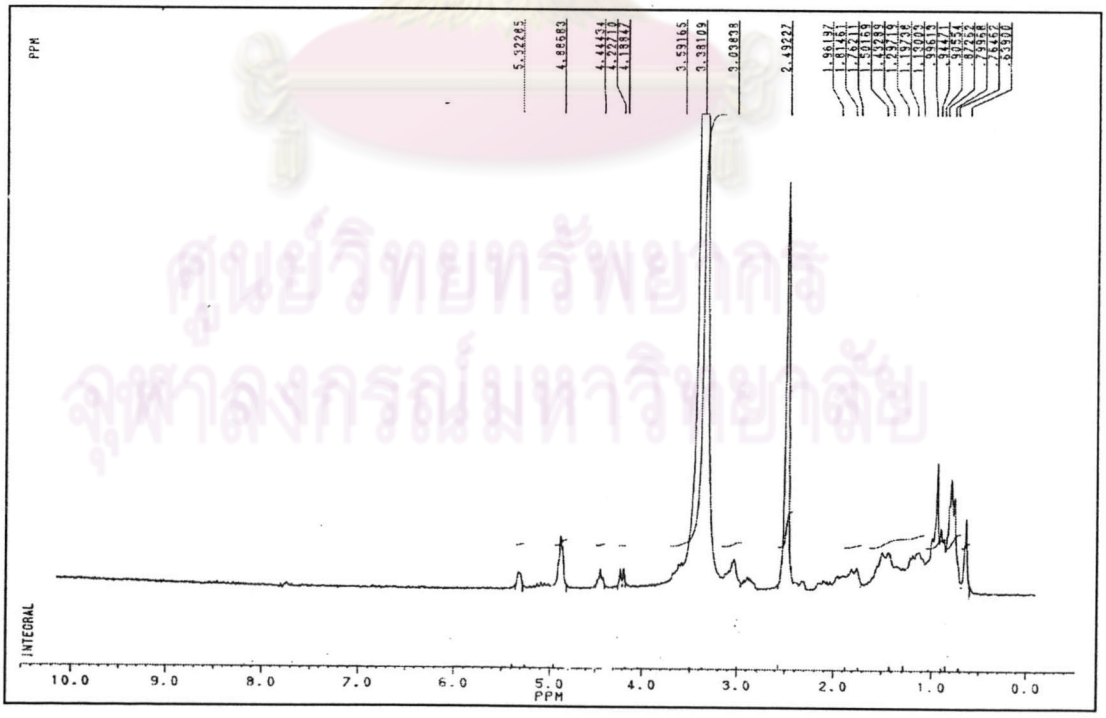

Fig. 3.22 The ^{1}H-NMR spectrum of Mixture **HS-5**

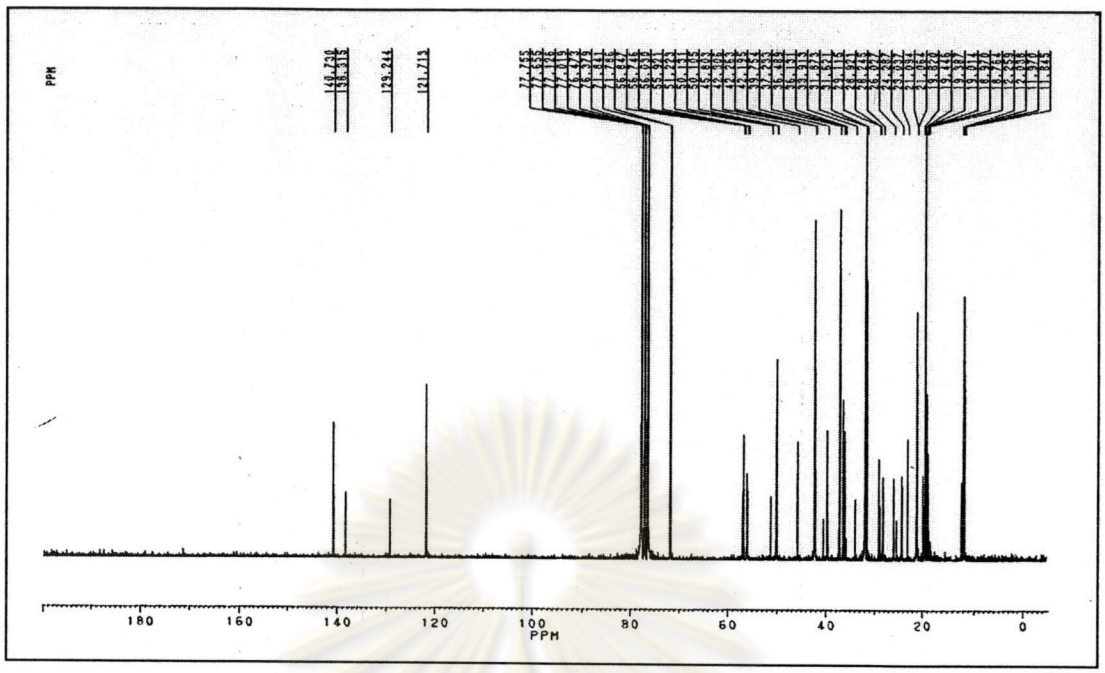

Fig. 3.23 The ^{13}C-NMR spectrum of Mixture **HS-5**

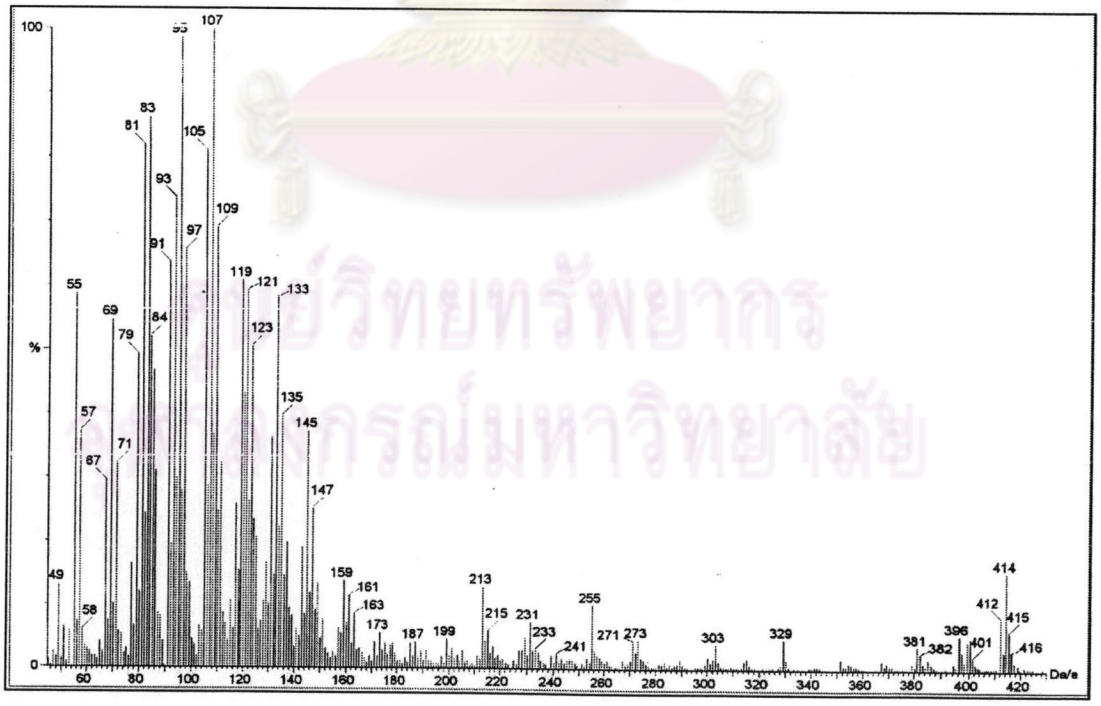

Fig. 3.24 The mass spectrum of Mixture **HS-5**

Table 3.10 Structure of steroidal glucoside in Mixture **HS-5**.

steroid glycoside compound	Structure
β-sitosteryl-3-*O*-β-D-glucopyranoside	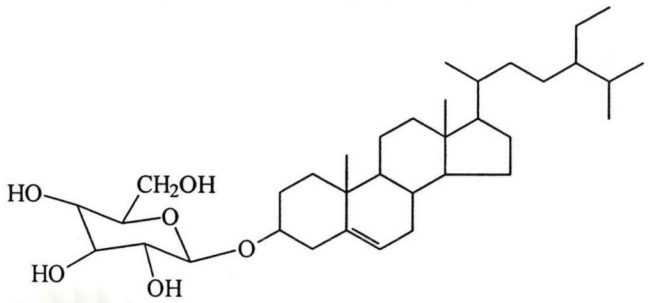
Stigmasteryl-3-*O*-β-D-glucopyranoside	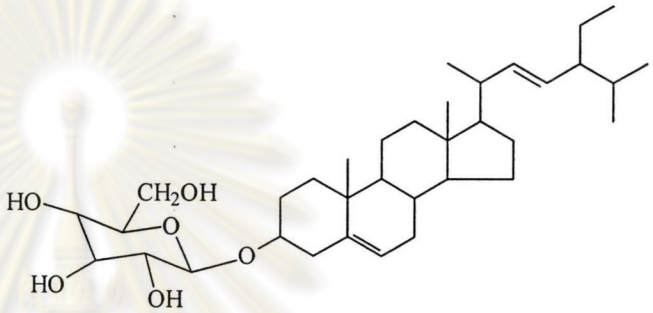

3.4.6 Structural Elucidation of Mixture HS-6

Mixture **HS-6** (51.6 mg, 0.022% w/w of dichloromethane extract) was isolated from dichloromethane crude extract. After recrystallization with methanol a solid of melting point 122-124 °C was gained. This mixture gave a pink-red color with Libermann-Burchard reagent, which implied the presence of a triterpenoidal structure.

EIMS spectrum (Fig. 3.25) gave the parent ion peak M^+, at m/z 448. The important fragmentation pattern was observed at m/z 95 (100), 55 (90), 149 (80), 412 (40) and 430 (47).

The IR-spectrum of Mixture **HS-6** (Fig. 3.26) of this mixture showed characteristic absorption peaks at 3600-3200 cm^{-1}(O-H stretching vibration of alcohol), 2970-2850 cm^{-1} of C-H stretching vibration of CH_2 and CH_3, 1480-1376 cm^{-1} of C-H bending of CH_2 and CH_3.

The ^{1}H-NMR spectrum of Mixture **HS-6** (Fig. 3.27) exhibited the olefinic protons at δ 4.95-5.17 ppm, and methyl protons at δ 0.64-1.25 ppm. The signal at δ 5.35 ppm was assigned to O-H.

The ^{13}C-NMR spectrum (Fig. 3.28) signals showed 48 carbon signals with four olefinic carbons at δ 140.8, 138.3, 129.3 and 121.7 ppm. The carbon signals at δ 71.8 ppm inferred the carbon attached to a hydroxy group. Other signals around 10 to 60 ppm should be methyl, methylene and methine carbons.

From the GC chromatogram (Fig. 3.29) of **HS-6**, there were two major peaks observed. Thus, **HS-6** contained at least two components.

From all spectroscopic data, one compound existed in this mixture was proposed to be a hydroxy triterpenoid with two double bonds in the skeleton.

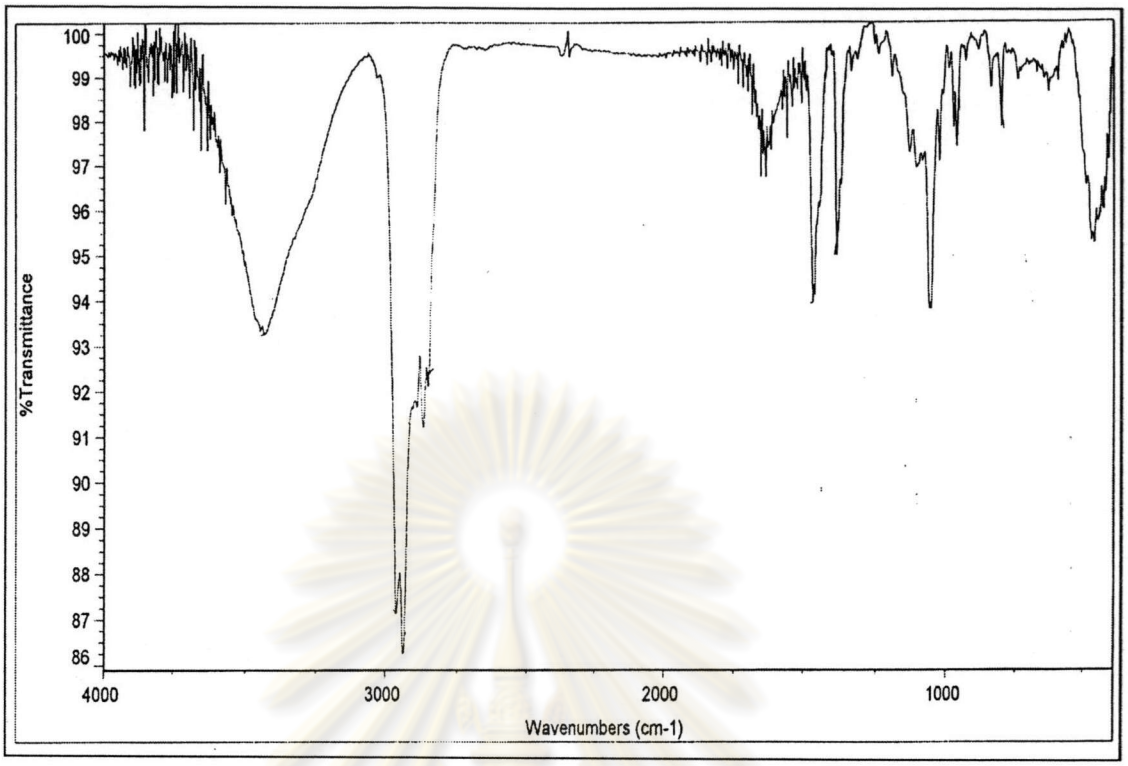

Fig. 3.25 The IR spectrum of Mixture **HS-6**

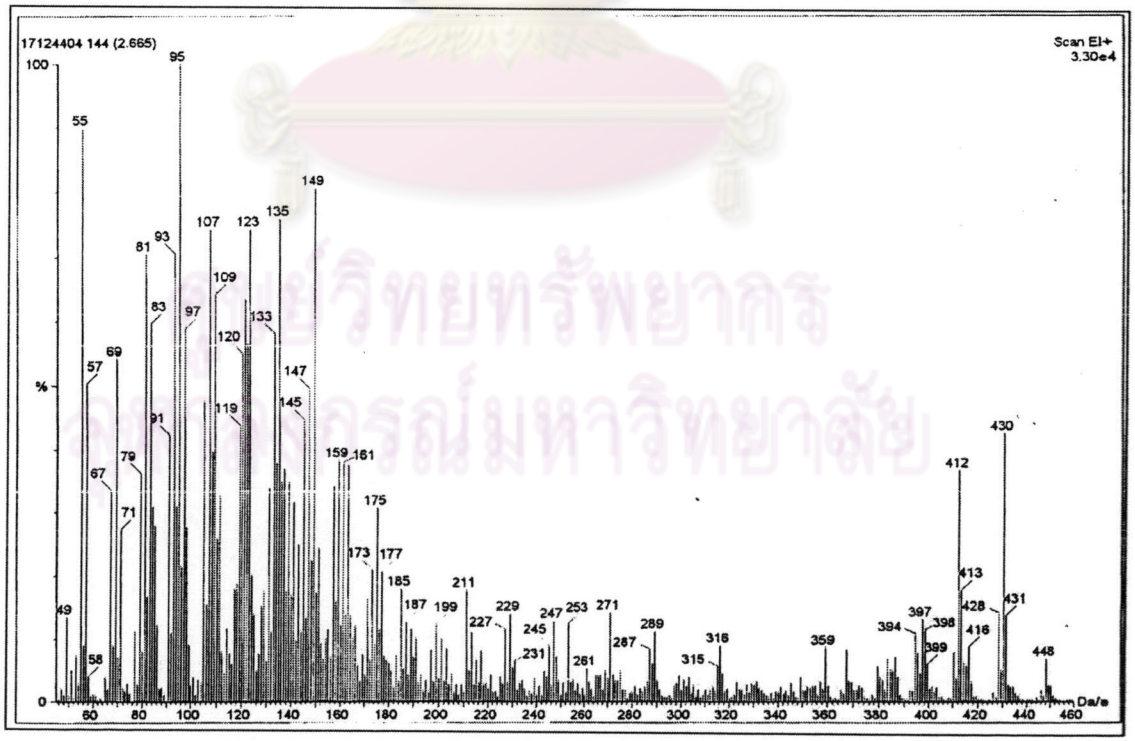

Fig. 3.26 The mass spectrum of Mixture **HS-6**

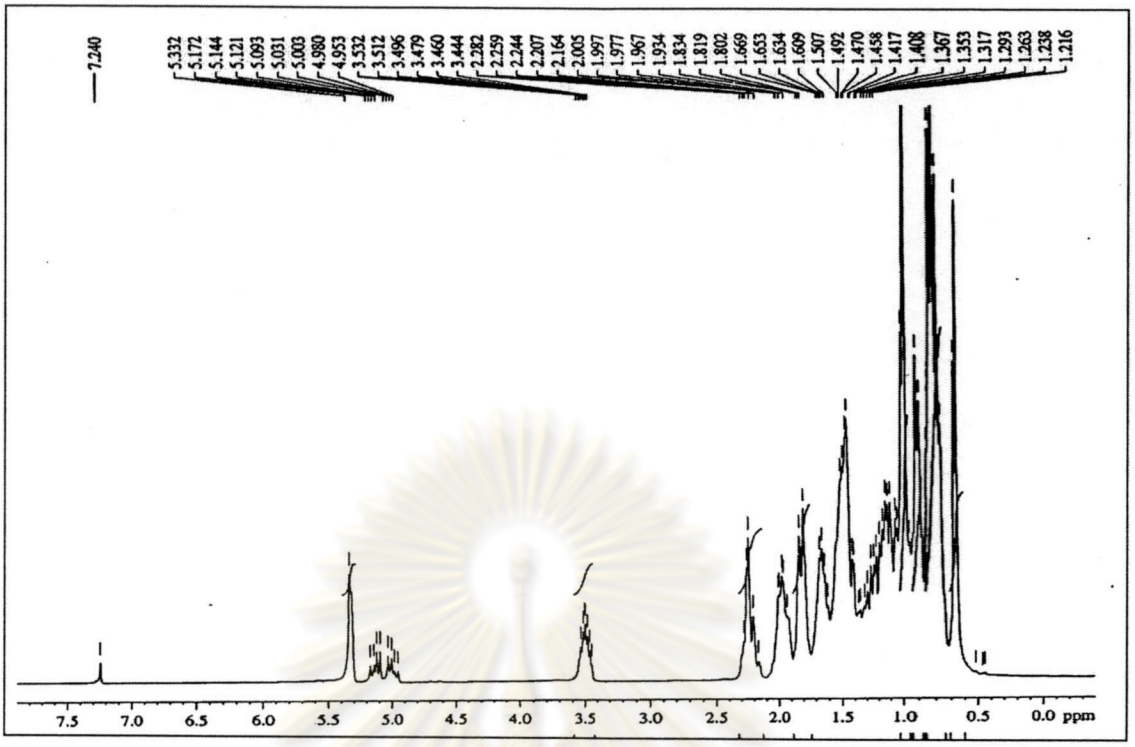

Fig. 3.27 The ^{1}H-NMR spectrum of Mixture **HS-6**

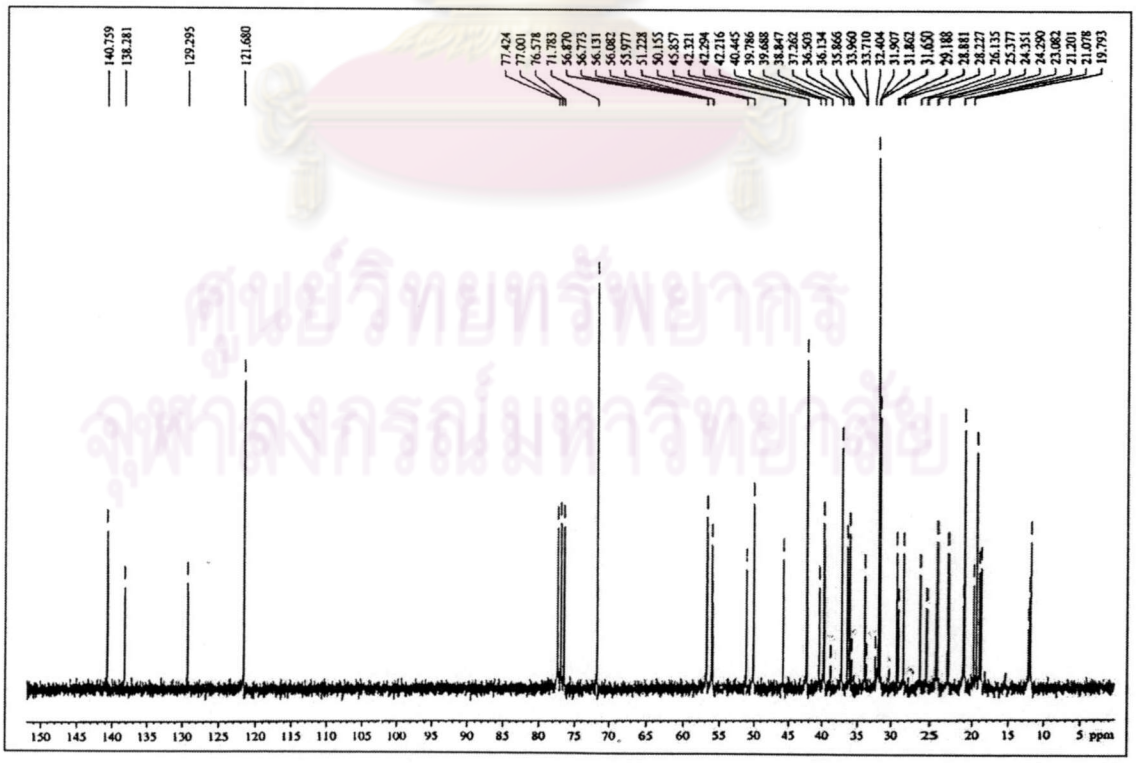

Fig. 3.28 The ^{13}C-NMR spectrum of Mixture **HS-6**

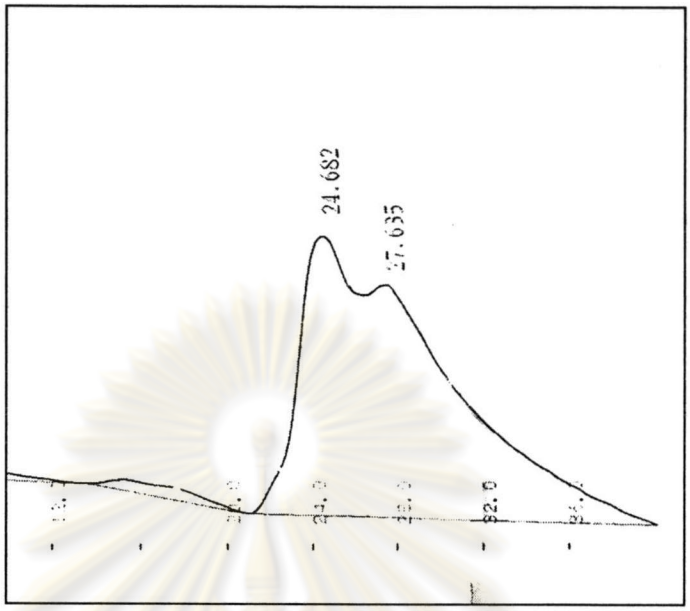

Fig. 3.29 The GC spectrum of Mixture **HS-6**

3.4.7 Structural Elucidation of Mixture HS-7

Mixture **HS-7** (17.5 mg, 0.007 % w/w of dichloromethane extract) was white amorphous solid, melting point 62-65°C with R_f value 0.68 (15% dichloromethane in hexane).

The IR spectrum (Fig. 3.30) exhibited the characteristic absorption peaks at 3452 cm^{-1}(OH stretching of hydroxyl group), 2914 and 2842 cm^{-1}(C-H stretching of CH_2, CH_3) and 1465 cm^{-1} (C-H asymmetric bonding of CH_2, CH_3).

From the comparison of physical properties and all spectroscopic data with an authentic sample of a mixture of long chain alcohols. Mixture **HS-7** should be a mixture of long chain alcohol.

CH_3-$(CH_2)_n$-CH_2-OH

Mixture **HS-7**: Mixture of long chain alcohol

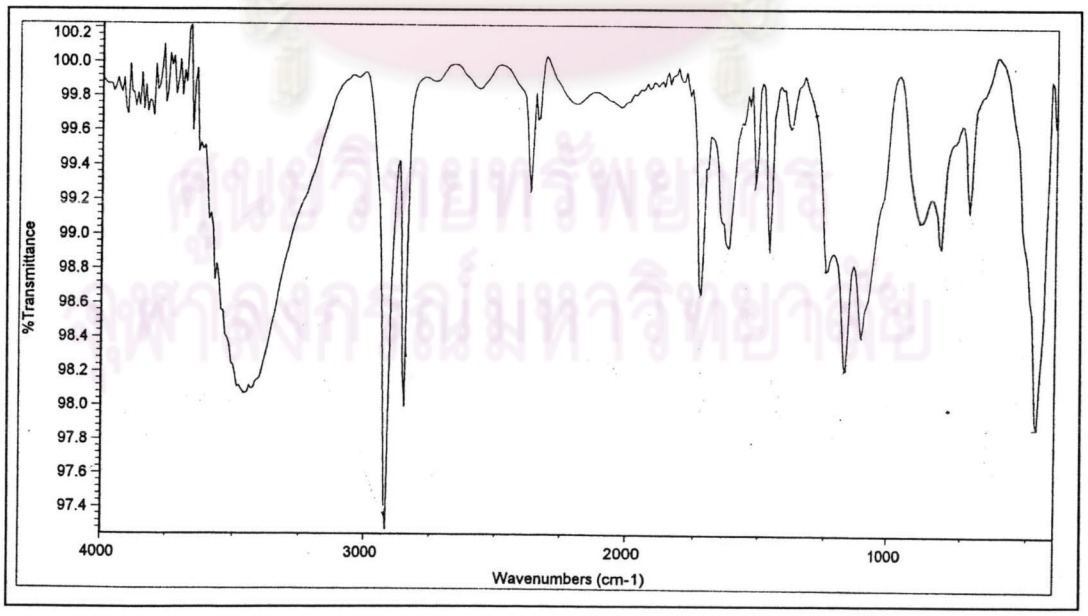

Fig. 3.30 The IR spectrum of Mixture **HS-7**

3.4.8 Structural Elucidation of Compound HS-8

Mixture **HS-8** as white amorphous solid, melting point 65-70 °C, (82.7 mg, 0.035 % w/w of dichloromethane extract) was obtained.

The IR spectrum (Fig. 3.31) showed characteristic absorption peaks at 2914, 2858 cm^{-1} (C-H stretching of CH_2, CH_3), 1736 cm^{-1}(C=O stretching), 1465 cm^{-1}(C-H bending vibration of $-CH_3$, $-CH_2-$).

The IR spectrum clearly supported that this mixture should be a mixture of long chain esters.

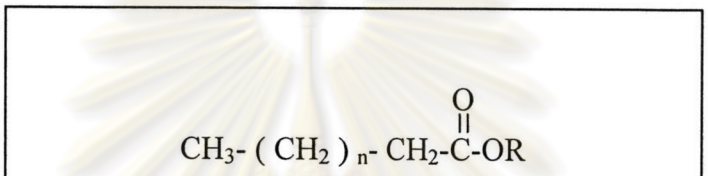

Mixture **HS-8** : Mixture of long chain ester

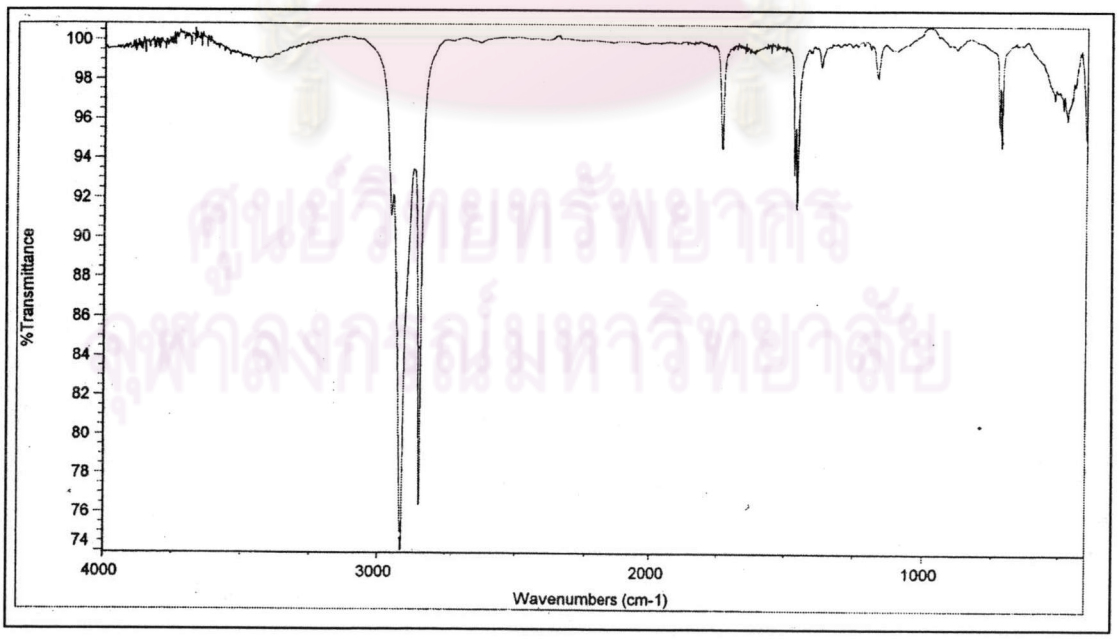

Fig. 3.31 The IR spectrum of Mixture **HS-8**

3.4.9 Structural Elucidation of Compound HS-9

Compound **HS-9** as white crystal was isolated from hexane extract. After recrystallization with acetone several times, the product with melting point 195-197 °C, 184.9 mg (0.15 % w/w of hexane extract) was achieved. This compound gave a violet color with Liebermann-Burchard's reagent which suggested the presence of triterpenoid skeleton.

The IR spectrum (Fig. 3.32) displayed a broad band in the range of 3400-3500 cm^{-1} belonging to O-H stretching and the absorption peak of C-O stretching vibration at 1035 cm^{-1}. The additional bands of trisubstituted olefinic moiety were also observed at 1634 and 815 cm^{-1}.

The molecular formula of Compound **HS-9** was proposed to be $C_{30}H_{50}O$ (MW. 426). This formula was supported by mass spectrum data.

The mass spectrum (Fig. 3.33) gave the parent ion peak M^+, at m/z 426. Other important fragmentation peaks at m/z 218 (100), 203 (36) and 219 (18) strongly pointed out that Compound **HS-9** was a member of either α-amyrin or β-amyrin series.

The ^{1}H-NMR spectrum of Compound **HS-9** (Fig. 3.34) exhibited methylene and methine proton signals at 0.6-2.1 ppm.

The ^{13}C-NMR spectrum (Fig. 3.35) displayed two olefinic carbons at 145.2 and 121.7 ppm. The signal at 79.0 ppm could be assigned for the carbon signal adjacent to oxygen atom. The other signals around 55.1-15.4 ppm were compatible with methyl, methylne, methine and quarternary carbons. The comparison of ^{13}C-NMR chemical shifts of Compound **HS-9** and those of β-amyrin was conducted and found that chemical shifts of Compound **HS-9** were well-coincided with those of β-amyrin (Mahato and Kundu, 1994). Its structure is shown below.

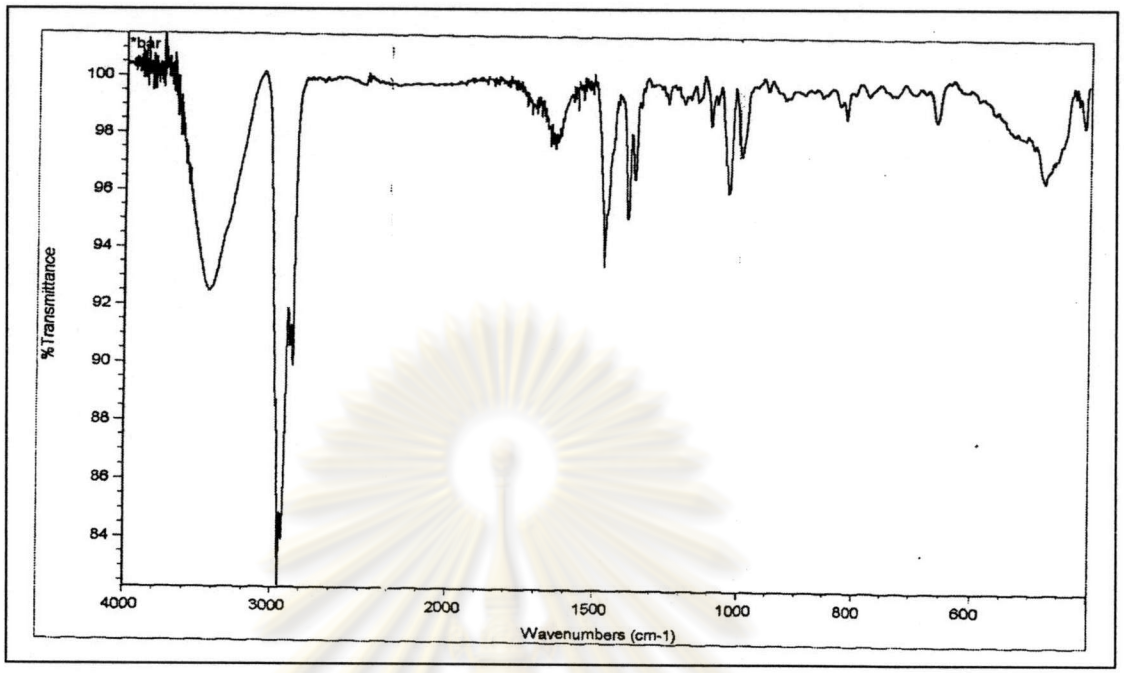

Fig. 3.32 The IR spectrum of Compound **HS-9**

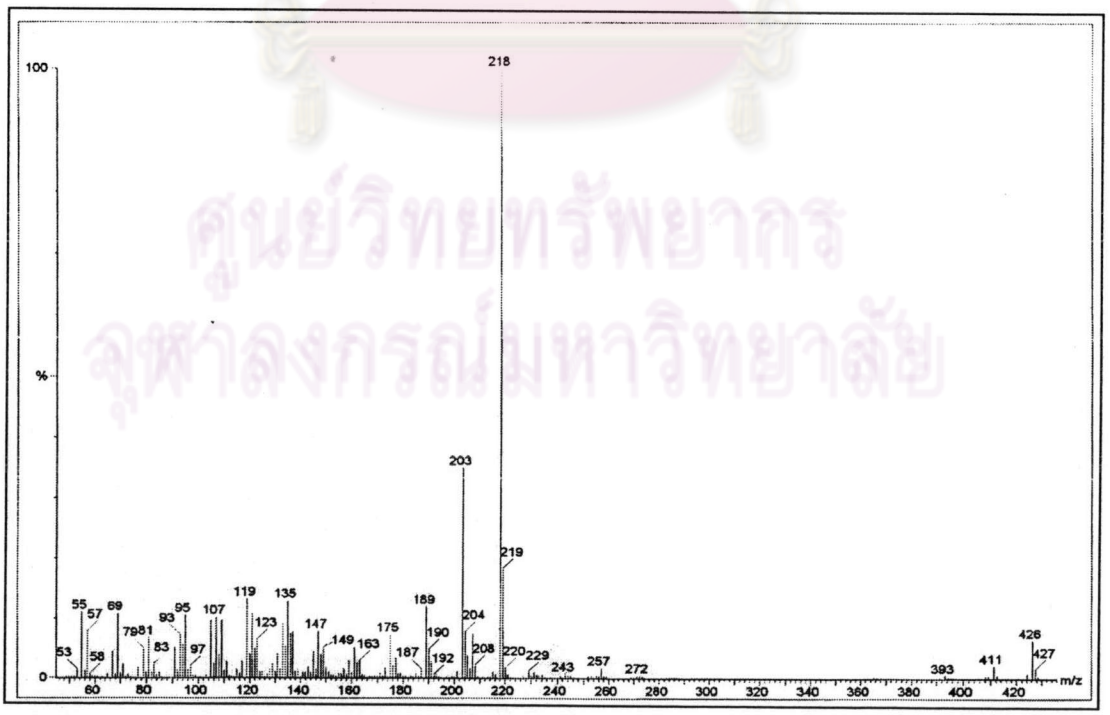

Fig. 3.33 The mass spectrum of Compound **HS-9**

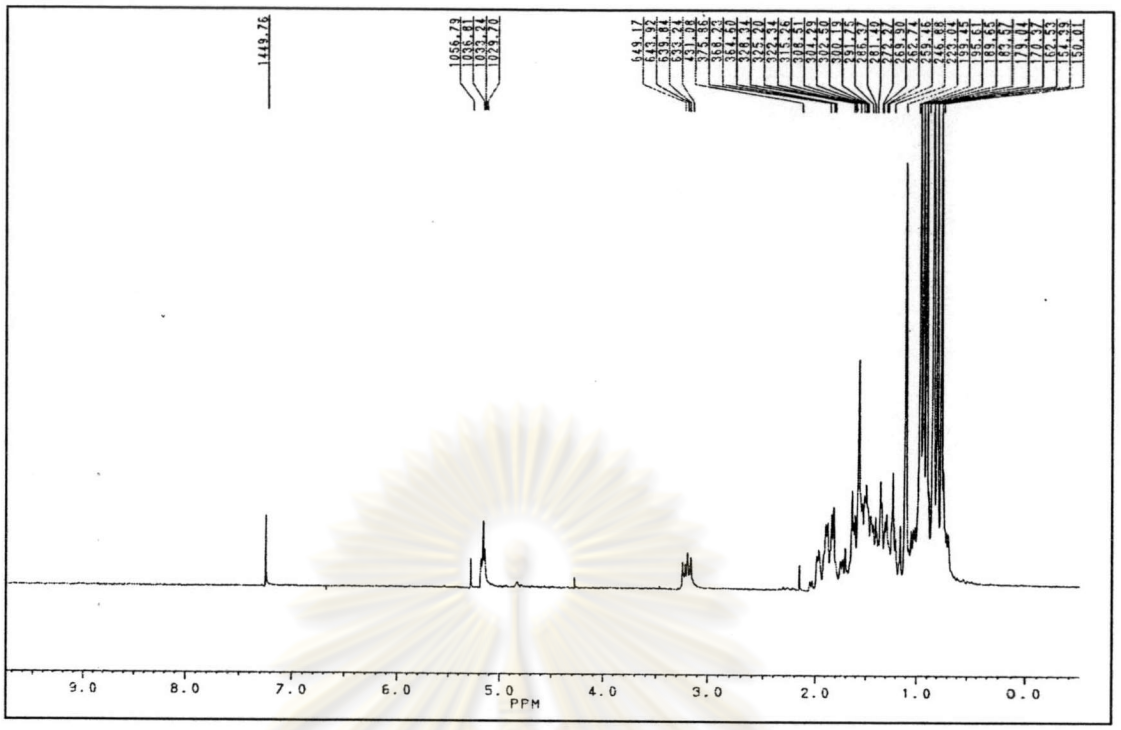

Fig. 3.34 The ^{1}H-NMR spectrum of Compound **HS-9**

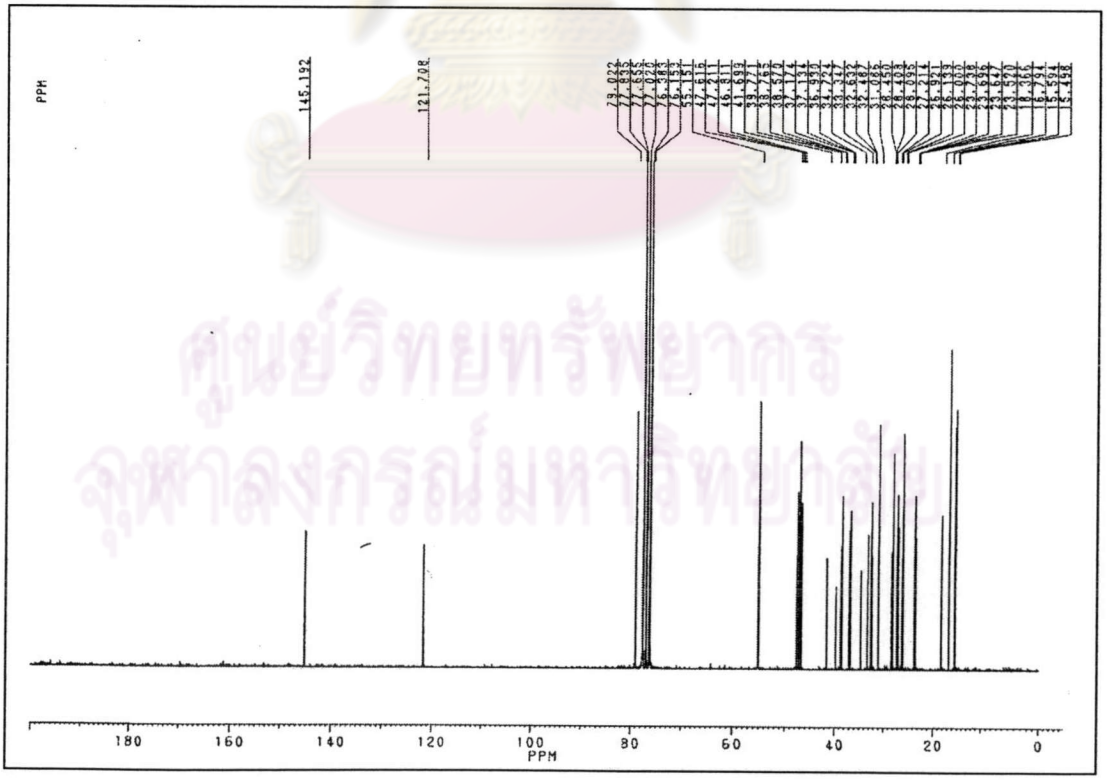

Fig. 3.35 The ^{13}C-NMR spectrum of Compound **HS-9**

Table 3.11. The ^{13}C-NMR chemical shift assignment of β-amyrin and Compound **HS-9** (in $CDCl_3$)

Carbon	Chemical shift (ppm)		Carbon	Chemical shift (ppm)	
	β-amyrin	**HS-9**		β-amyrin	**HS-9**
1	38.5	38.5	16	26.2	26.1
2	27.0	26.9	17	32.5	32.4
3	78.9	79.0	18	47.2	47.2
4	38.7	38.7	19	46.8	46.8
5	55.1	55.1	20	31.1	31.0
6	18.3	18.3	21	34.8	34.7
7	32.6	32.6	22	37.2	37.1
8	39.7	39.7	23	28.1	28.0
9	47.6	47.6	24	15.5	15.4
10	37.1	37.1	25	15.5	15.5
11	23.4	23.5	26	16.8	16.7
12	121.7	121.7	27	26.1	25.9
13	145.2	145.1	28	27.3	27.3
14	41.7	41.6	29	33.2	33.3
15	28.3	28.4	30	23.6	23.6

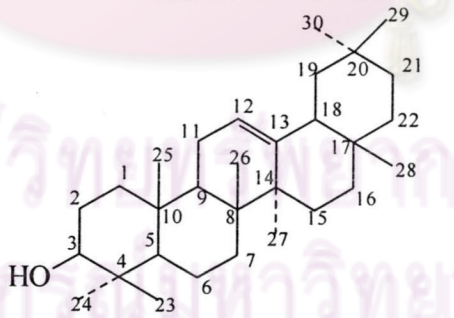

Compound **HS-9** : *β*-amyrin

3.4.5 Structural Elucidation of Compound HS-10

Compound **HS-10** as white crystal was isolated from hexane extract. After recrystallization with acetone several times, the product with melting point 186-188 °C, 24.4 mg (0.017 % w/w of hexane extract) was obtained.

This compound gave a violet color with Liebermann-Burchard's reagent which suggested the presence of triterpenoid skeleton.

The IR spectrum (Fig. 3.36) displayed a broad band in the range of 3400-3500 cm^{-1} belonging to O-H stretching and the absorption peak of C-O stretching vibration at 1035 cm^{-1}. The additional bands of trisubstituted olefinic moiety were also observed at 1634 and 815 cm^{-1}.

The molecular formula of Compound **HS-10** was proposed to be $C_{30}H_{50}O$ (MW. 426). This formula was supported by the mass spectral data.

The mass spectrum (Fig. 3.37) gave the parent ion peak M^+, at m/z 426. The important fragmentation pattern at m/z 218 (100), 95 (54), 69 (48) and 203 (41) strongly pointed out that Compound **HS-10** was of α-amyrin.

The ^{1}H-NMR spectrum of Compound **HS-10** (Fig. 3.38) exhibited methylene and methine proton signals at 0.6-2.1 ppm.

The ^{13}C-NMR spectrum (Fig. 3.39) displayed two olefinic carbons at 139.5 and 124.4 ppm. The signal at 79.0 ppm could be assigned for the carbon signal adjacent to oxygen atom. Other signals around 55.1-15.4 ppm were compatible with methyl, methylene, methine and quaternary carbons. The comparison of the ^{13}C-NMR chemical shifts of Compound **HS-10** and the of α-amyrin was presented in Table 3.12 (Seo, Tomita and Tori, 1974).

Table 3.12. The ^{13}C-NMR chemical shift assignment of *a*-amyrin and Compound **HS-10** (in $CDCl_3$)

Carbon	Chemical shift (ppm)		Carbon	Chemical shift (ppm)	
	a-amyrin	**HS-10**		*a*-amyrin	**HS-10**
1	38.7	38.71	16	26.6	26.6
2	27.2	27.2	17	33.7	33.7
3	78.8	79.0	18	58.9	59.0
4	38.7	38.6	19	39.6	39.6
5	55.2	52.2	20	39.6	39.6
6	18.3	18.3	21	31.2	31.2
7	32.9	32.9	22	41.5	41.5
8	40.0	39.9	23	28.1	28.1
9	47.7	47.7	24	15.6	15.6
10	36.9	36.9	25	15.6	15.6
11	17.4	17.4	26	16.8	16.8
12	124.3	124.4	27	23.3	23.3
13	139.3	139.5	28	28.1	28.1
14	42.0	42.0	29	23.3	33.2
15	28.7	28.7	30	21.3	21.3

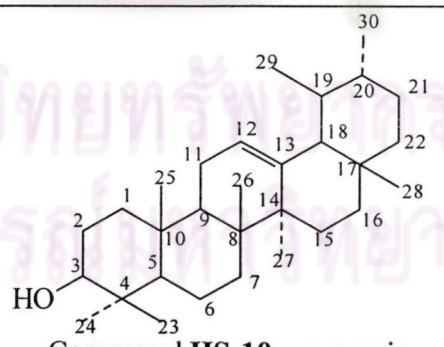

Compound **HS-10** : *α*-amyrin

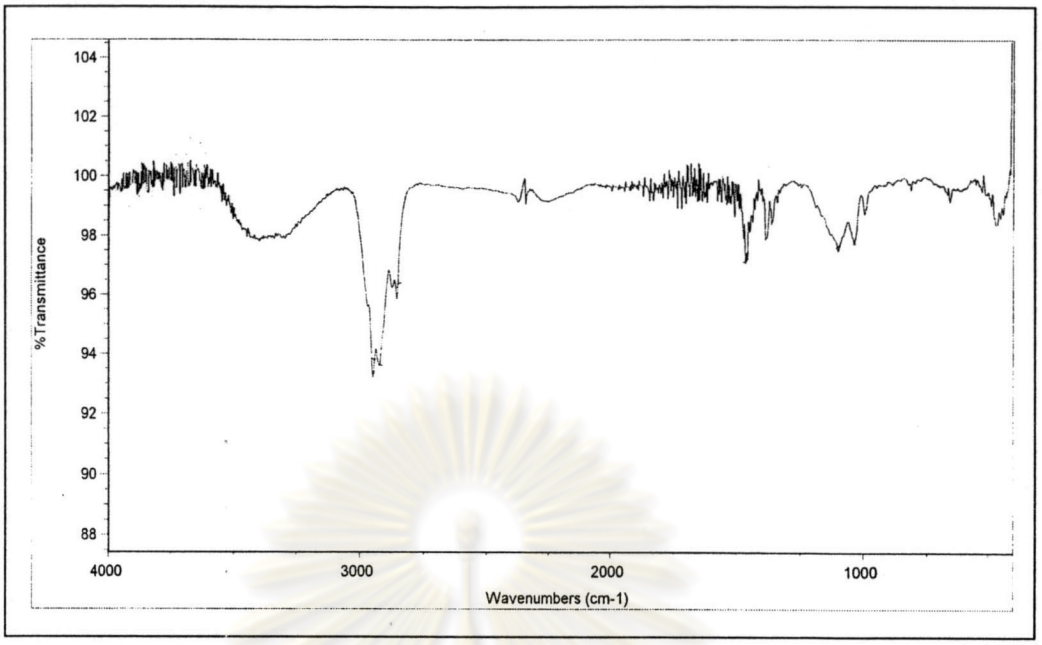

Fig. 3.36 The IR spectrum of Compound **HS-10**

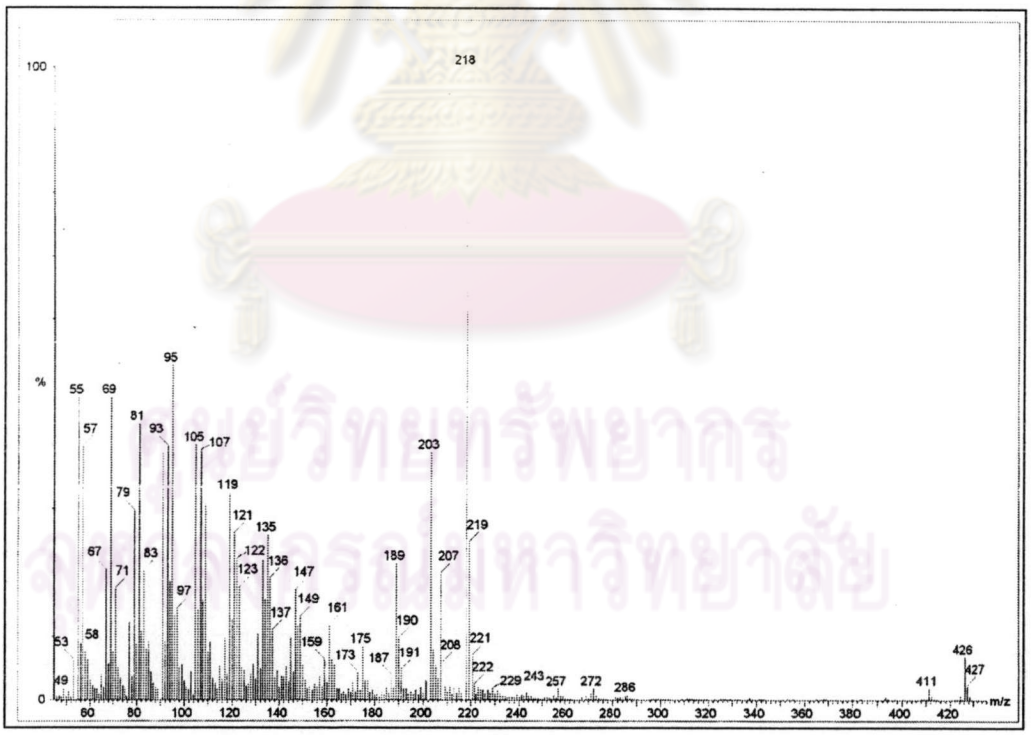

Fig. 3.37 The mass spectrum of Compound **HS-10**

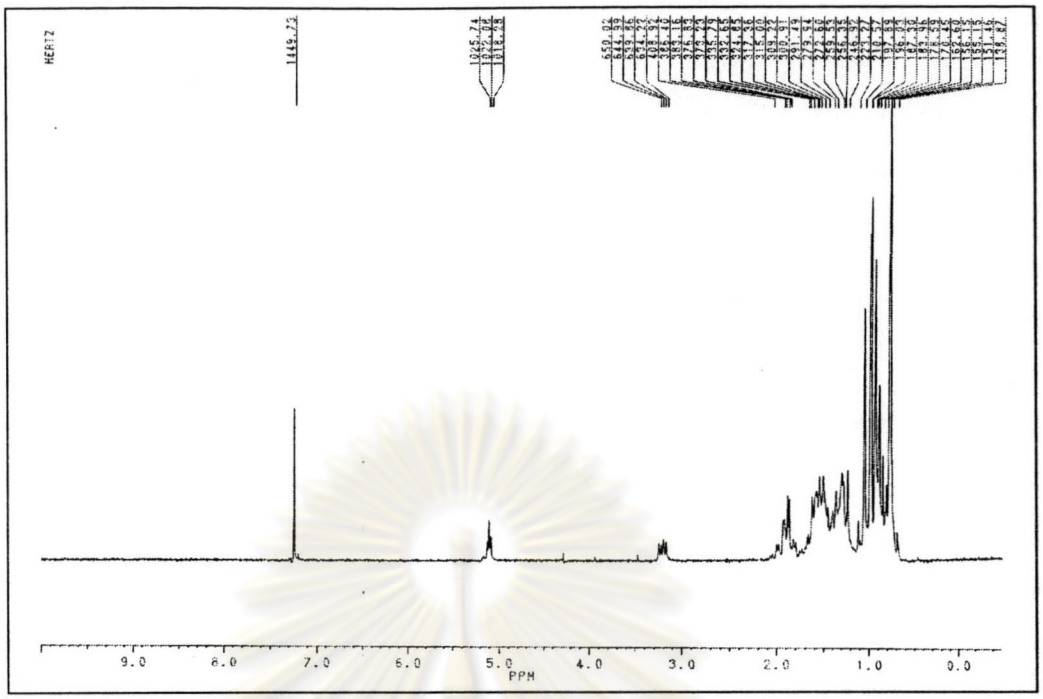

Fig. 3.38 The ^{1}H-NMR spectrum of Compound **HS-10**

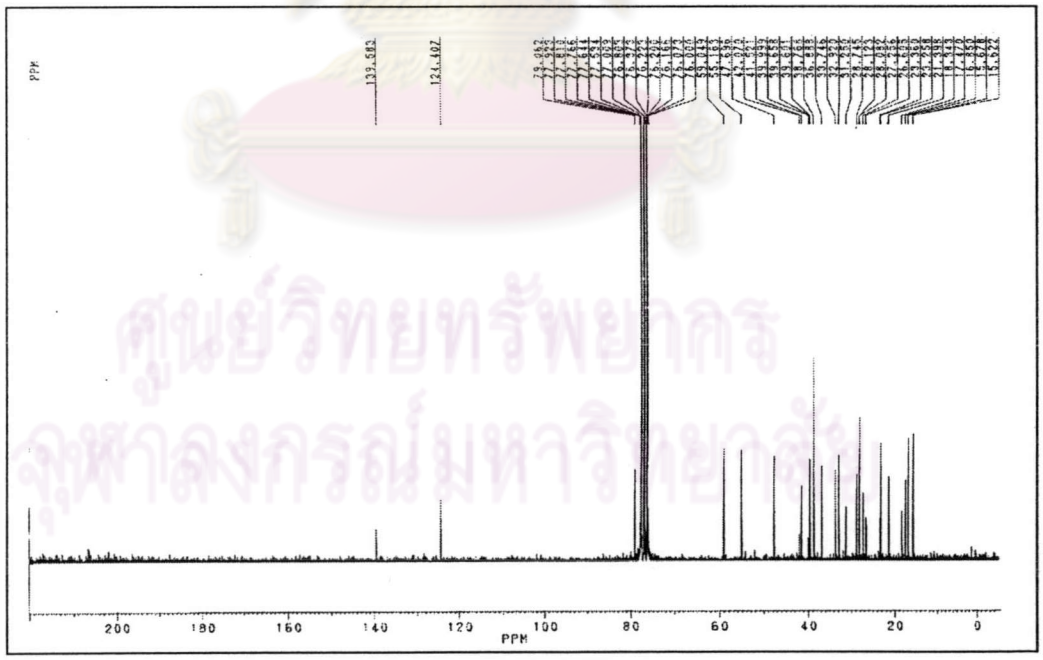

Fig. 3.39 The ^{13}C-NMR spectrum of Compound **HS-10**

3.4.6 Structural Elucidation of Compound HS-11

Compound HS 11 was obtained as colorless needles (42.7 mg, 0.018 % w/w of dichloromethane extract), m.p. 215°C. This compound gave a violet color with Liebermann-Burchard's reagent, suggesting the presence of a triterpenoid nucleus. The EIMS spectrum of Compound **HS-11** (Fig. 3.40) displayed the molecular ion [M^+] at m/z 426, corresponding to $C_{30}H_{50}O$.

The IR spectrum (Fig. 3.41) revealed the absorption bands at 3350 (O-H stretching), 2944 and 2872 (C-H stretching), 1641 (C=C stretching), 1455 and 1382 (C-H bending) and 1042 (C-O stretching).

The ^{1}H-NMR spectrum of Compound **HS-11** (Fig. 3.42) showed seven methyl signals at δ 0.73-1.65 ppm, which could be assigned comparison to lupeol (Mahato and Kundu, 1994) as shown in Table 3.13. The signals at δ 1.05-2.00 were the signal of methylene and methine protons. The signal at δ 3.15 (2H, dd, J = 5.10, 10.50 Hz) could be assigned to H-3 whereas the resonance at δ 2.37 (m) could be assigned to H-19. The signals at 4.54 (br, s) and δ 4.66 (br, s) could be assigned to H-29 (2H).

Table 3.13 The ^{1}H NMR chemical shift assignments of Compound **HS-11** and lupeol (in $CDCl_3$)

Position	δ_H (ppm)	
	lupeol	**HS-11**
H-23	0.98	0.94
H-24	0.77	0.73
H-25	0.84	0.80
H-26	1.04	1.00
H-27	0.97	0.92
H-28	0.97	0.76
H-30	1.69	1.65

The ^{13}C-NMR spectrum (Fig. 3.43) disclosed the presence of 30 carbon resonances. To confirm the structure, this compound was compared the ^{13}C-NMR spectrum with that of lupeol (Mahato and Kundu, 1994). Their carbon chemical shift assignments are shown in Table 3.14.

Comparison of its ^{1}H and ^{13}C-NMR spectra with those reported (Mahato and Kundu, 1994), it was suggested that Compound **HS-11** be identical with lupeol.

Table 3.14 The ^{13}C-NMR chemical shift assignment of lupeol and Compound **HS-11** (in $CDCl_3$)

Carbon	Chemical shift (ppm)		Carbon	Chemical shift (ppm)	
	lupeol	**HS-11**		lupeol	**HS-11**
1	38.67	36.6	16	35.54	35.5
2	27.35	27.3	17	42.95	42.9
3	78.94	79.0	18	48.24	48.2
4	83.81	38.8	19	47.94	47.9
5	55.25	55.2	20	150.88	150.9
6	18.28	18.3	21	29.80	29.8
7	34.23	34.2	22	39.96	39.9
8	40.78	40.8	23	27.95	27.9
9	50.38	50.4	24	15.35	15.3
10	37.11	37.1	25	16.09	16.1
11	20.89	20.9	26	15.94	15.9
12	25.08	25.1	27	14.51	14.5
13	38.00	38.0	28	17.97	17.9
14	42.78	42.8	29	109.31	109.3
15	27.41	27.4	30	19.28	19.3

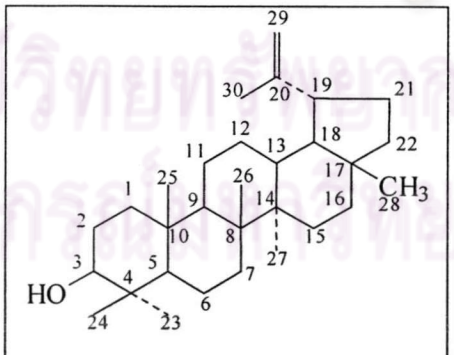

Compound HS-11 : Lupeol

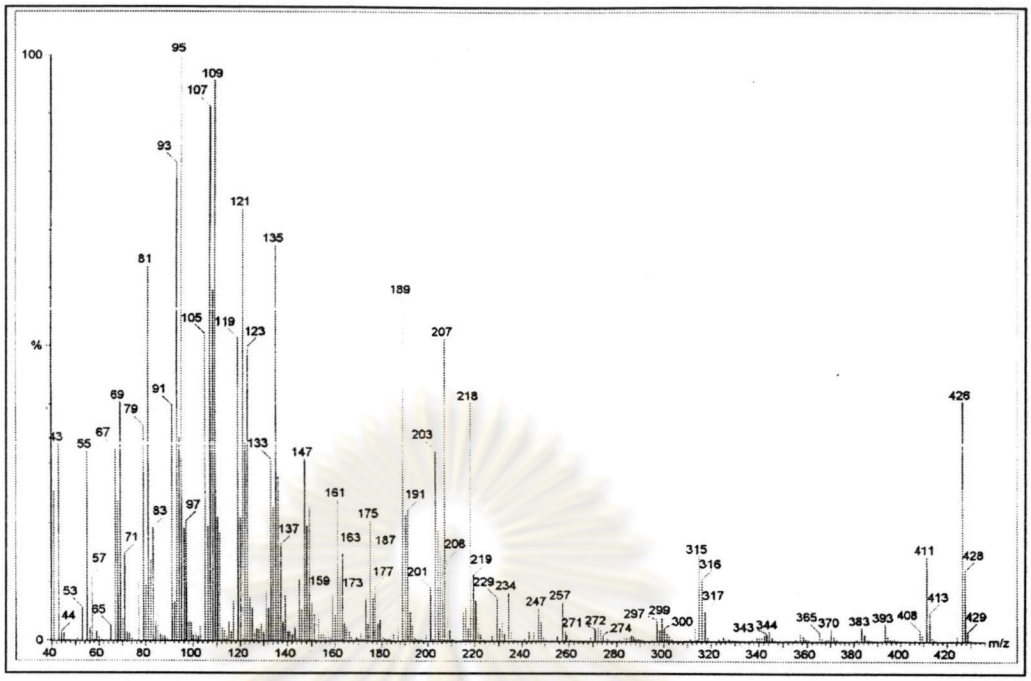

Fig. 3.40 The mass spectrum of Compound **HS-11**

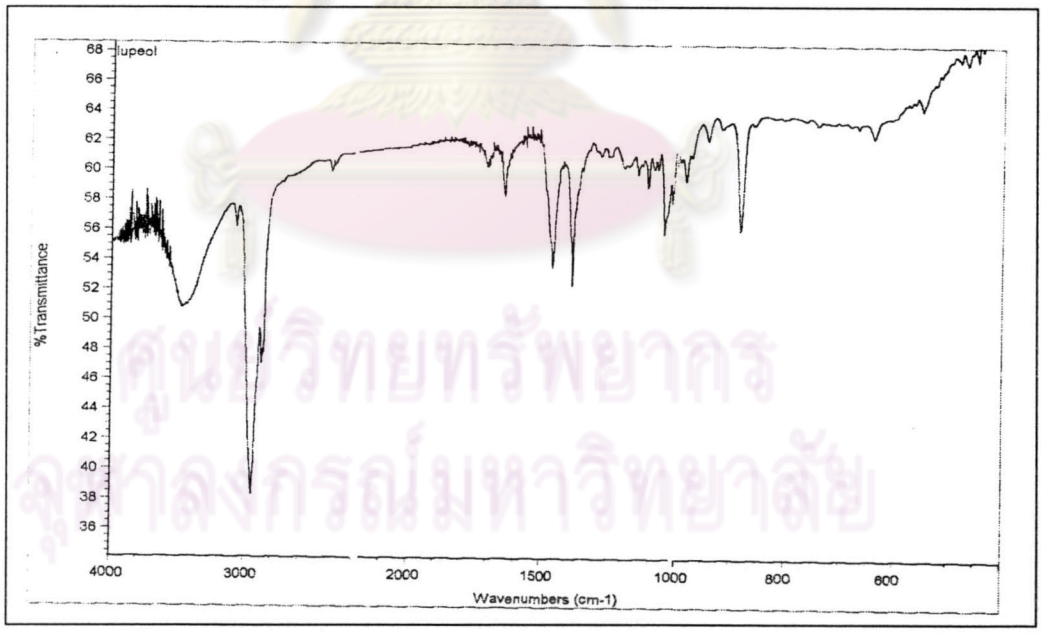

Fig. 3.41 The IR spectrum of Compound **HS-11**

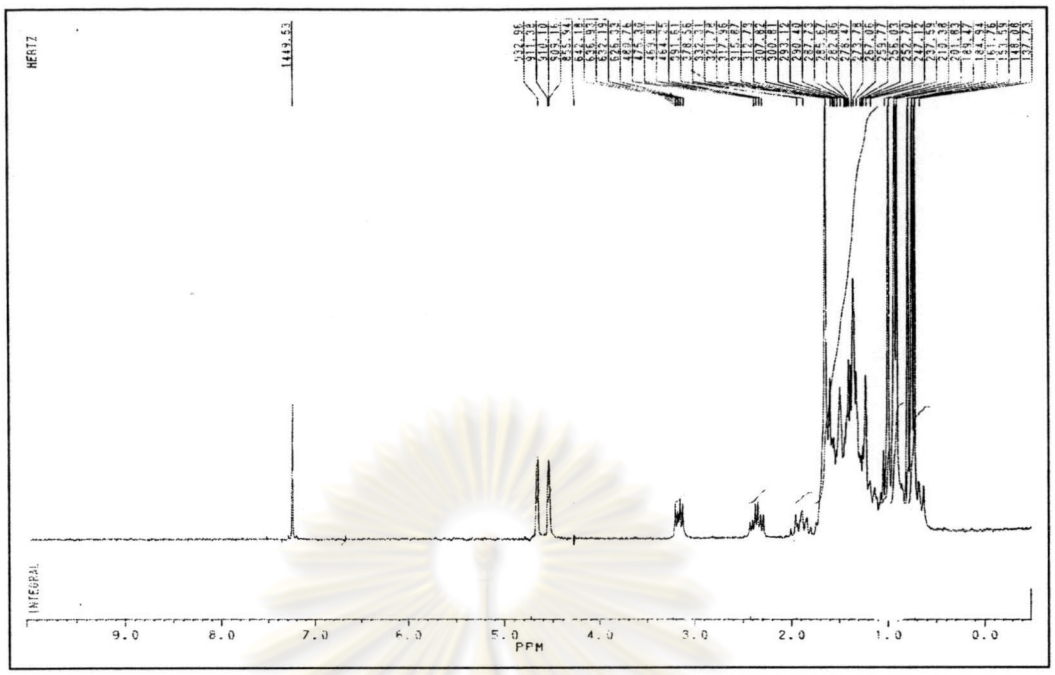

Fig. 3.42 The ^{1}H-NMR spectrum of Compound **HS-11**

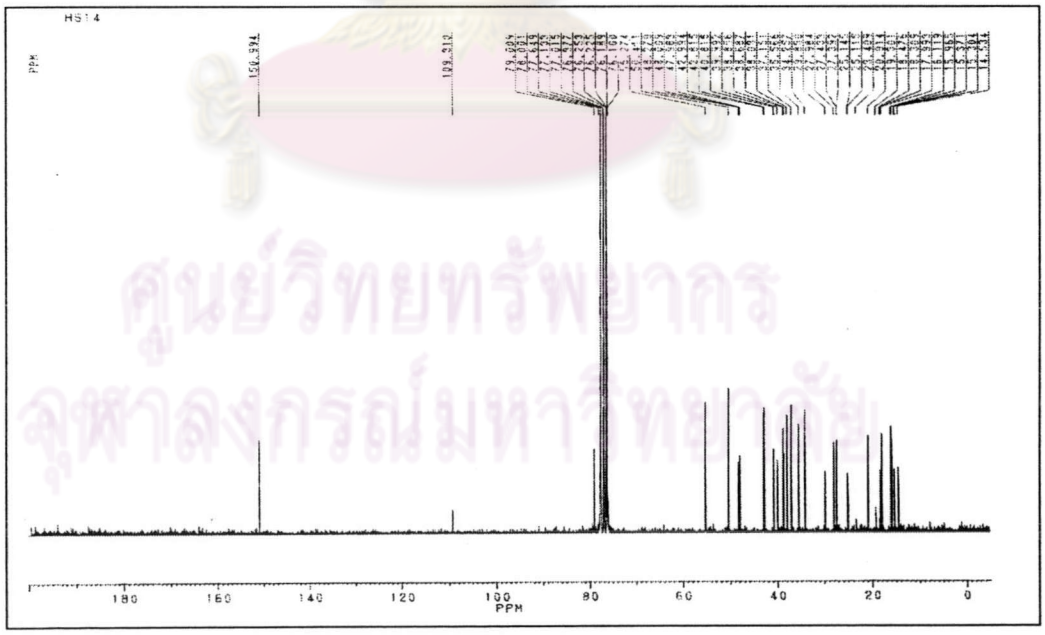

Fig. 3.43 The ^{13}C-NMR spectrum of Compound **HS-11**

3.4.12 Structural Elucidation of Compound HS-12

Compound **HS-12** (29.7 mg, 0.066 % w/w of fraction C) m.p. 278-280 °C was obtained as colorless needles from Fraction I 13 through recrystallization from methanol. A Libermann-Burchard test gave a positive red color indicative of a triterpeniodal skeleton.

The EIMS spectrum of Compound **HS-12** (Fig. 3.44) revealed a molecular ion at m/z 456, suggesting a molecular formula of $C_{30}H_{48}O_3$. The IR spectrum (Fig. 3.45) revealed absorption bands at 3457 cm^{-1}(O-H stretching).

By comparing the ^1H and ^{13}C-NMR spectra of Compound **HS-12** with previously reported data (Mahato and Kundu, 1994), Compound **HS-12** was identified as betulinic acid.

The ^1H-NMR spectrum of Compound **HS-12** (Fig. 3.46) showed a methyl signal at δ 0.64-1.67 ppm which could be assigned by comparison with betulinic acid as shown in Table 3.15. The signals at δ 4.58 (br, s) and δ 4.71 (br, s) could be assigned for two vinyl protons of C -29.

Table 3.15 The ^1H NMR chemical shift assignments of Compound **HS-12** and betulinic acid (in $CDCl_3$)

Position	δ_H (ppm)	
	Betulinic acid	**HS-12**
H-23	0.93	0.91
H-24	0.75	0.73
H-25	0.82	0.80
H-26	0.96	0.95
H-27	0.97	0.97
H-30	1.68	1.67

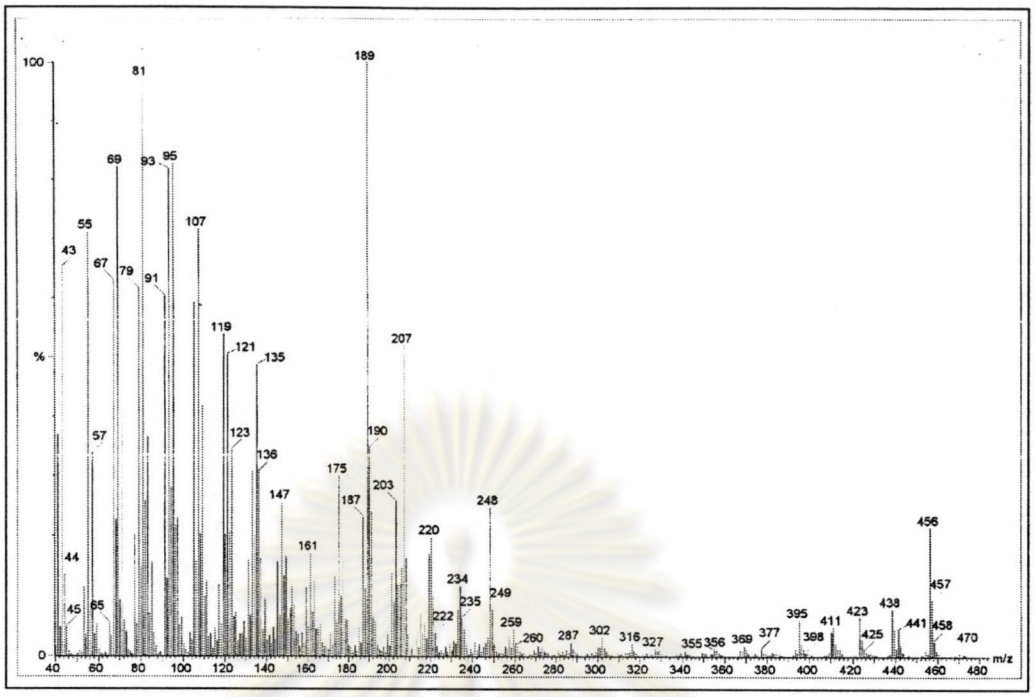

Fig. 3.44 The mass spectrum of Compound **HS-12**

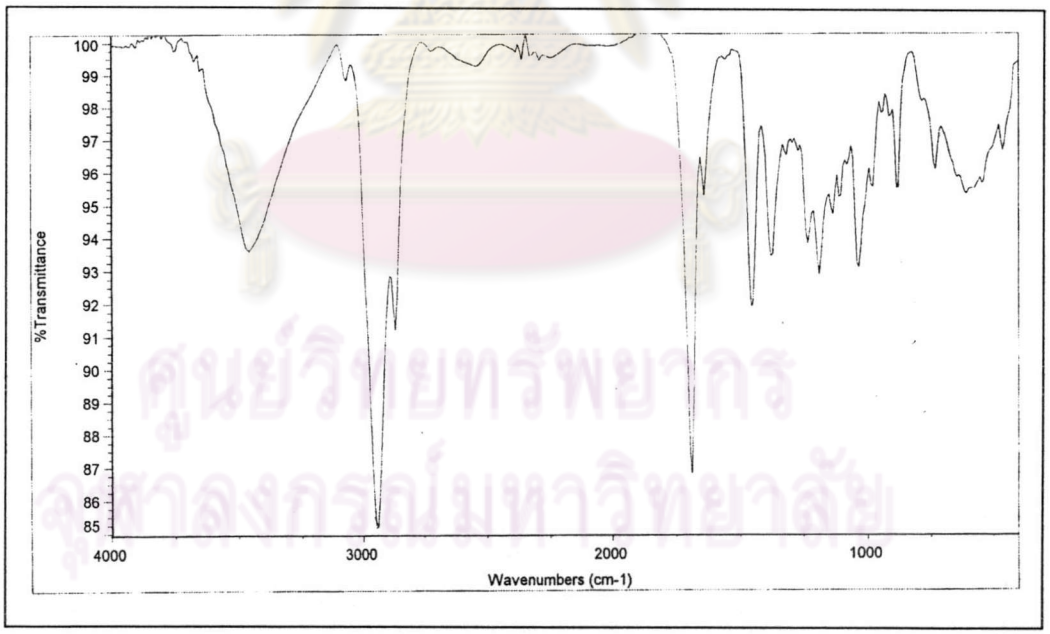

Fig. 3.45 The IR spectrum of Compound **HS-12**

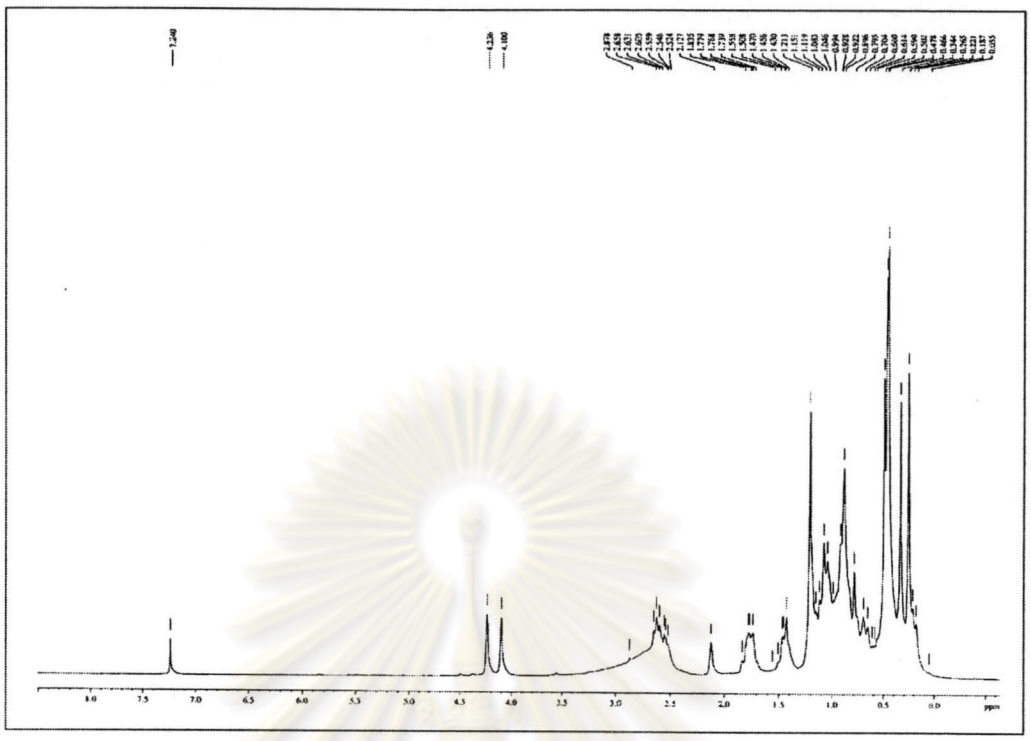

Fig. 3.46 The ^{1}H-NMR spectrum of Compound **HS-12**

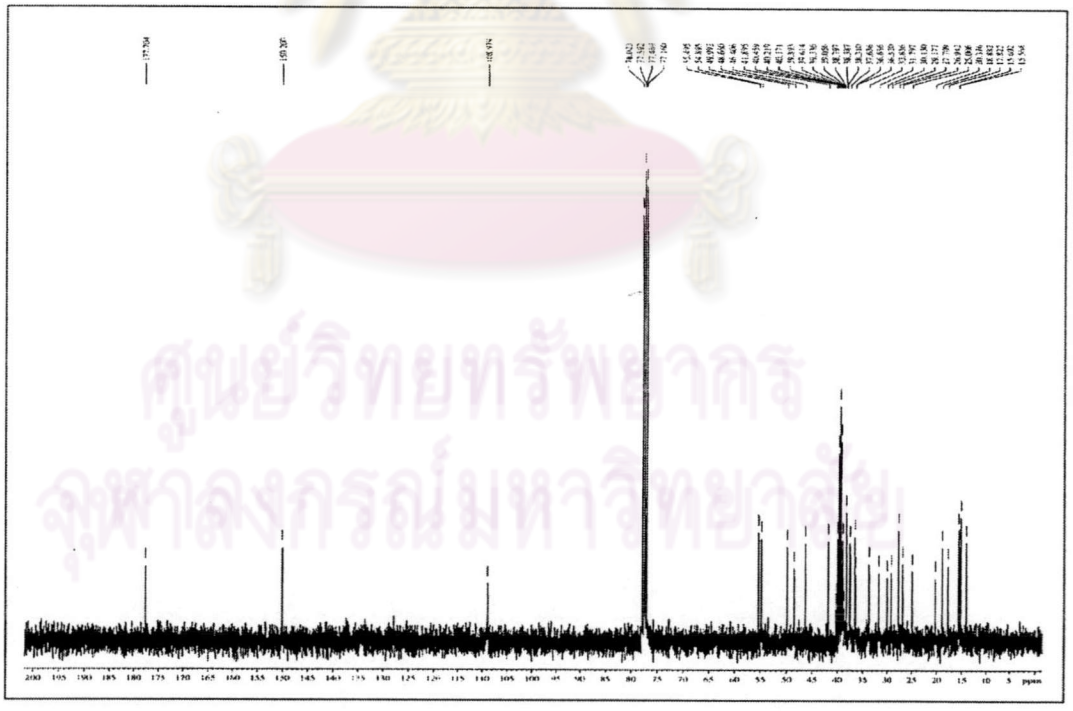

Fig. 3.47 The ^{13}C-NMR spectrum of Compound **HS-12**

The ^{13}C-NMR spectrum (Fig. 3.47) displayed 30 carbon signals which were in good agreement with those of betulinic acid. The complete carbon assignments of Compound **HS-12** and betulinic acid are shown in Table 3.16.

Table 3.16 The ^{13}C-NMR spectral assignment of betulinic acid and Compound **HS-12** (in $CDCl_3$)

Carbon	Chemical shift (ppm)		Carbon	Chemical shift (ppm)	
	betulinic acid	**HS-12**		betulinic acid	**HS-12**
1	38.7	38.6	16	32.1	32.1
2	24.4	25.4	17	56.3	56.3
3	79.9	79.0	18	46.8	46.8
4	38.8	38.8	19	49.2	49.2
5	55.3	55.3	20	150.3	150.2
6	18.3	18.4	21	29.7	29.6
7	34.3	34.3	22	37.0	37.0
8	40.7	40.6	23	27.9	27.9
9	50.5	50.4	24	15.3	15.3
10	37.2	37.	25	16.0	16.0
11	20.8	20.8	26	16.1	16.1
12	25.5	25.5	27	14.7	14.6
13	38.4	38.4	28	180.5	177.7
14	42.4	42.4	29	109.6	108.8
15	30.5	30.5	30	19.4	19.3

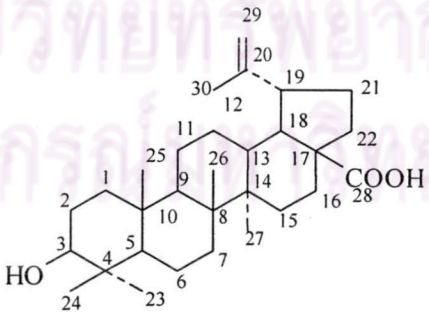

Compound HS-12: Betulinic acid

3.4.13 Structural Elucidation of Compound HS-13

Compound HS 13 (1.42 g, 1.17% w/w of hexane extract) was isolated from hexane extract. After recrystallization with ethanol white amorphous solid, melting poit 238-242 °C was gained.

Compound **HS-13** gave a violet color to with Liebermann-Burchard's reagent, suggesting the presence of a triterpenoidal nucleus, in its molecule.

The IR spectrum (Fig. 3.48) showed absorption bands at 3350 (O-H stretching), 2944 and 2872 (C-H stretching), 1641 (C=C stretching), 1455 and 1382 (C-H bending) and 1042 (C-O stretching) cm^{-1}.

The EIMS spectrum of Compound **HS-13** (Fig. 3.49) showed the molecular ion $[M^+]$ at m/z 456, corresponding to $C_{30}H_{48}O_3$. The important fragmentation pattern at m/z 248 (100), 133 (72), 149 (80), 203 (49) and 119 (34) was observed.

The ^{1}H-NMR spectrum of Compound **HS-13** (Fig. 3.50) showed methyl signal at δ 0.70-1.60 ppm. The signals at δ 1.05-2.25 ppm were the signals of methylene and methine protons.

The ^{13}C-NMR spectrum (Fig. 3.51) displayed two olefinic carbons at 138.1 and 124.5 ppm. The signal at 76.8 ppm could be assigned for the carbon signal adjacent to oxygen atom. Other signals around 54.8-15.2 ppm were compatible with methyl, methylene, methine and quaternary carbons.

Comparison of its ^{13}C-NMR spectra with those reported data (Lin *et al*, 1987), it was conceivable to conclude that Compound **HS-13** was identical with ursolic acid. The complete carbon assignments of Compound **HS-13** and ursolic acid are shown in Table 3.17.

Table 3.17 The ^{13}C-NMR spectral assignment of betulinic acid and Compound **HS-13** (in $CDCl_3$)

Carbon	Chemical shift (ppm)		Carbon	Chemical shift (ppm)	
	ursolic acid	**HS-13**		ursolic acid	**HS-13**
1	38.7	38.5	16	24.2	23.8
2	27.2	26.9	17	47.5	47.0
3	78.2	76.8	18	52.7	52.4
4	38.8	38.3	19	39.1	39.1
5	55.2	54.8	20	38.8	38.4
6	18.3	18.0	21	30.7	30.2
7	33.0	32.7	22	36.7	36.3
8	39.5	38.5	23	28.0	27.5
9	47.5	46.8	24	15.7	16.0
10	36.9	36.5	25	15.4	15.2
11	17.1	16.9	26	17.0	17.0
12	125.2	125.5	27	23.5	22.8
13	138.3	138.2	28	179.9	178.3
14	42.0	41.6	29	23.2	23.3
15	28.2	28.2	30	21.2	21.1

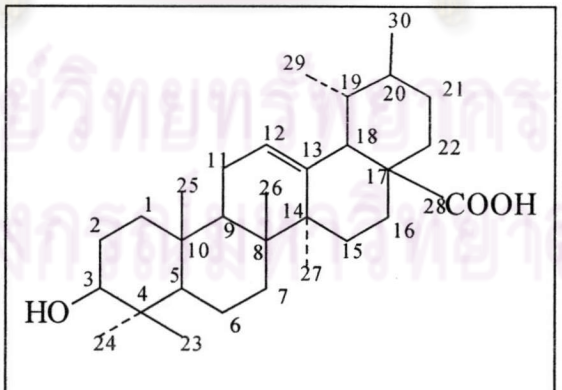

Compound HS-13 : Ursolic acid

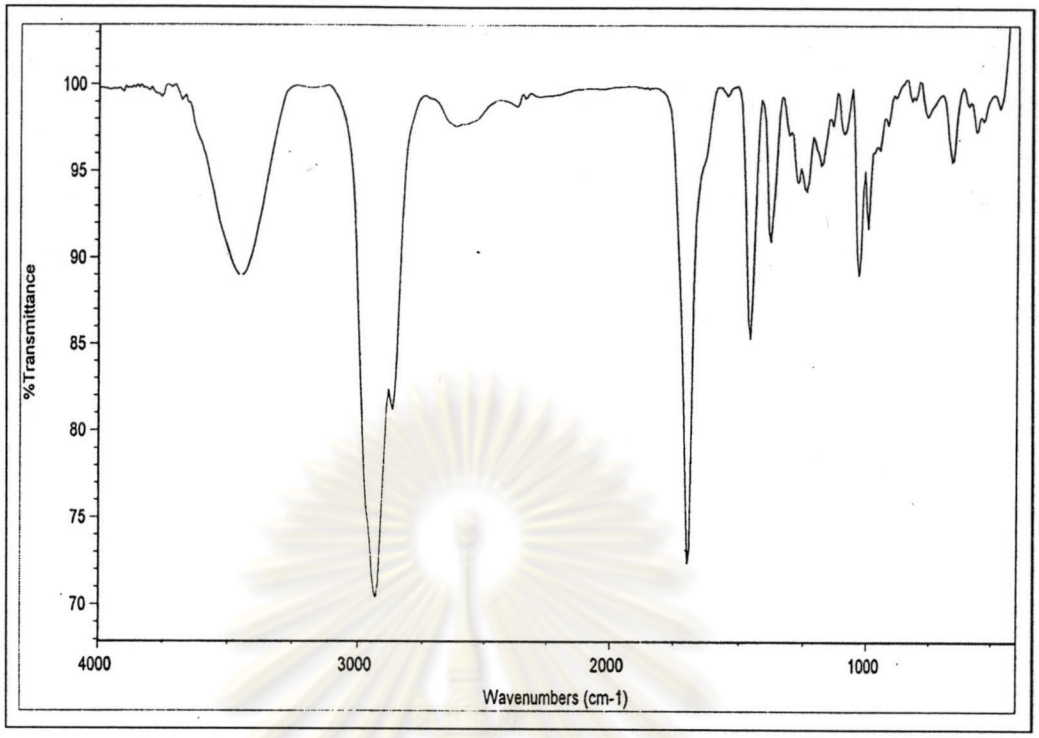

Fig. 3.48 The IR spectrum of Compound **HS-13**

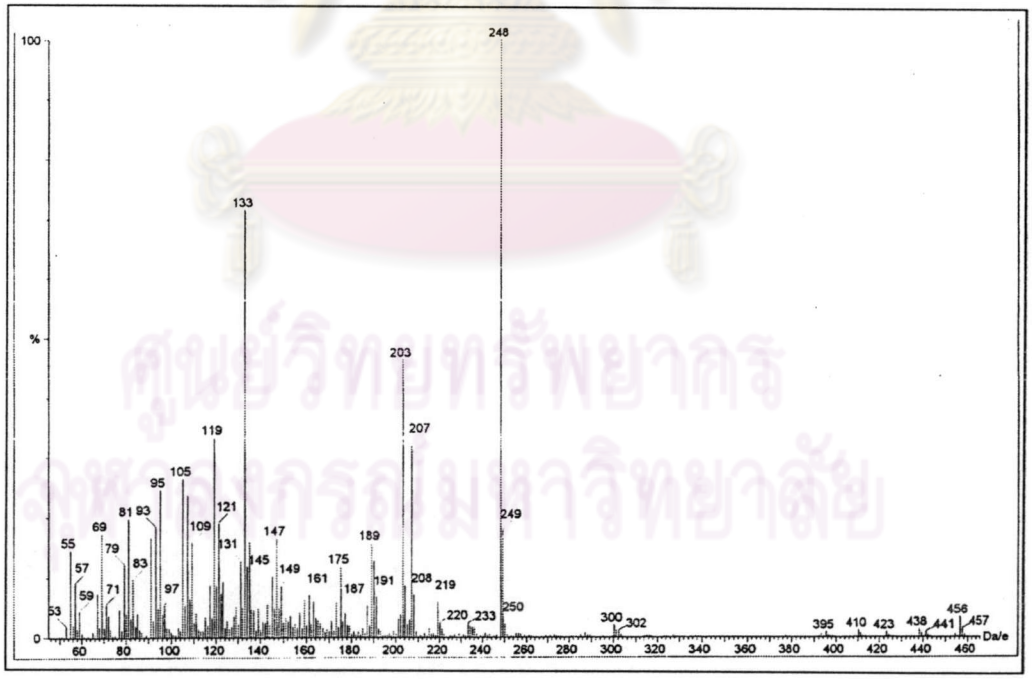

Fig. 3.49 The mass spectrum of Compound **HS-13**

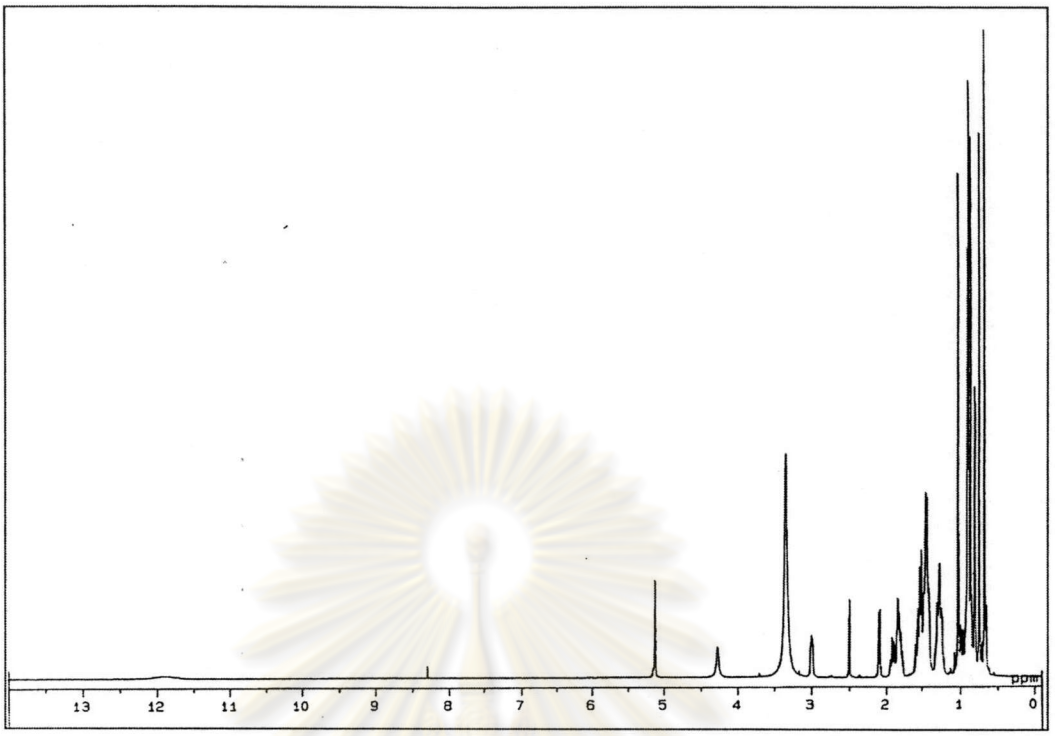

Fig. 3.50 The ^{1}H-NMR spectrum of Compound **HS-13**

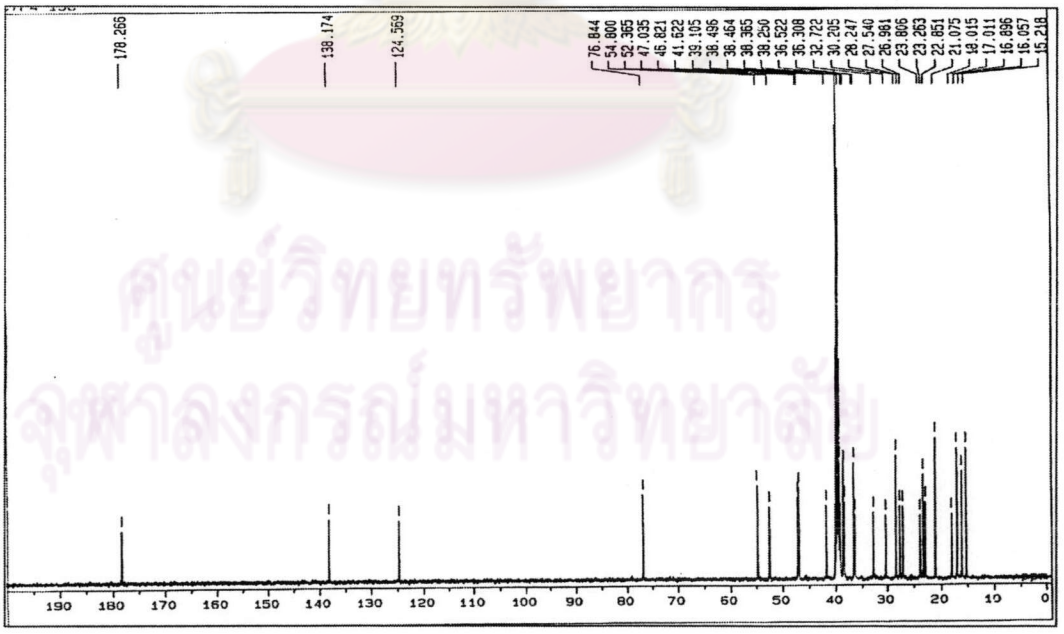

Fig. 3.51 The ^{13}C-NMR spectrum of Compound **HS-13**

3.5 Weed Growth Inhibition Activity of Isolated Substances.

From the fractionation and purification of *H. suaveolens* Poit. crude extracts, thirteen substances were isolated. Eight substances, including a mixture of two steroids **(HS-1)**, oleanolic acid **(HS-2)**, genkwanin **(HS-3)**, 5-hydroxy methyl furfuraldehyde **(HS-4)**, a mixture of two steroid glycosides **(HS-5)**, a mixture of two steroid **(HS-6)**, a mixture of long chain alcohols **(HS-7)** and a mixture of long chain esters **(HS-8)** were isolated from dichloromethane extract. β-Amyrin **(HS-9)**, α-amyrin **(HS-10)**, lupeol **(HS-11)**, betulinic acid **(HS-12)** and ursolic acid **(HS-13)** were isolated from hexane extract.

In order to reach the goal of this research, all isolated substances were subjected to weed growth inhibitory test. The results are shown in Table 3.18 and Fig. 3.52.

Table 3.18. Inhibitory effect of isolated substances from *H. suaveolens* Poit. on the growth of *E. crus-galli* Beauv.

Substances	% Inhibition at various concentration			
	Growth of *E. crus-galli* parts	10 ppm	100 ppm	1000 ppm
HS-1	root	-10.32	-7.25	8.65
	shoot	-15.65	4.14	17.94
HS-2	root	-12.13	-22.18	-27.20
	shoot	-20.66	-11.52	3.02
HS-3	root	10.65	23.18	45.61
	shoot	-12.61	-7.22	18.54
HS-4	root	-12.38	33.46	82.13
	shoot	10.22	21.17	-10.83
HS-5	root	17.17	18.80	17.29
	shoot	-4.82	0.57	-4.22
HS-6	root	-34.03	-33.05	10.32
	shoot	50.00	53.03	59.60
HS-7	root	-14.37	-15.90	22.87
	shoot	50.77	55.90	60.00
HS-8	root	1.26	8.37	24.97
	shoot	-60.95	-46.23	-31.00
HS-9	root	8.15	12.28	12.91
	shoot	-18.00	-7.22	4.23
HS-10	root	-31.38	-11.85	2.93
	shoot	56.92	59.49	62.56
HS-11	root	-9.90	-15.03	-3.18
	shoot	10.87	8.46	3.04
HS-12	root	-23.68	12.78	52.01
	shoot	33.51	36.51	45.49
HS-13	root	-8.51	-9.48	10.04
	shoot	49.73	52.61	63.95

The plant growth inhibition agents isolated from *H. suaveolens* Poit. which had affected on *E. crus-galli* Beauv. could be listed as follows: 5-hydroxy methyl furfuraldehyde **(HS-4)**, betulinic acid **(HS-12)** and genkwanin **(HS-3)** revealed root inhibition effect with 82.13%, 52.01% and 45.61%, respectively at 1000 ppm. Substances that exhibited shoot growth inhibition were ursolic acid **(HS-13)**, α-amyrin **(HS-10)**, a mixture of long chain alcohols **(HS-7)**, a mixture of two triterpenoids **(HS-6)**, and betulinic acid **(HS-12)** revealed root inhibition effect with 63.95%, 62.56%, 60.00%, 59.60% and 45.49%, respectively at 1000 ppm. **HS-8** showed shoot growth promotion effect 60.95% at 10 ppm. The results of substances on *E. crus-galli* Beauv. growth inhibition are shown in Fig. 3.52.

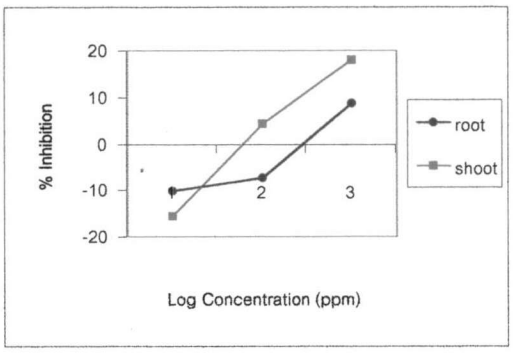

Mixture **HS-1**

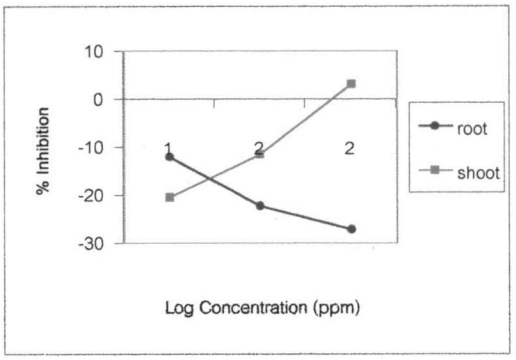

Compound **HS-2**

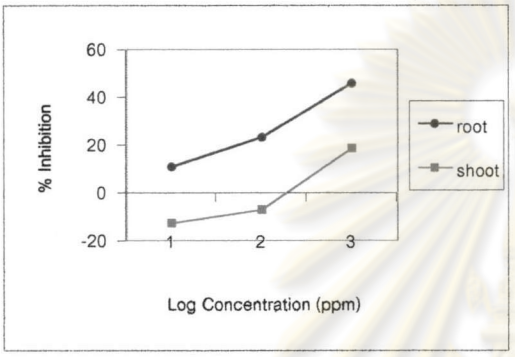

Compound **HS-3**

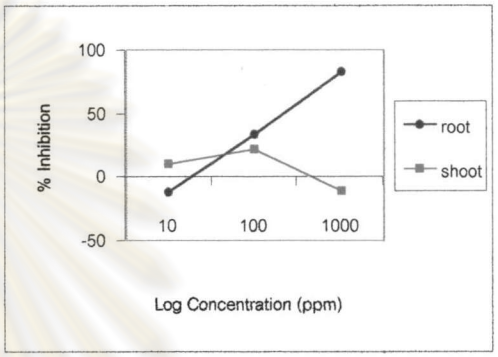

Compound **HS-4**

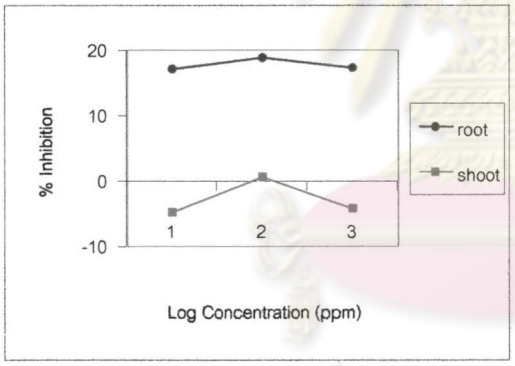

Mixture **HS-5**

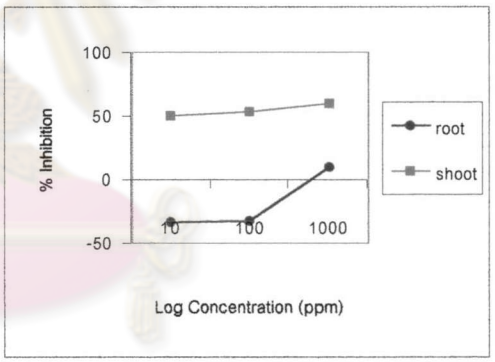

Mixture **HS-6**

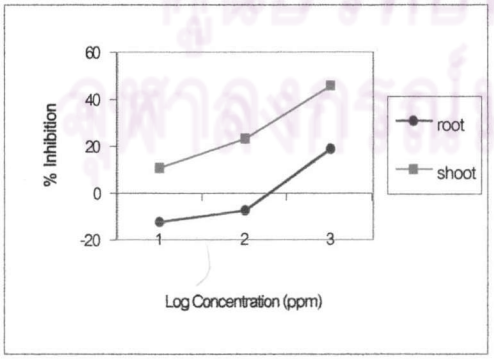

Mixture **HS-7**

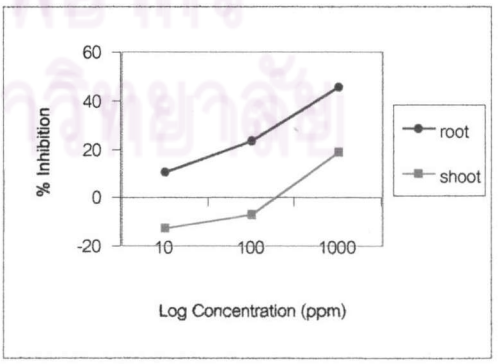

Mixture **HS-8**

Fig. 3.52 Inhibitory effect of isolated substances from *H. suaveolens* Poit. on the growth of *E. crus-galli* Beauv.

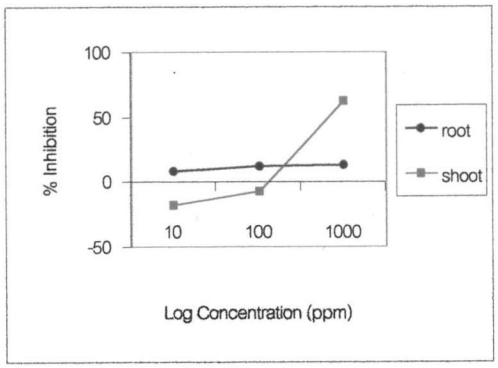

Compound **HS-9**

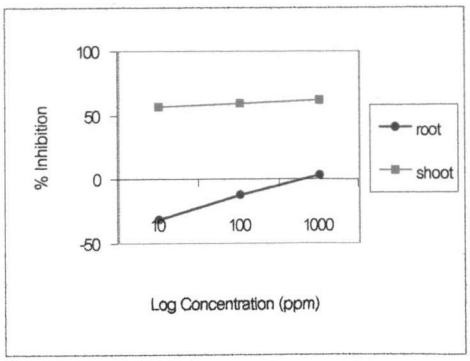

Compound **HS-10**

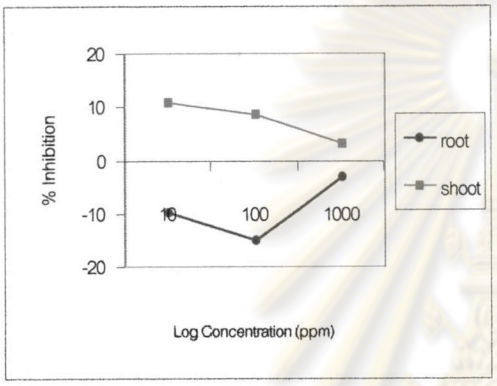

Compound **HS-11**

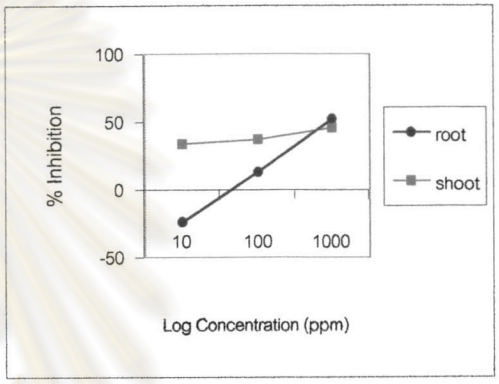

Compound **HS-12**

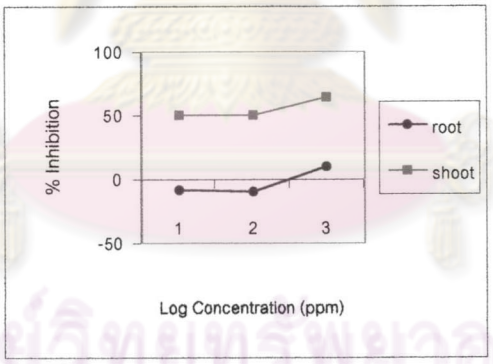

Compound **HS-13**

Fig. 3.52 Inhibitory effect of isolated substances from *H. suaveolens* Poit. on the growth of *E. crus-galli* Beauv. (continued)

In addition, some isolated substances with sufficient amount were further bioassayed for plant growth inhibition against various weeds and selected plants. These specimens are *Lactuca sativa* Linn. (ผักกาดหอม), *Trianthema portulacastrum* Linn. (ผักเบี้ยหิน), *Bidens pilosa* Linn. (กันจ้ำขาว), *Brassica chinense* Jusl. (ผักกาดขาว),

Dactyloctenium aegyptium Willd. (หญ้าปากควาย) and *Pennisetum polystachyon* Schult. (ขจรจบดอกใหญ่). The results of inhibitory effect compounds are shown in Tables 3.19-3.24 and Fig. 3.53-3.64.

Table 3.19 Inhibitory effect of isolated substances from *H. suaveolens* Poit. on the growth of *Lactuca sativa* Linn. (ผักกาดหอม)

Substances	% Inhibition at various concentration			
	Growth of *L. sativa* parts	10 (ppm)	100 (ppm)	1000 (ppm)
HS-1	root	-36.18	-30.20	-47.58
	shoot	34.17	41.08	42.17
HS-2	root	-31.05	-15.95	64.39
	shoot	27.26	35.26	63.99
HS-3	root	16.24	-28.21	-46.72
	shoot	27.62	33.08	37.44
HS-4	root	-3.80	-12.30	44.37
	shoot	1.71	6.84	13.68
HS-5	root	24.22	-29.91	-54.13
	shoot	3.98	17.08	25.80
HS-6	root	-35.90	-82.63	-131.34
	shoot	21.44	28.35	49.08
HS-7	root	-10.84	-9.21	-0.52
	shoot	-3.42	-2.56	8.55
HS-8	root	1.66	7.09	13.07
	shoot	-6.84	5.98	17.09
HS-9	root	-28.77	-29.91	-43.02
	shoot	25.08	29.44	27.99
HS-10	root	-83.48	-16.48	-17.66
	shoot	-20.02	28.35	29.44
HS-11	root	-3.78	1.66	13.07
	shoot	14.53	17.39	20.51
HS-12	root	-53.56	-45.87	-4.84
	shoot	33.81	27.26	23.99
HS-13	root	-26.50	27.07	65.24
	shoot	27.99	30.53	39.63

The allelopatic agents isolated from *H. suaveolens* Poit. that had affected on *Lactuca sativa* Linn. growth inhibition could be listed as follows: a mixture of two steroids **(HS-6)**, a mixture of two steroid glycosides **(HS-5)**, a mixture of β-sitosterol and stigmasterol **(HS-1)** and genkwanin **(HS-3)** revealed root promotion effect with 131.34%, 54.13%, 47.58% and 46.72%, respectively at 1000 ppm. Whereas substances that exhibited root growth inhibition were **HS-13**, **HS-2** and **HS-4** with 65.24%, 64.39% and 44.37%, respectively, at 1000 ppm.

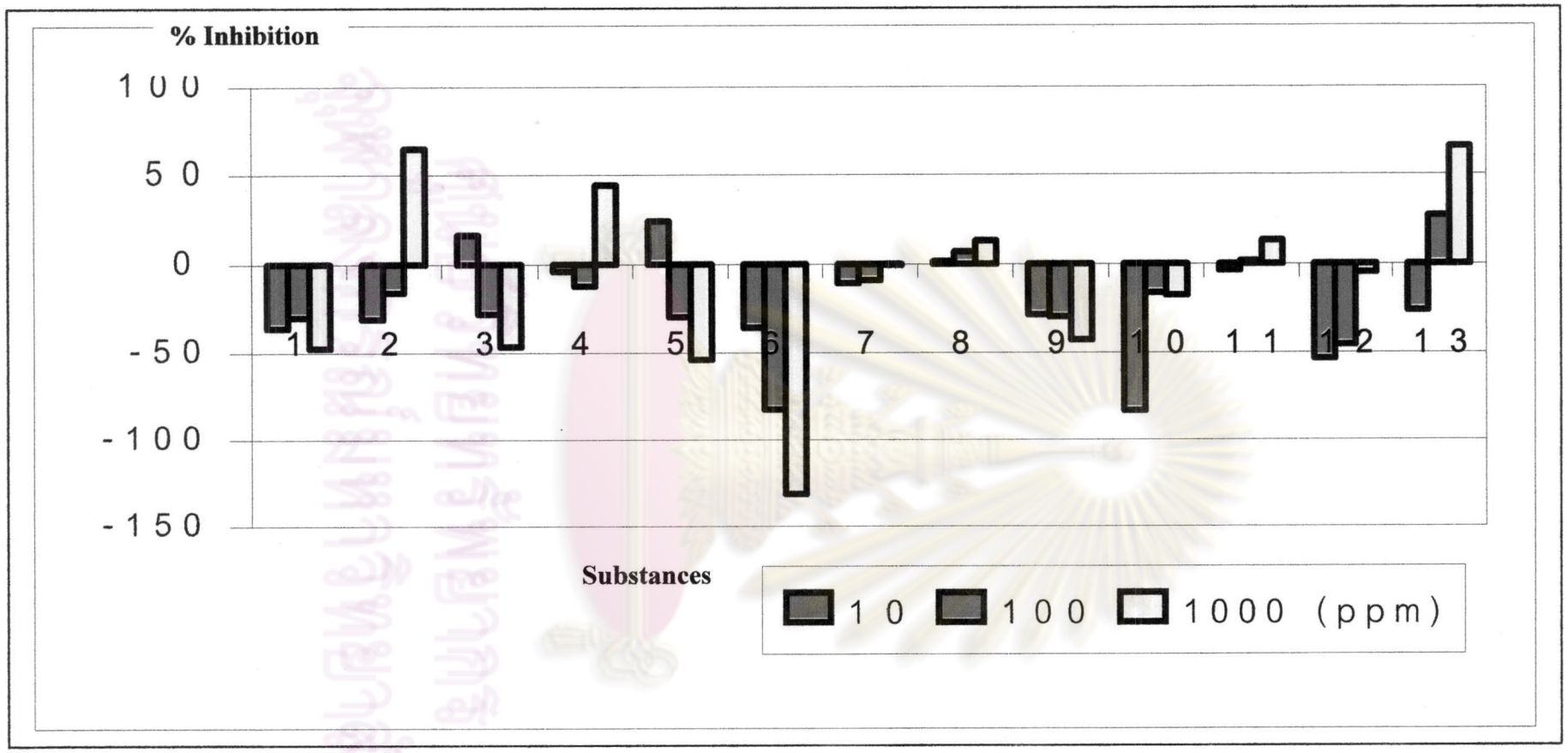

Fig. 3.53 Inhibitory effect of isolated substances from *Hyptis suaveolens* Poit. on the root growth of *Lactuca sativa* Linn.

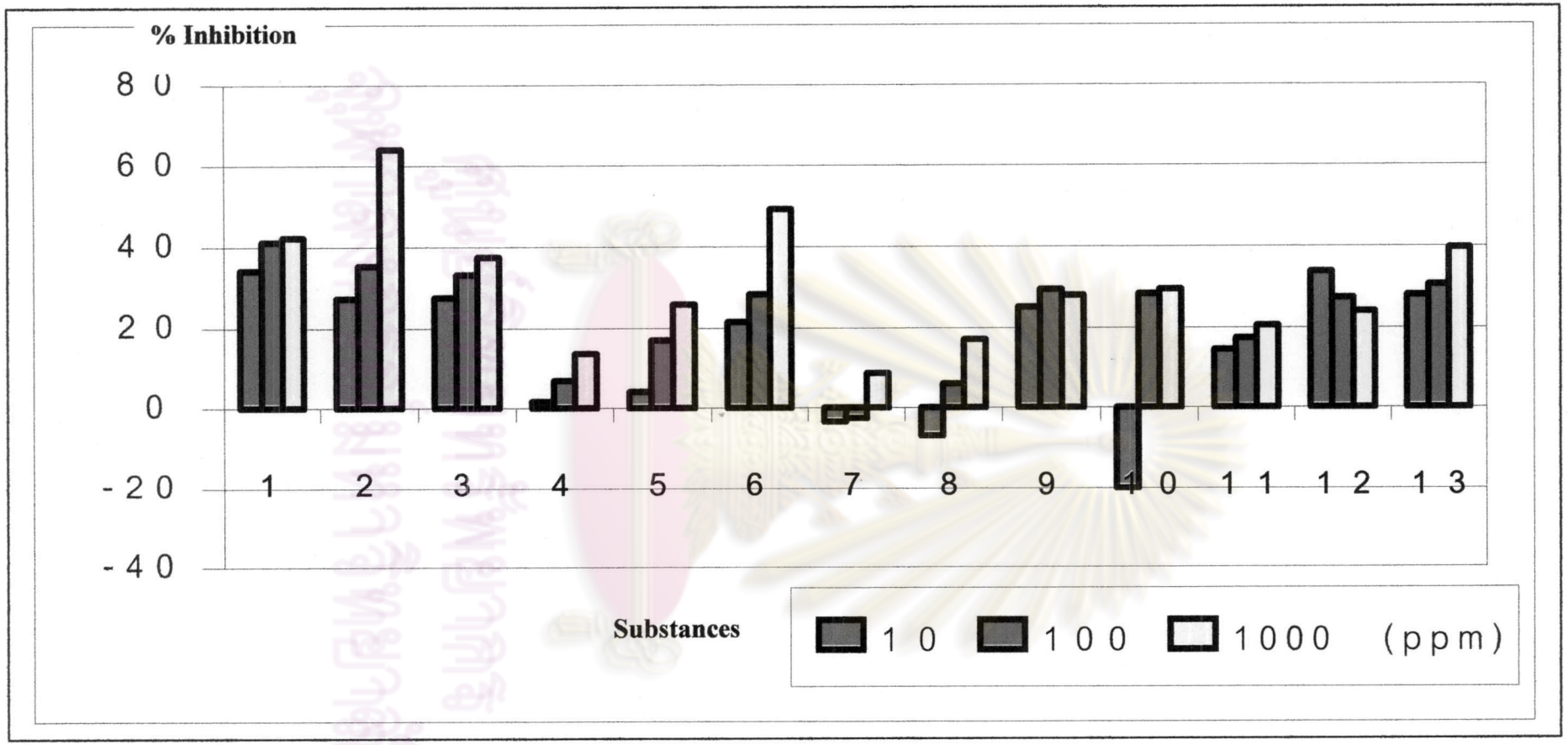

Fig. 3.54 Inhibitory effect of isolated substances from *Hyptis suaveolens* Poit. on the shoot growth of *Lactuca sativa* Linn.

Table 3.20 Inhibitory effect of isolated substances from *H. suaveolens* Poit. on the growth of *Dactyloctenium aegyptium* Willd. (หญ้าปากควาย)

Substances	% Inhibition at various concentration			
	Growth of *D. aegyptium* parts	10 (ppm)	100 (ppm)	1000 (ppm)
HS-1	root	-14.77	8.02	28.69
	shoot	-16.96	-16.40	9.03
HS-2	root	-9.24	7.23	18.47
	shoot	-14.67	-10.95	6.46
HS-3	root	-13.06	-10.46	-27.36
	shoot	-17.27	-3.61	-1.61
HS-4	root	7.21	14.96	43.04
	shoot	-5.88	3.92	13.73
HS-5	root	-2.69	11.75	29.13
	shoot	-5.88	9.80	13.73
HS-6	root	-28.11	-10.04	11.65
	shoot	-13.06	-10.46	-23.46
HS-7	root shoot	NT	NT	NT
HS-8	root shoot	NT	NT	NT
HS-9	root	-40.51	16.88	36.71
	shoot	-80.64	-28.65	9.03
HS-10	root shoot	NT	NT	NT
HS-11	root	-51.05	-27.00	5.49
	shoot	-13.06	-10.46	-27.36
HS-12	root	-7.65	12.41	48.69
	shoot	-21.09	-1.02	31.57
HS-13	root	-18.07	2.81	8.43
	shoot	-13.06	-3.96	9.03

NT = Not Tested

Betulinic acid **(HS-12)** and 5-hydroxy methyl furfuraldehyde **(HS-4)** showed root growth inhibitory effect 48.69% and 43.04%, respectively at 1000 ppm. While β-Amyrin **(HS-9)** promoted the shoot growth 80.64% at 1000 ppm. Lupeol **(HS-11)** showed root growth promotion effect 51.05% at 1000 ppm.

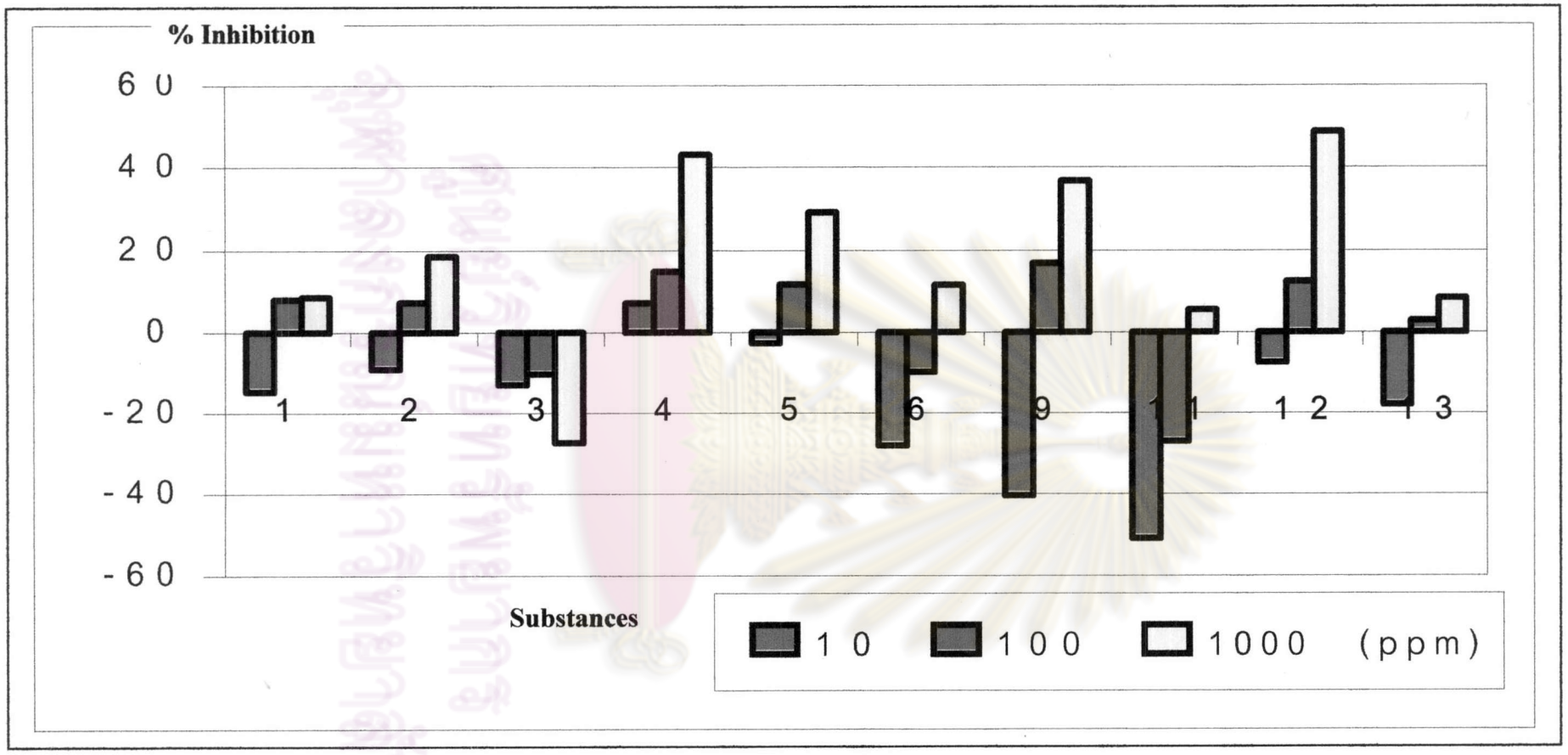

Fig. 3.55 Inhibitory effect of isolated substances from *Hyptis suaveolens* Poit. on the root growth of *Dactyloctenium aegyptium* Willd.

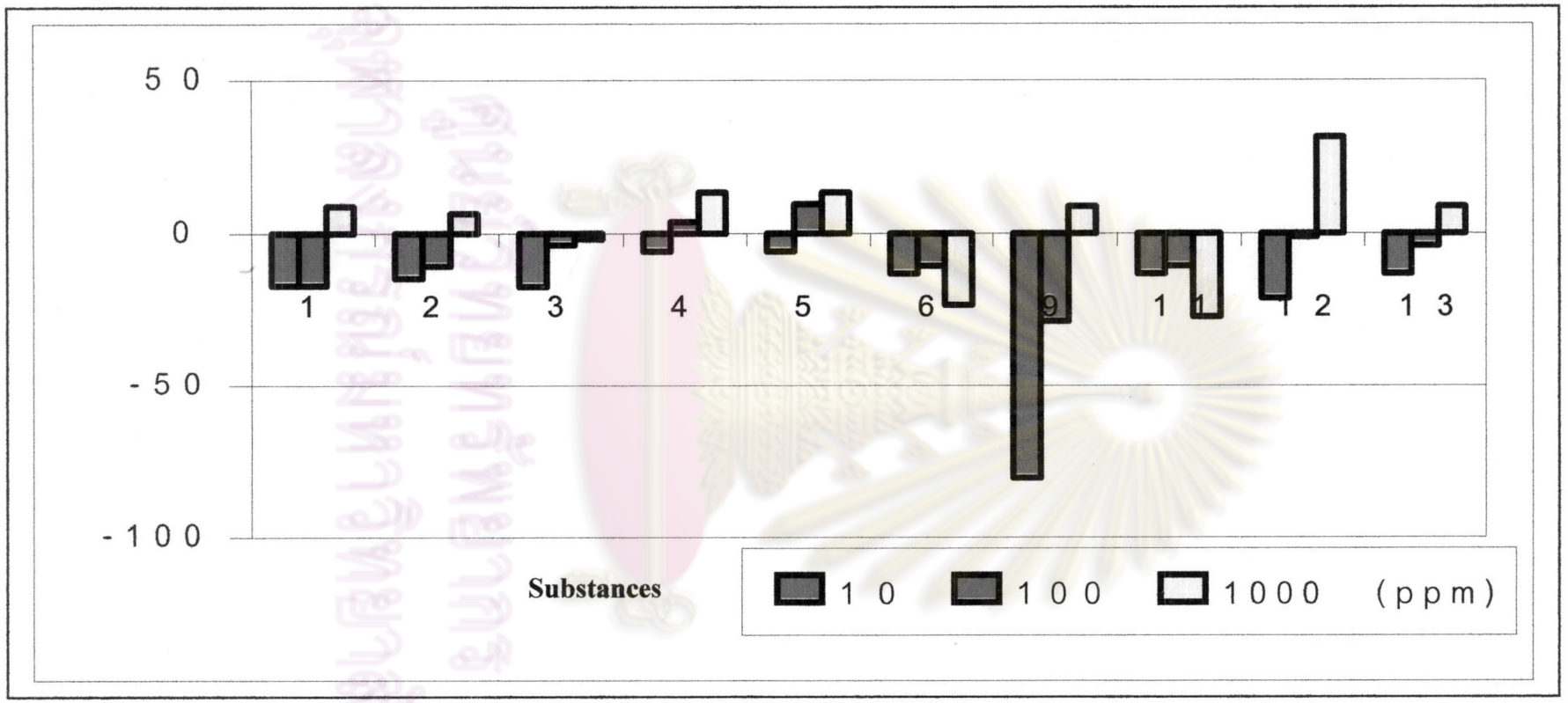

Fig. 3.56 Inhibitory effect of isolated substances from *Hyptis suaveolens* Poit. on the shoot growth of *Dactyloctenium aegyptium* Willd.

Table 3.21 Inhibitory effect of isolated substances from *H. suaveolens* Poit. on the growth of *Trianthema portulacastrum* Linn. (ผักเบี้ยหิน)

Substances	% Inhibition at various concentration			
	Growth of *T. portulacastrum* parts	10 (ppm)	100 (ppm)	1000 (ppm)
HS-1	root	10.14	-11.01	-14.60
	shoot	13.25	33.54	40.60
HS-2	root	0.96	7.12	11.34
	shoot	-8.06	17.22	26.01
HS-3	root	-4.40	8.42	16.12
	shoot	-18.65	-12.81	3.07
HS-4	root	1.28	10.75	55.37
	shoot	-19.17	-12.47	35.39
HS-5	root	-6.74	1.64	5.65
	shoot	0.45	3.33	12.90
HS-6	root	2.75	15.55	66.93
	shoot	-4.40	8.42	16.12
HS-7	root shoot	NT	NT	NT
HS-8	root shoot	NT	NT	NT
HS-9	root	-40.61	-33.21	-25.17
	shoot	30.01	28.54	37.36
HS-10	root shoot	NT	NT	NT
HS-11	root	-0.43	-15.46	-16.50
	shoot	16.19	26.48	32.66
HS-12	root	7.79	18.48	33.44
	shoot	-6.78	5.68	16.36
HS-13	root	-7.79	-2.12	4.04
	shoot	12.82	10.99	21.98

NT = Not Tested

Three compounds, namely a mixture two of triterpenoids **(HS-6)**, 5-hydroxy methyl furfuraldehyde **(HS-4)** and a mixture of β-sitosterol and stigmasterol **(HS-1)** showed root growth inhibitory effect 66.93%, 55.37% and 40.60% at 1000 ppm, respectively.

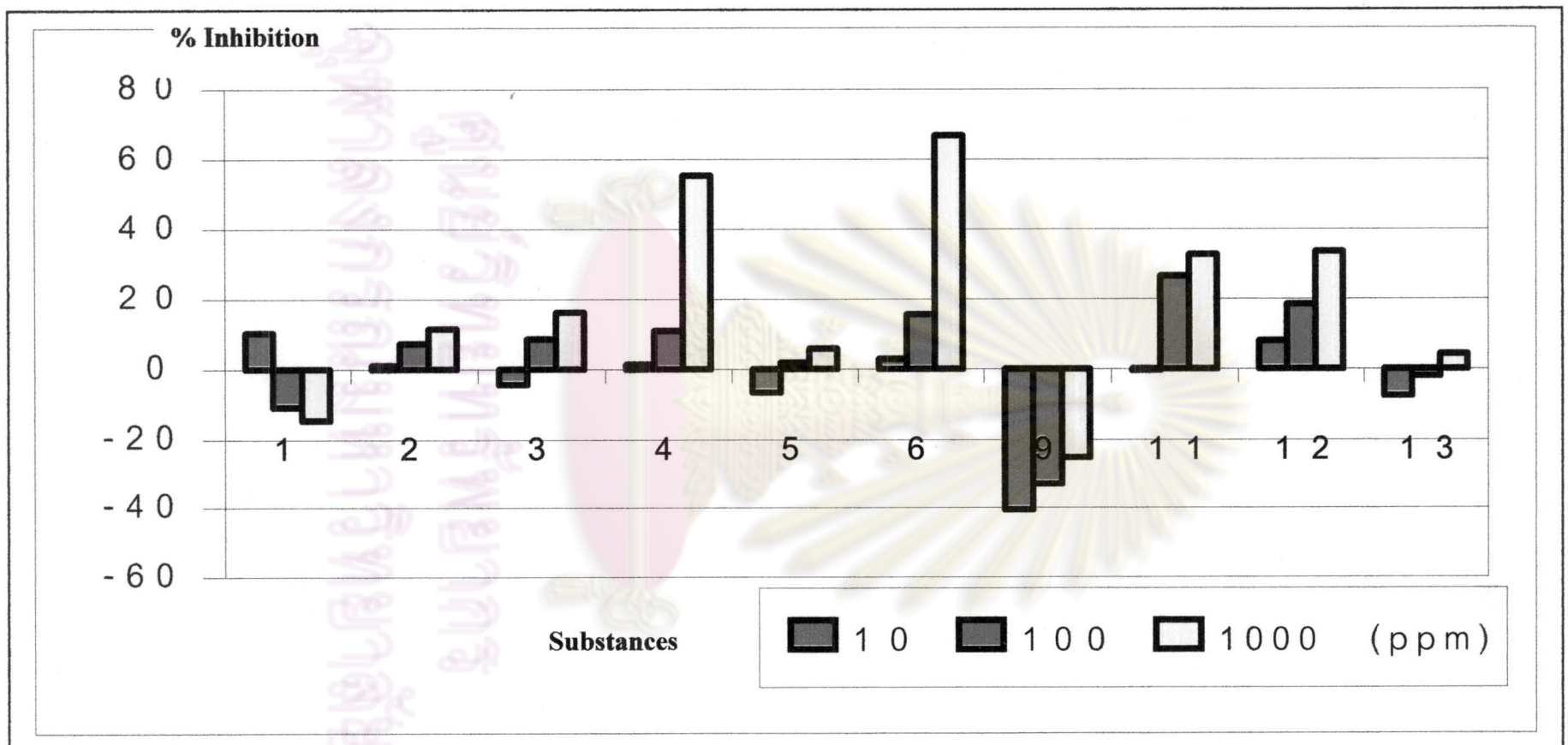

Fig. 3.57 Inhibitory effect of isolated substances from *Hyptis suaveolens* Poit. on the root growth of *Trianthema portulacastrum* Linn.

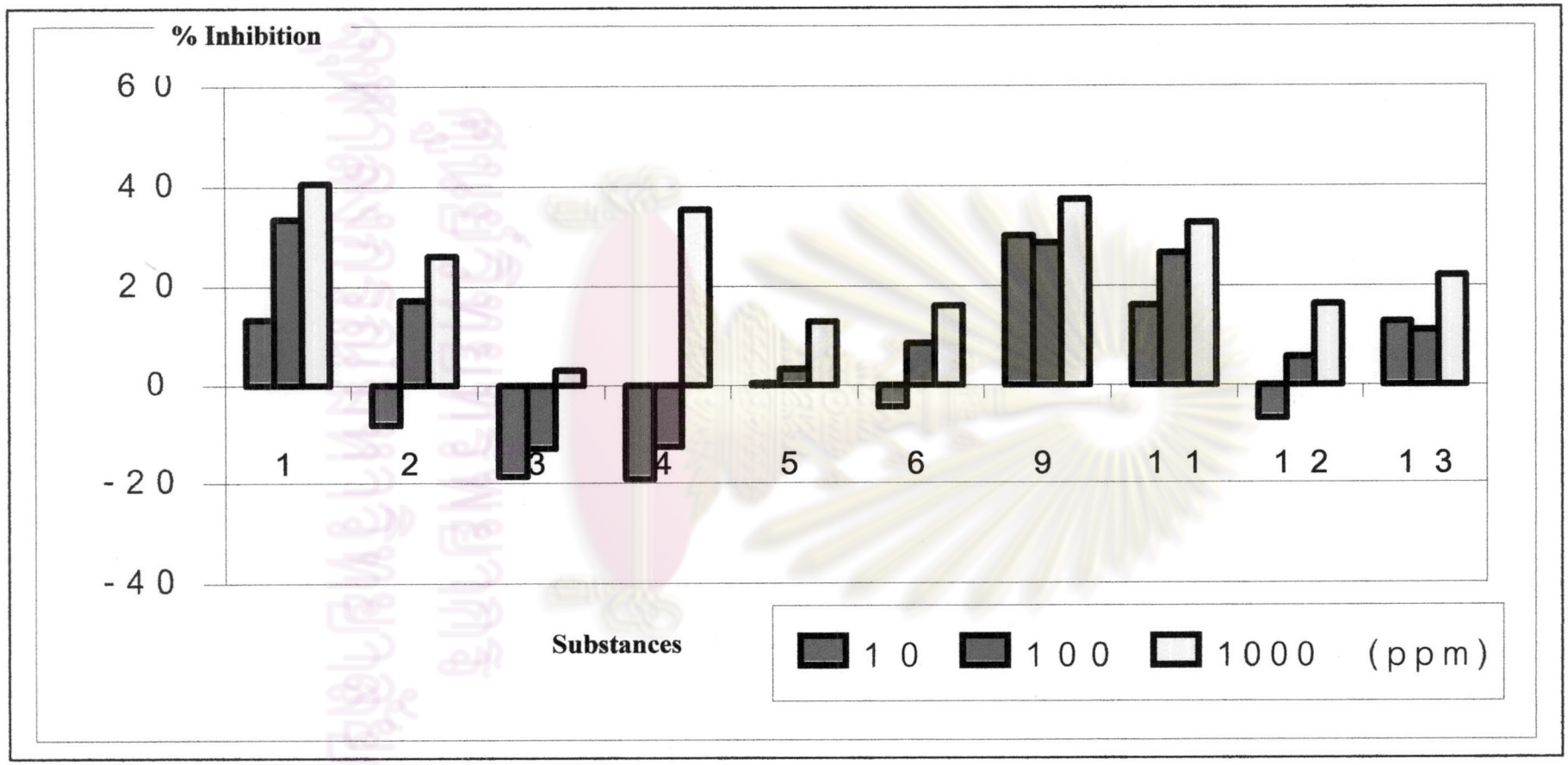

Fig. 3.58 Inhibitory effect of isolated substances from *Hyptis suaveolens* Poit. on the shoot growth of *Trianthema portulacastrum* Linn

Table 3.22 Inhibitory effect of isolated substances from *H. suaveolens* Poit. on the growth of *Pennisetum polystachyon* Schult. (ขจรจบดอกใหญ่)

Substances	% Inhibition at various concentration			
	Growth of *P. polystachyon* parts	10 (ppm)	100 (ppm)	1000 (ppm)
HS-1	root	-0.91	11.72	16.74
	shoot	1.42	8.73	10.92
HS-2	root	-5.56	9.72	12.43
	shoot	-7.14	0.97	3.17
HS-3	root	-27.78	-14.29	9.52
	shoot	-19.58	-10.82	-0.15
HS-4	root	-4.88	16.76	67.76
	shoot	3.02	12.18	25.93
HS-5	root	-0.72	0.71	3.72
	shoot	6.07	9.89	14.47
HS-6	root	-0.95	3.03	24.05
	shoot	-26.98	-14.29	9.52
HS-7	root	NT	NT	NT
	shoot			
HS-8	root	NT	NT	NT
	shoot			
HS-9	root	-2.44	2.13	-3.81
	shoot	-29.24	-17.56	3.61
HS-10	root	NT	NT	NT
	shoot			
HS-11	root	10.81	13.85	21.77
	shoot	-48.96	-5.15	16.76
HS-12	root	3.87	15.13	20.34
	shoot	41.43	45.38	50.64
HS-13	root	-16.07	1.60	16.73
	shoot	-32.54	-21.43	-4.76

NT = Not Tested

While 5-hydroxy methyl furfuraldehyde **(HS-4)** reveled root growth inhibitory effect 67.76 %, at 1000 ppm, lupeol **(HS-11)** showed shoot growth promotion effect 48.96 %, at 10 ppm. In addition, betulinic acid **(HS-12)** displayed shoot growth inhibitory effect 50.64%, 45.38% and 41.43% at 1000, 100 and 10 ppm, respectively.

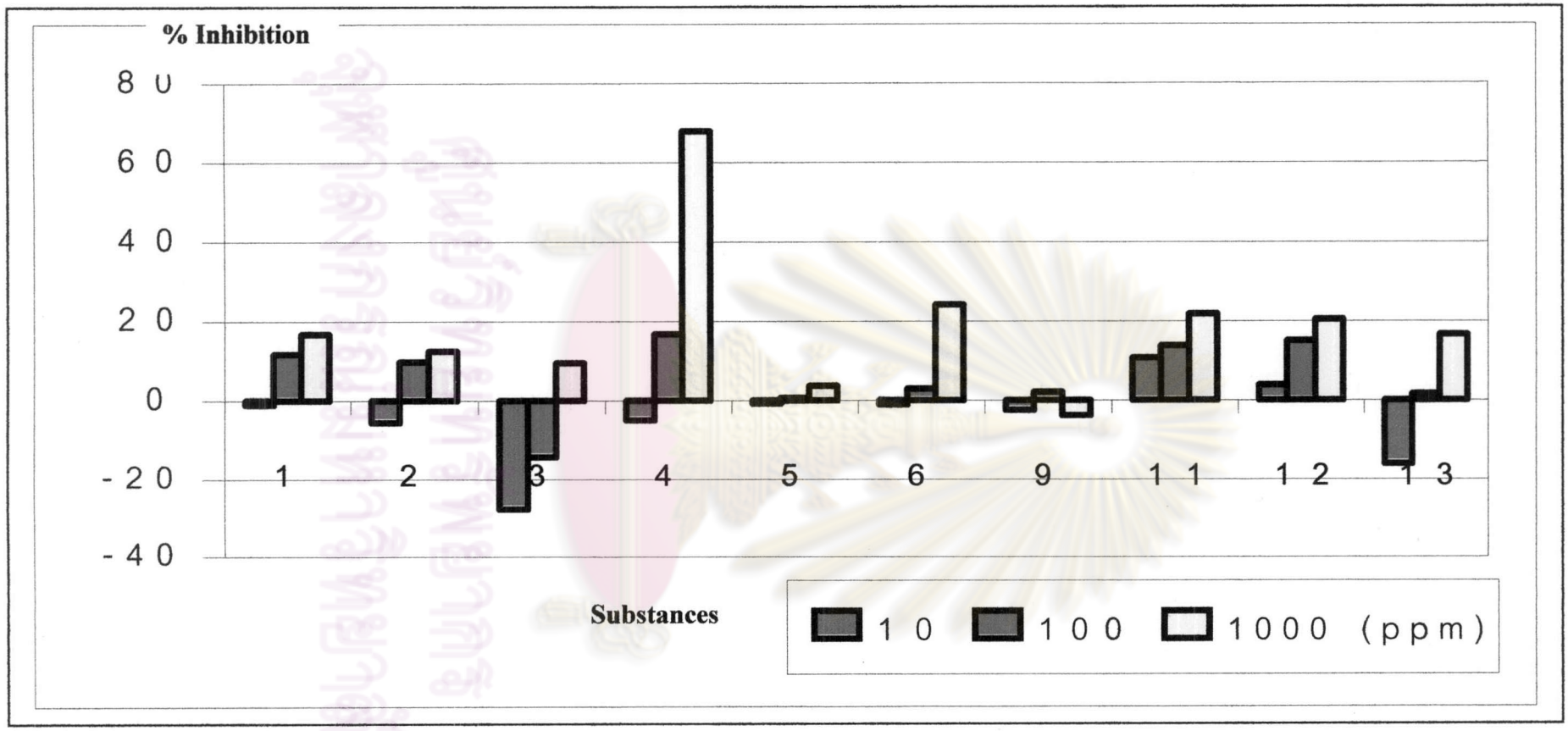

Fig. 3.59 Inhibitory effect of isolated substances from *Hyptis suaveolens* Poit. on the root growth of *Pennisetum polystachyon* Schult.

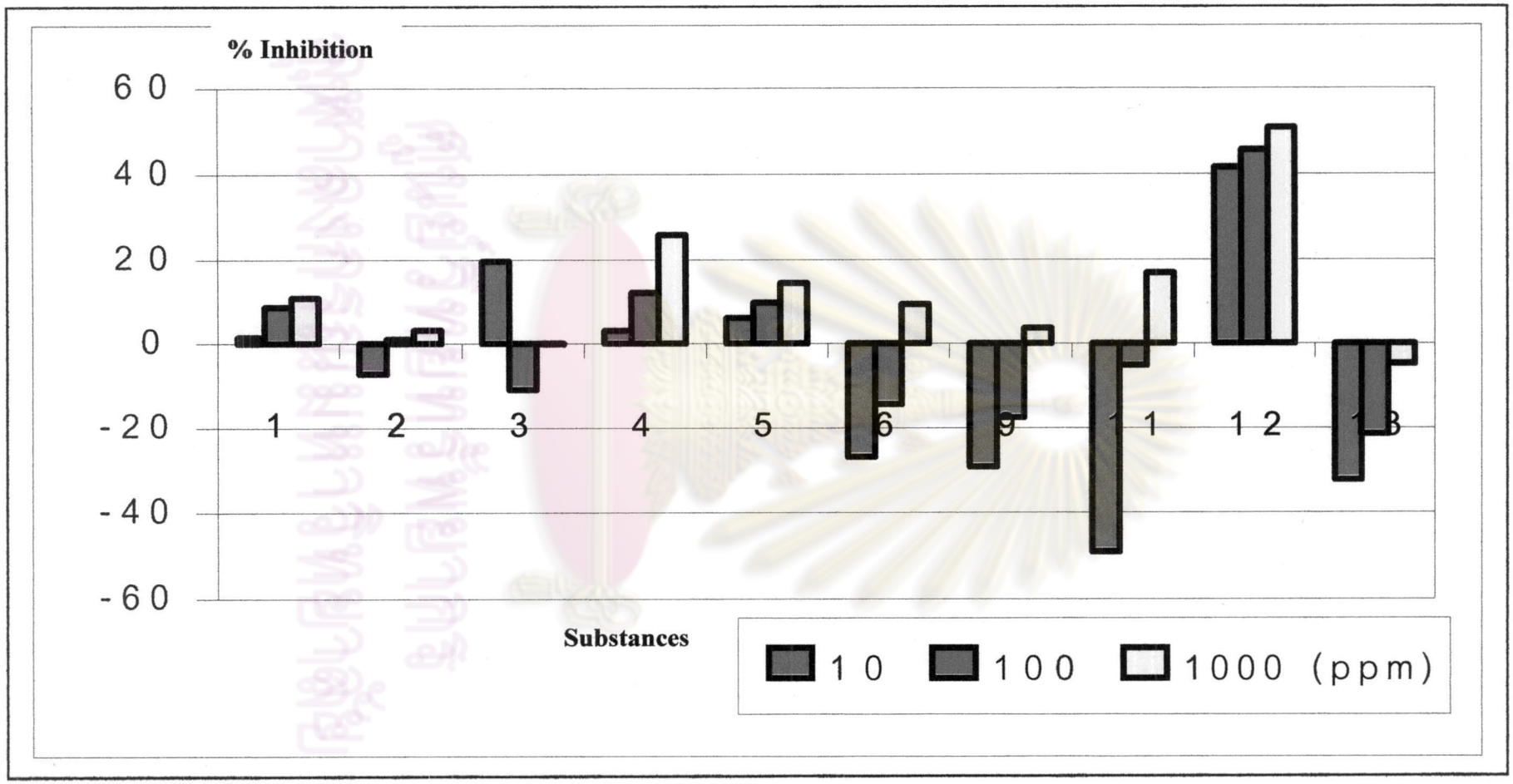

Fig. 3.60 Inhibitory effect of isolated substances from *Hyptis suaveolens* Poit. on the shoot growth of *Pennisetum polystachyon* Schult.

Table 3.23 Inhibitory effect of isolated substances from *H. suaveolens* Poit. on the growth of *Bidens pilosa* Linn. (กันจ้ำขาว)

Substances	% Inhibition at various concentration			
	Growth of *Bidens pilosa* parts	10 (ppm)	100 (ppm)	1000 (ppm)
HS-1	root	-7.06	1.58	3.63
	shoot	-15.70	13.60	23.66
HS-2	root	6.39	11.05	26.60
	shoot	-14.33	14.62	24.56
HS-3	root	-31.87	-22.51	-7.02
	shoot	-2.59	3.28	5.01
HS-4	root	7.21	19.92	46.40
	shoot	-0.31	5.81	16.51
HS-5	root	-21.60	-28.16	-56.55
	shoot	4.28	5.81	6.12
HS-6	root	7.94	23.14	52.16
	shoot	-4.09	3.51	10.53
HS-7	root shoot	NT	NT	NT
HS-8	root shoot	NT	NT	NT
HS-9	root	-15.92	-13.65	-5.24
	shoot	-12.44	6.50	17.44
HS-10	root shoot	NT	NT	NT
HS-11	root	-19.79	3.17	7.94
	shoot	-5.34	2.35	9.45
HS-12	root	1.78	8.44	34.67
	shoot	-16.57	-10.36	15.50
HS-13	root	-6.56	3.97	11.92
	shoot	-11.11	7.60	18.42

NT = Not Tested

5-Hydroxy methyl furfuraldehyde **(HS-4)** and a mixture of two triterpenoids **(HS-6)** exhibited root growth inhibitory effect 46.40%, 52.16%, respectively at 1000 ppm. A mixture of two steroid glycosides **(HS-5)** showed root growth promotion effect 56.55%, at 1000 ppm.

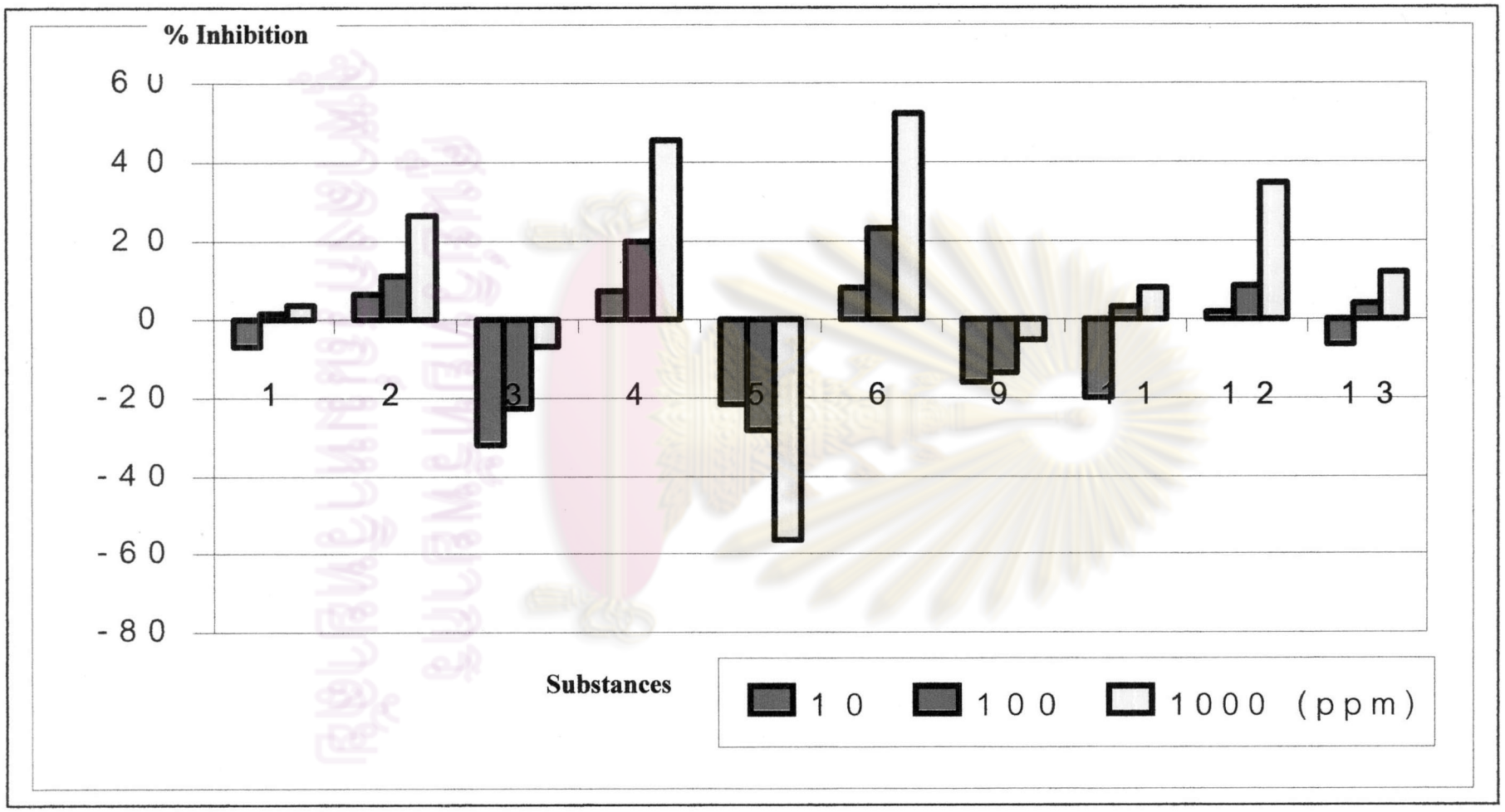

Fig. 3.61 Inhibitory effect of isolated substances from *Hyptis suaveolens* Poit. on the root growth of *Bidens pilosa* Linn.

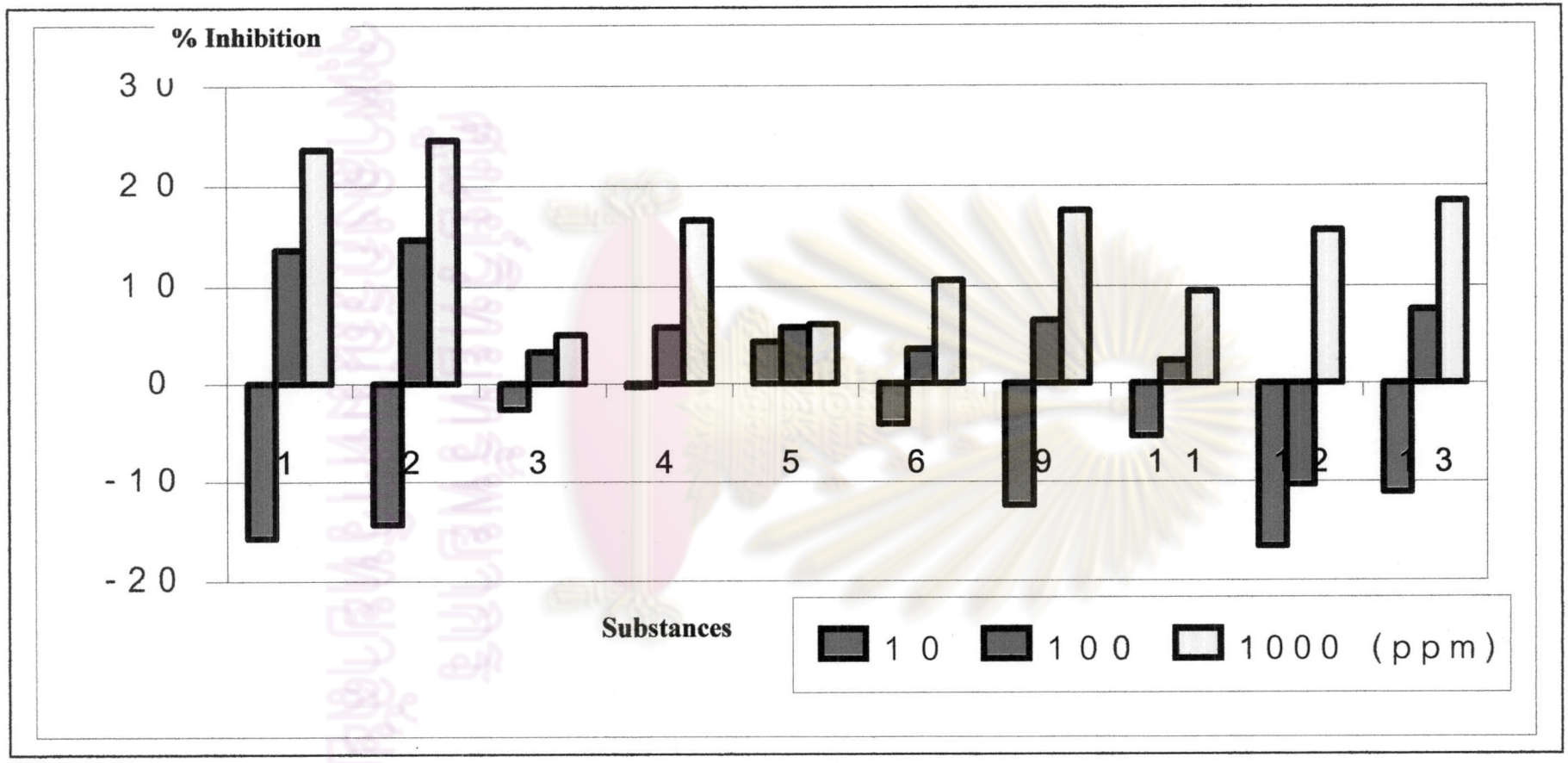

Fig. 3.62 Inhibitory effect of isolated substances from *Hyptis suaveolens* Poit. on the shoot growth of *Bidens pilosa* Linn.

Table 3.24 Inhibitory effect of isolated substances from *H. suaveolens* Poit. on the growth of *Brassica chinense* Jusl.

Substances	% Inhibition at various concentration			
	Growth of *Brassica chinese* parts	10 (ppm)	100 (ppm)	1000 (ppm)
HS-1	root shoot	-21.12 -24.84	0.95 -11.76	27.83 4.27
HS-2	root shoot	-2.74 0.68	19.41 4.72	39.82 21.09
HS-3	root shoot	NT	NT	NT
HS-4	root shoot	-24.12 -7.51	14.16 18.78	86.79 22.54
HS-5	root shoot	NT	NT	NT
HS-6	root shoot	NT	NT	NT
HS-7	root shoot	NT	NT	NT
HS-8	root shoot	NT	NT	NT
HS-9	root shoot	5.61 -24.88	10.04 -19.81	37.64 12.98
HS-10	root shoot	NT	NT	NT
HS-11	root shoot	NT	NT	NT
HS-12	root shoot	22.44 -1.58	27.41 9.83	47.60 29.69
HS-13	root shoot	0.75 -25.01	3.95 -21.49	18.82 10.67

NT = Not Tested

5-Hydroxy methyl furfuraldehyde **(HS-4)** and betulinic acid **(HS-12)** showed root growth inhibitory effect 86.79% and 47.60%, respectively, at 1000 ppm. Compounds **HS-3**, **HS-5**, **HS-6**, **HS-7**, **HS-8**, **HS-10** and **HS-11** did not test because of its insufficience of samples.

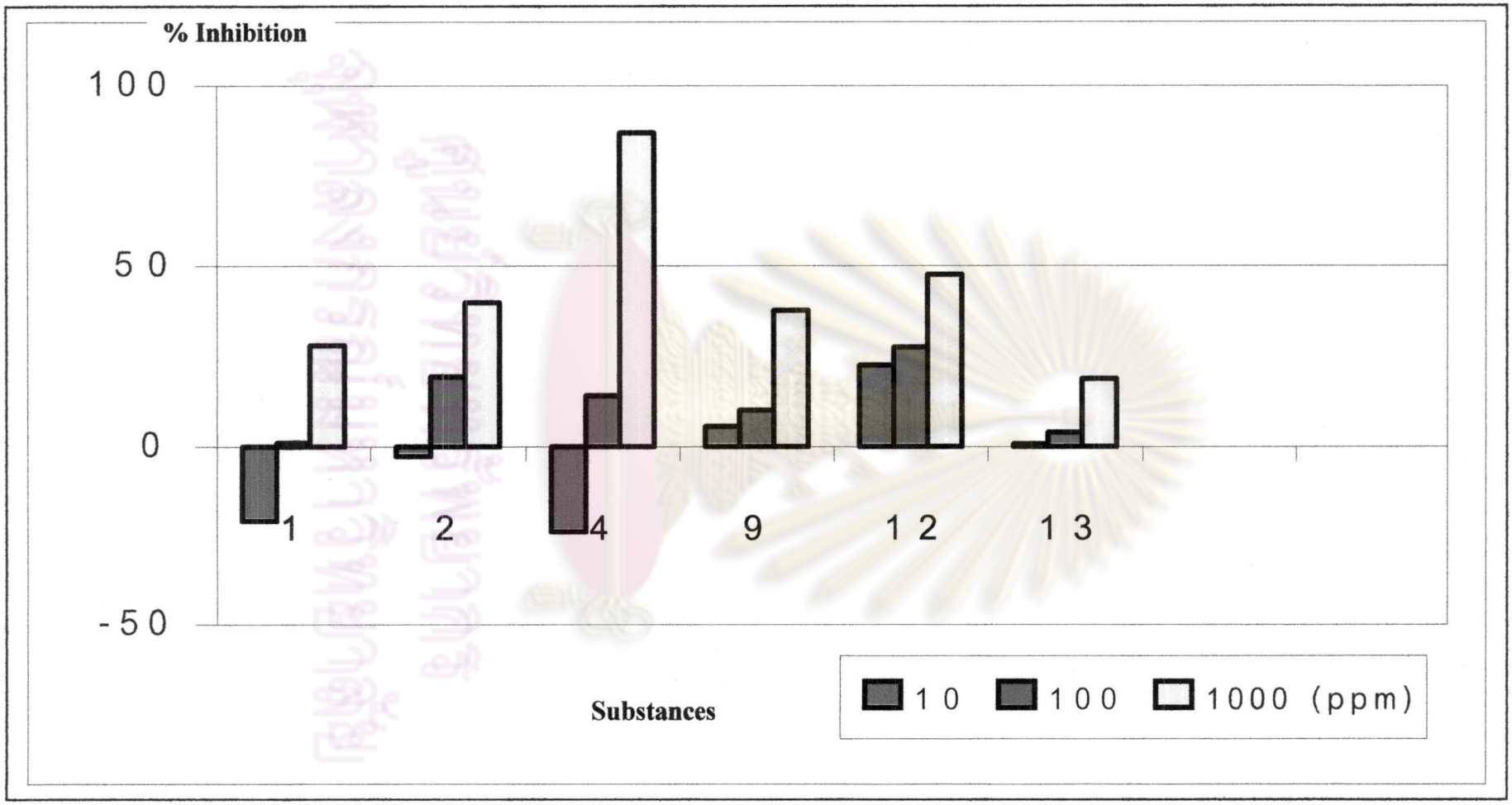

Fig. 3.63 Inhibitory effect of isolated substances from *Hyptis suaveolens* Poit. on the root growth of *Brassica chinense.* Jusl.

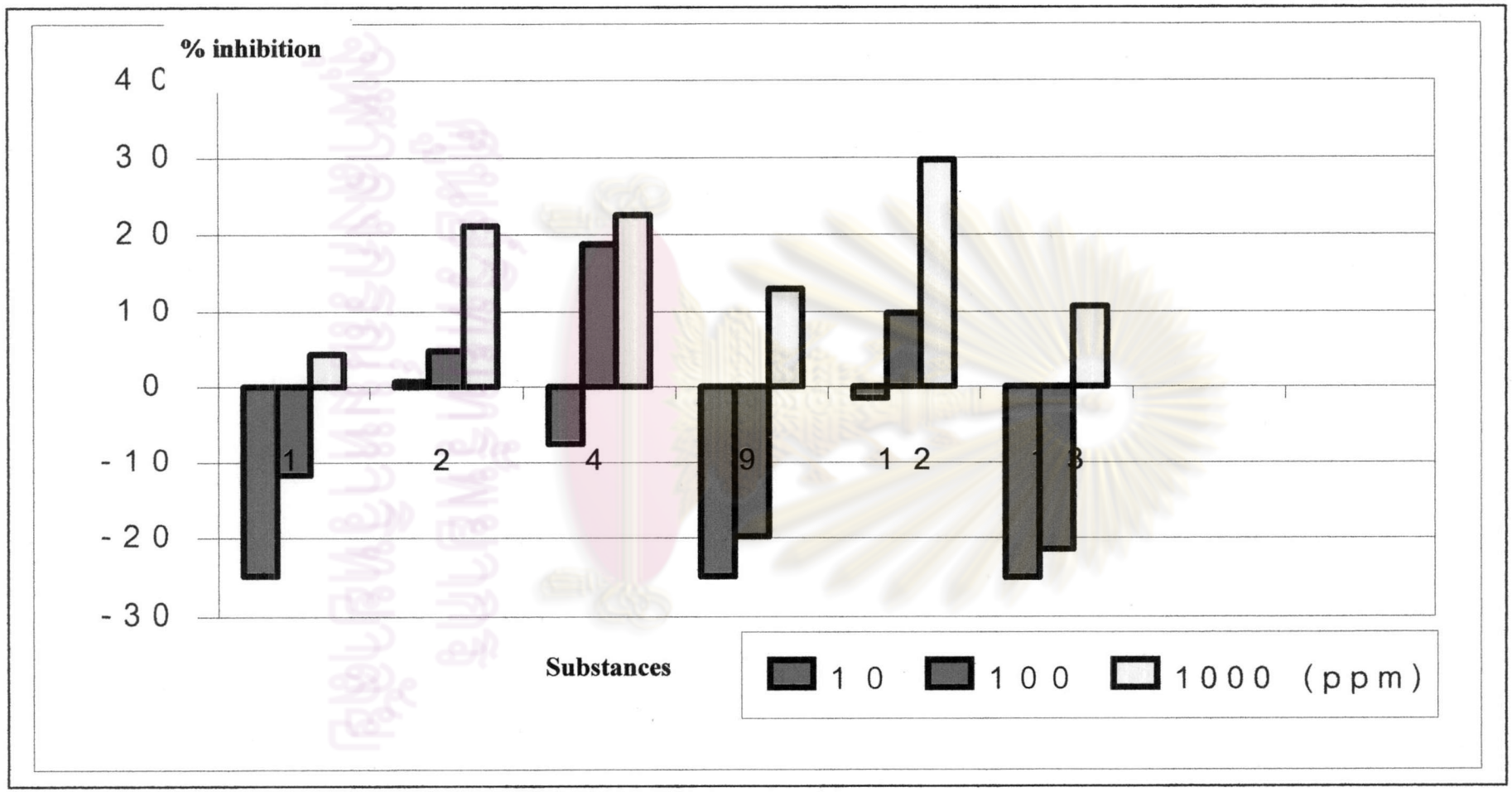

Fig. 3.64 Inhibitory effect of isolated substances from *Hyptis suaveolens* Poit. on the shoot growth of *Brassica chinense* Jusl.

From the preliminary bioassay for seedling growth inhibition activity, it was revealed that a mixture of two steroids **(HS-1)** showed root growth promotion effect on *L. sativa* Linn. and *T. portulacastrum* Linn., but exhibited slightly inhibition effect against root and shoot on other plants. Oleanolic acid **(HS-2)** revealed root growth promotion effect on *E. crus-galli* Beauv., exhibited moderately inhibition effect against root and shoot on *L. sativa* Linn., and showed slightly inhibition effect against root and shoot on other plants. Genkwanin **(HS-3)** showed root growth promotion effect on *L. sativa* Linn., *B. pilosa* Linn. and *D. aegyptium* Willd., showed root growth promotion effect on *D. aegyptium* Willd. and *P. polystachyon* Schult., displayed moderatelyly inhibition effect against root on *E. crus-galli* Beauv. and exhibited slightly inhibition effect against shoot on *L. sativa* Linn., *T. portulacastrum* Linn., *B. pilosa* Linn. and *E. crus-galli* Beauv. 5-Hydroxy methyl furfuraldehyde **(HS-4)** revealed strongly inhibition effect against root on *B. chinense* Jusl. and *E. crus-galli* Beauv., displayed moderately inhibition effect against root on *L. sativa* Linn., *T. portulacastrum* Linn., *B. pilosa* Linn., *P. polystachyon* Schult. and *D. aegyptium* Willd., showed slightly inhibition effect against shoot on *L. sativa* Linn., *T. portulacastrum* Linn., *B. pilosa* Linn., *P. polystachyon* Schult. and *D. aegyptium* Willd., but exhibited shoot growth promotion effect on *E. crus-galli* Beauv. A mixture of two steroid glycosides **(HS-5)** revealed root growth promotion effect on *L. sativa* Linn. and *B. pilosa* Linn., showed shoot growth promotion effect on *E. crus-galli* Beauv., displayed slightly inhibition effect against root and shoot on *T. portulacastrum* Linn., *P. polystachyon* Schult., and *D. aegyptium* Willd., showed slightly inhibition effect against shoot on *L. sativa* Linn., and *B. pilosa* Linn. A mixture of two triterpenoids **(HS-6)** showed root growth promotion effect on *L. sativa* Linn. and *E. crus-galli* Beauv., exhibited shoot growth promotion effect on *D. aegyptium* Willd., showed moderately inhibition effect against root on *T. portulacastrum* Linn. and *B. pilosa* Linn., displayed moderately inhibition effect against shoot on *L. sativa* Linn. and *E. crus-galli* Beauv., revealed slightly inhibition effect against root on *P. polystachyon* Schult. and *D. aegyptium* Willd., showed slightly inhibition effect against shoot on *T. portulacastrum* Linn., *B. pilosa* Linn. and on *P. polystachyon* Schult. A mixture of long chain alcohols **(HS-7)** showed root growth promotion on *L. sativa* Linn., exhibited slightly inhibition effect against root on *E. crus-galli* Beauv., displayed slightly inhibition effect against shoot on *L. sativa* Linn., showed moderately inhibition effect against shoot on *E. crus-galli* Beauv. A

mixture of long chain esters **(HS-8)** revealed shoot growth promotion on *E. crus-galli* Beauv., displayed slightly inhibition effect against root and shoot on *L. sativa* Linn., showed slightly inhibition effect against root on *E. crus-galli* Beauv. β-Amyrin **(HS-9)** revealed root growth promotion effect on *L. sativa* Linn., *T. portulacastrum* Linn., *B. pilosa* Linn. and *P. polystachyon* Schult., showed root and shoot growth promotion effect on *D. aegyptium* Willd., displayed slightly inhibition effect against root and shoot on *B. chinense* Jusl. and *E. crus-galli* Beauv., exhibited slightly inhibition effect against shoot on *L. sativa* Linn., *T. portulacastrum* Linn., *B. pilosa* Linn. and *P. polystachyon* Schult. α-Amyrin **(HS-10)** revealed root growth promotion effect on *L. sativa* Linn. and *E. crus-galli* Beauv., showed moderately inhibition effect against shoot on *E. crus-galli* Beauv., and exhibited slightly inhibition effect against shoot on *L. sativa* Linn. Lupeol **(HS-11)** revealed root growth promotion effect on *T. portulacastrum* Linn., *E. crus-galli* Beauv. and *D. aegyptium* Willd., showed shoot growth promotion effect on *P. polystachyon* Schult., *D. aegyptium* Willd., displayed slightly inhibition effect against root and shoot on *E. crus-galli* Beauv. and ., *B. pilosa* Linn., *L. sativa* Linn. and *T. portulacastrum* Linn., and exhibited slightly inhibition effect against root on *L. sativa* Linn., *B. pilosa* Linn. and *P. polystachyon* Schult. Betulinic acid **(HS-12)** revealed root growth promotion effect on *L. sativa* Linn., showed moderately inhibition effect against root on *B. chinense* Jusl., *E. crus-galli* Beauv. and *D. aegyptium* Willd., displayed moderately inhibition effect against shoot on *P. polystachyon* Schult. and *E. crus-galli* Beauv., and exhibited slightly inhibition effect against root and shoot on other plants. Ursolic acid **(HS-13)** revealed shoot growth promotion effect on *P. polystachyon* Schult., showed moderately inhibition effect against root on *L. sativa* Linn., showed moderately inhibition effect against shoot on *E. crus-galli* Beauv., and displayed slightly inhibition effect against root and shoot on other plants. The results of allelopathy effect of isolated substances from *H. suaveolens* Poit. are summarized in Table 3.25.

Table. 3.25 Allelopathic effect of isolated substances from *Hyptis suaveolens* Poit on various plants.

Substances	Dicotyledon								Monocotyledon					
	LS		TP		BP		BC		PP		EC		DA	
	R	S	R	S	R	S	R	S	R	S	R	S	R	S
HS-1	x	++	x	+	+	+	+	+	+	+	+	+	+	+
HS-2	++	++	+	+	+	+	+	+	+	+	x	+	+	+
HS-3	x	+	+	+	x	+	-	-	+	x	++	+	x	x
HS-4	++	+	++	+	++	+	+++	+	++	+	+++	x	++	+
HS-5	x	+	+	+	x	+	-	-	+	+	+	x	+	+
HS-6	x	++	++	+	++	+	-	-	+	+	x	++	+	x
HS-7	x	+	-	-	-	-	-	-	-	-	+	++	-	-
HS-8	+	+	-	-	-	-	-	-	-	-	+	x	-	-
HS-9	x	+	x	+	x	+	+	+	x	+	+	+	x	x
HS-10	x	+	-	-	-	-	-	-	-	-	x	++	-	-
HS-11	+	+	x	+	+	+	-	-	+	x	x	+	x	x
HS-12	x	+	+	+	+	+	++	+	+	++	++	++	++	+
HS-13	++	+	+	+	+	+	+	+	+	x	+	++	+	+

note: LS = *L. sativa* Linn., TP = *T. portulacastrum* Linn., BP = *B. pilosa* Linn., PP = *P. polystachyon* Schult., BC = *B. chinense* Jusl., EC = *E. crus-galli* Beauv., DA = *D. aegyptium* Willd., R = Root, S = Shoot, " + " = 1-40% inhibition, " ++ " = 41-79% inhibition, " +++ " = 80-100% inhibition, " x " = Plant growth promotion and " - " = not tested.

According to the activity against monocotyledon and dicotyledon plants, it can briefly summarized that the substance exhibited root growth promotion on monocotyledon α-amyrin **(HS-10)**, while showed that shoot growth promotion is a mixture of long chain esters **(HS-8)**. The substances that displayed root growth inhibition on monocotyledon are a mixture of two steroids **(HS-1)**, 5-hydroxy methyl furfuraldehyde **(HS-4)**, a mixture of two steroid glycosides **(HS-5)**, a mixture of long chain alcohols **(HS-7)**, a mixture of long chain esters **(HS-8)**, betulinic acid **(HS-12)** and ursolic acid **(HS-13)**. While those showed shoot growth inhibition are a mixture of two steroids **(HS-1)**, oleanolic acid **(HS-2)**, a mixture of long chain alcohols **(HS-7)**, α-amyrin **(HS-10)** and betulinic acid **(HS-12)**. Oleanolic acid **(HS-2)**, genkwanin **(HS-3)**, a mixture of two triterpenoids **(HS-6)**, β-amyrin **(HS-9)** and lupeol **(HS-11)** displayed both root growth inhibition and root growth promotion. In addition, a mixture of two steroids **(HS-1)**, oleanolic acid **(HS-2)**, a mixture of long chain alcohols **(HS-7)**, α-amyrin **(HS-10)** and betulinic acid **(HS-12)** showed shoot growth inhibition and shoot growth promotion.

For dicotyledon plants, the substances exhibited root growth promotion on dicotyledon are a mixture of long chain alcohols **(HS-7)** and α-amyrin **(HS-10)**. The substances that displayed root growth inhibition are oleanolic acid **(HS-2)**, 5-hydroxy methyl furfuraldehyde **(HS-4)**, a mixture of long chain esters **(HS-8)** and ursolic acid **(HS-13)**. The substances a mixture of two steroids **(HS-1)**, genkwanin **(HS-3)**, a mixture of two steroid glycosides **(HS-5)**, a mixture of two triterpenoids **(HS-6)**, β-amyrin **(HS-9)**, lupeol **(HS-11)** and betulinic acid **(HS-12)** displayed both root growth inhibition and showed shoot growth promotion. While all substances showed shoot growth inhibition on dicotyledon depended on which tested plants were used. The results of allelopathic effect of isolated substances from *Hyptis suaveolens* Poit. against monocotyledons and dicotyledons are summarized in Table 3.26.

Table 3.26 The summary of allelopathic effect of isolated substances from *Hyptis suaveolens* Poit. against monocotyledon and dicotyledon.

allelopathy	Monocotyledon		Dicotyledon.	
	Root	Shoot	Root	Shoot
Inhibition	**HS-1, HS-4, HS-5, HS-7, HS-8, HS-12, HS-13**	**HS-1, HS-2, HS-7, HS-10, HS-12**	**HS-2, HS-4, HS-8, HS-13**	**HS-1, HS-2, HS-3, HS-4, HS-5, HS-6, HS-7, HS-8, HS-9, HS-10, HS-11, HS-12, HS-13**
Promotion	**HS-10**	**HS-8**	**HS-7, HS-10**	-
Inhibition and Promotion	**HS-2, HS-3, HS-6, HS-9, HS-11**	**HS-3, HS-4, HS-5, HS-6, HS-9, HS-11, HS-13**	**HS-1, HS-3, HS-5, HS-6, HS-9, HS-11, HS-12**	-

From the list of isolated substances, it could draw a conclusion that for *H. suaveolens*, the plant growth inhibition activity of pure substances was found to comparatively be less than that of hexane and dichloromethane crude extracts, likely because hexane and dichloromethane crude extracts were fractionated. The marked plant growth inhibition activity of hexane and dichloromethane crude extracts may be contributed to be pure substances and other minor plant growth inhibition components in hexane and dichloromethane crude extracts. The real active components isolated were indeed synergist. Furthermore, for the worse case, the active principles may be decomposed during separation isolation step.